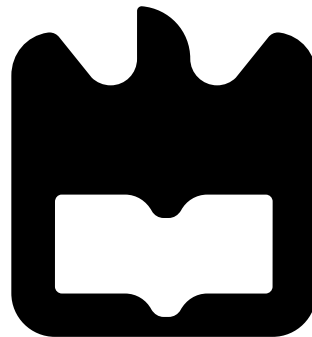




**Alison Willian Pereira**

**Sistema Automático de 'Load-Pull' com Base  
num Sintonizador de Impedância Eletromecânico**

**Fully-Automated Load-Pull System based on  
Mechanical Tuners**





**Alison Willian Pereira**

**Sistema Automático de 'Load-Pull' com Base  
num Sintonizador de Impedância Eletromecânico**

**Fully-Automated Load-Pull System based on  
Mechanical Tuners**

Dissertação apresentada à Universidade de Aveiro para cumprimento dos requisitos necessários à obtenção do grau de Mestre em Engenharia Electrónica e Telecomunicações, realizada sob a orientação científica de José Carlos Esteves Duarte Pedro, Pedro Miguel da Silva Cabral, Professores do Departamento de Electrónica da Universidade de Aveiro e Dr. Francesc Martin Purroy líder de grupo na área de amplificadores de potência em rádio frequência (RF) na empresa Huawei Technologies Suécia.

Dissertation presented to the University of Aveiro for the fulfilment of the requisites necessary to obtain the degree of Master In electronics and Telecommunication Engineering, developed under the scientific guidance of José Carlos Esteves Duarte Pedro, Pedro Miguel da Silva Cabral, Professors in the Department of Electronics, Telecommunication and Informatics of the University of Aveiro, and Dr. Francesc Martin Purroy the team leader of radio-frequency (RF) power amplifier (PA) in HUAWEI Technologies Sweden.

## O Júri / The Jury

Presidente / President

**Prof. Doutor Nuno Miguel Borges de Carvalho**  
Professor Catedrático da Universidade de Aveiro

Arguente Principal / Main  
Examiner

**Prof. Doutor João Manuel Torres Caldinhas Simões Vaz**  
Professor Auxiliar do Instituto Superior Técnico da Universidade de Lisboa

Orientador / Advisor

**Prof. Doutor José Carlos Esteves Duarte Pedro**  
Professor Catedrático da Universidade de Aveiro

Co-Orientador / Co-Advisor

**Prof. Doutor Pedro Miguel da Silva Cabral**  
Professor Auxiliar Convidado da Universidade de Aveiro

## **Agradecimentos / Acknowledgments**

É com muita satisfação que expresso a minha gratidão aos meus orientadores Prof. Dr. José Carlos Esteves Duarte Pedro e Prof. Dr. Pedro Miguel da Silva Cabral pela ajuda fornecida, conhecimento transmitido e tempo disponibilizado.

Agradeço ao meu co-orientador, Dr. Francesc Purroy pela sua disponibilidade, atenção dispensada, paciência, dedicação e profissionalismo em todas as fases que levaram à concretização deste trabalho.

O meu profundo agradecimento a todos os colegas que contribuíram para a concretização desta dissertação, estimulando-me intelectual e emocionalmente. Em particular, agradeço o Dr. Eng. Luís Cótimos por me ter ajudado inúmeras vezes.

À Universidade de Aveiro e o Instituto de telecomunicações de Aveiro pela aprendizagem transmitida, assim como o acesso as suas facilidades.

Esta dissertação foi realizada com o apoio e colaboração da empresa HUAWEI Technologies AB - Suécia. Agradeço esta instituição pelo interesse no trabalho desenvolvido.

Por último, tendo plena consciência que sem ela nada disso seria possível, dirijo-me a minha mãe, pelo incentivo, compreensão e encorajamento ao longo de todos os anos da minha vida. A ela dedico este trabalho!

## palavras-chave

carga virtual, calibração absoluta de potência, malha-fechada, malha-aberta, realimentação para frente, sintonizador de impedância eletromecânico, sintonizador de impedância eletrônico

## Resumo

Por razões de potência, linearidade e eficiência o amplificador é um componente limitador de performance em qualquer tipo de aplicações relacionadas com estações base de voz e dados, motivando a indústria das telecomunicações a investir em sistemas capazes de ajudar o projetista de Amplificador de Potência (AP) a obter o máximo deste elemento ativo.

O sistema de 'load-pull' é uma ferramenta essencial para auxiliar o projeto de amplificadores de potência, permitindo determinar as condições ideais de impedância que maximizam a sua performance.

Esta dissertação insere-se na área de caracterização e projeto de AP, em rádio frequência e visa a concepção, implementação e validação de um sistema automático de 'load-pull' passivo.

Neste trabalho, realizou-se um estudo sobre os mais diversos tipos de sistemas de 'load-pull' utilizados na caracterização de transistores de alta potência.

De modo a cumprir a finalidade desta dissertação, construí-se um sistema passivo automatizado de 'load-pull' capaz de lidar com potência 250W forma de onda contínua (CW) e 2.5 kW de potência de pico em relação a envolvente de modulação (PEP), onde a repetibilidade da malha de saída deste sistema é -60dB a uma frequência correspondente de 1.8GHz, garantindo uma boa precisão das impedâncias apresentadas ao transistor de microondas.

**Keywords**

active injection, absolute power calibration, closed-loop, load-pull characterization, electromechanical tuner, electronic tuners, feed-forward, harmonic impedance synthesis, load-pull, open-loop, virtual load

**Abstract**

Due to power, linearity and efficiency reasons the PA is the performance limiting component in any state-of-the-art mobile voice and data base station, motivating the telecommunications industry to invest in systems capable of helping the designer of PA to get the most of the active devices.

The load-pull system is an essential tool to assist the design of PA, allowing to determine the optimum matching conditions that maximizes the PA performance parameters.

This dissertation fits in the area of radio frequency characterization and PA design, aiming the artful conception, implementation and validation of an automated passive load-pull system.

In this work a study was also performed on the most diverse types of load-pull systems that are used in the characterization of high power transistors.

In order to fulfill the purpose of this dissertation, an automated load-pull system was built, being capable to handle 250W of power in continuous wave (CW) and 2.5kW in peak-to-envelope (PEP), where the system repeatability of its output network is -60dB at a frequency of 1.8GHz, granting a good accuracy of impedances presented to the microwave transistor.

# Contents

<b>Contents</b>	<b>i</b>
<b>List of Figures</b>	<b>iii</b>
<b>List of Tables</b>	<b>v</b>
<b>Acronyms</b>	<b>vi</b>
<b>1 Introduction</b>	<b>1</b>
1.1 Motivation . . . . .	1
1.2 Objectives . . . . .	2
1.3 Organization and structure . . . . .	2
<b>2 Load-Pull Systems</b>	<b>3</b>
2.1 Introduction . . . . .	3
2.2 Figures of Merit (FoM) . . . . .	4
2.3 Load-pull measurements: Traditional, VNA and Six-Port. . . . .	5
2.4 Load-pull techniques: Passive, Active and Hybrid . . . . .	10
2.5 Comparison of the different kinds of load-pull setups . . . . .	25
2.6 Reflection coefficient enhancement techniques . . . . .	26
<b>3 Design and implementation of an automated tuner-based load-pull system</b>	<b>31</b>
3.1 Introduction . . . . .	31
3.2 Diagram of the automated load-pull system . . . . .	32
3.3 System description . . . . .	33
3.4 Characterization of the load-pull system . . . . .	37
3.5 Characterization of the system components . . . . .	37
3.6 Characterization of tuner . . . . .	38
3.7 MATLAB routines . . . . .	40
3.8 Automated load-pull system verification . . . . .	43
<b>4 Conclusion and Future Work</b>	<b>51</b>
4.1 Conclusion . . . . .	51
4.2 Future work . . . . .	52
<b>Bibliography</b>	<b>53</b>

<b>A</b>	<b>MATLAB Routines</b>	<b>57</b>
A.1	Pre-Characterization . . . . .	57
A.2	Power Calibration . . . . .	61
A.3	Load-Pull Measurements . . . . .	65
<b>B</b>	<b>MT981EU10_Setup - HUAWEI</b>	<b>73</b>
<b>C</b>	<b>GaN Load-Pull - Target impedances</b>	<b>76</b>
<b>D</b>	<b>3-port to 2-port network conversion</b>	<b>77</b>
D.1	LPS - Output Network . . . . .	77
D.2	LPS - Input Network . . . . .	78

# List of Figures

2.1	Representative diagram of load-pull and its applications. . . . .	3
2.2	Representative diagram of the load-pull measurement capabilities. . . . .	5
2.3	Representative schematic of a traditional automated load-pull measurement [5]. . . . .	6
2.4	Generic block diagram of a real-time passive load-pull setup based on [6]. . . . .	7
2.5	Simplified automated load-pull setup based on SP reflectometer technique. . . . .	8
2.6	Representation of a passive load-pull system, copied from [5]. . . . .	10
2.7	Example of an electromechanical tuner (EMT) with 2 RF probes. . . . .	11
2.8	(a) Tuner RF probe. (b) Impact of parallel susceptance in the magnitude of $ \Gamma $ reflection coefficient. . . . .	11
2.9	A Solid-state electronic tuner, copied from [15]. . . . .	12
2.10	Example of an ETS assisting noise parameters in on-wafer measurements. . . . .	12
2.11	Shows the tuner distribution of ETS vs EMT. Copied from [18] . . . . .	13
2.12	This architecture was on of the first passive harmonic load-pull setups. . . . .	15
2.13	The harmonic rejection tuner based three-harmonic load-pull architecture. . . . .	16
2.14	Tuning coverage at $f_0$ , $2f_0$ and $3f_0$ using the triplexer method. [23] . . . . .	16
2.15	The harmonic rejection tuner based three-harmonic load-pull architecture. . . . .	17
2.16	Tuning coverage at $f_0$ , $2f_0$ and $3f_0$ using a PHT and fundamental tuner.[23] . . . . .	17
2.17	The multipurpose single tuner based harmonic load-pull architecture. . . . .	18
2.18	Tuning coverage at $f_0$ , $2f_0$ and $3f_0$ using the multi purpose single tuner. . . . .	18
2.19	Representative loop of an ideal active closed-loop LPS. system. . . . .	20
2.20	Block diagram of a realizable active closed-loop LPS. . . . .	21
2.21	A generic schematic of feed-forward active load-pull architecture [5] . . . . .	22
2.22	Functional diagram of an active open-loop load-pull system. . . . .	23
2.23	Hybrid-Active fo load-pull system copied from [28] . . . . .	24
2.24	Circuit model of a mechanical tuner with pre-match and tuning probe. . . . .	26
2.25	Functional diagram (a) and the signal flow of an enhaced load-pull setup (b) copied from [29]. . . . .	27
2.26	Comparison of the maximum achievable reflection coefficient between a commercial pre-matched tuner and a loop enhanced tuner at 1.8 GHz base on [29]. . . . .	27
2.27	Illustration of the quarter-wave transformer technique in (c). The $Z_T^l$ represents the synthesizable loads that are inside of the light blue circles. Moreover, the $Z_L$ are the loads presented after the quarter-wave transformation that are inside of the light purple circles. Those ones that possess a characteristic line impedance of $50 \Omega$ are depicted in (a) and those ones that possess a characteristic line impedance of $20 \Omega$ are represented in (b). . . . .	28

2.28	Fixtures with $\lambda/4$ - transformers for load-pull measurements (a) no-bias (b) bias. Copied from [30]. . . . .	28
2.29	Maury load pull low-loss test fixture. [32] . . . . .	29
3.1	Automated load-pull system implementation flow chart. . . . .	32
3.2	Scheme of the built automated load-pull system. . . . .	33
3.3	Functional diagram of the system source block. . . . .	34
3.4	Functional diagram of the system load block. . . . .	35
3.5	Illustrate how the reflection coefficient of a slide screw tuner change, with a conductive probe moving in two directions within a slabe line, being represented on the admittance smith chart. . . . .	36
3.6	Equivalent 2-port of the input network of the LPS. . . . .	37
3.7	Interpolation result based on the pre-characterized load impedances. . . . .	38
3.8	Representation of the output network of the developed load-pull system. . . . .	41
3.9	Normalized load-pull results obtained in the characterization of one load impedance, displaying the achieved gain(dB) and efficiency as function of output power ( $P_{out}$ ). . . . .	42
3.10	Obtained results of the repeatability check test at 1.8 GHz. . . . .	43
3.11	Characterization and tuner repeatability setup. . . . .	44
3.12	Displayed repeatability test over the Smith chart. . . . .	44
3.13	Scheme of the outputnetwork repeatability test. . . . .	45
3.14	Pre-characterization magnitude and phase error results. . . . .	46
3.15	Precision of poorly calibrated prediction loads. . . . .	47
3.16	Precision of the well performed prediction loads. . . . .	47
3.17	Estimated tuner impedances based on target impedances for the DUT characterization. . . . .	48
3.18	Load-Pull contours at the Z-plane. . . . .	49
3.19	Load-Pull contour at 3dB gain compression point. . . . .	49
3.20	Load-Pull contour at 3dB gain compression point where $Z_0 = 10 \Omega$ . . . . .	50
3.21	Final bench at Huawei Sweden of an automated tuner based load-pull system. . . . .	50
D.1	Conversion of a 3-port network to 2-port network. . . . .	77
D.2	Conversion from 3-port to 2-port s-parameters of the input network. . . . .	78

# List of Tables

2.1	Comparison of the load-pull measurement capabilities. Modified from [11]	9
2.2	Pros and Cons of ETS and EMT. Copied from [8]	14
2.3	Characteristic of harmonic tuning methods. Copied from [23]	19
2.4	Comparison between the passive and active techniques. Based on [5].	25
C.1	Target impedances of the used microwave transistor.	76

# Acronyms

<b>ACPR</b>	Adjacent-channel power ratio
<b>ALC</b>	Automatic leveling control
<b>AWR</b>	Applied wave research
<b>CAD</b>	Computer aided design
<b>CW</b>	Continuous wave
$\eta_D$	Drain efficiency
<b>DLL</b>	Dynamic-link library
<b>DUT</b>	Device under test
<b>EMT</b>	Electromechanical tuner
<b>ETS</b>	Electronic tuners
<b>FoM</b>	Figures of merit
<b>GaN</b>	Gallium nitride
<b>GPIO</b>	General purpose interface bus
<b>HRT</b>	Harmonic rejection tuner
<b>IF</b>	Intermediate frequency
<b>IMD</b>	Intermodulation distortion
<b>LNA</b>	Low Noise Amplifier
<b>LPS</b>	Load-pull system
<b>LUT</b>	Look up table
<b>MPST</b>	Multi-purpose single tuner
<b>MWO</b>	Microwave office
<b>NVNA</b>	Nonlinear vector network analyzer
<b>PA</b>	Power amplifier

<b>PAE</b>	Power-added efficiency
<b>PAPR</b>	Peak-to-average power ratio
$P_{DC}$	DC power supply
$P_{del}$	Power delivered
<b>PEP</b>	Peak-to-envelope
$P_{in}$	Input power
$P_{LP}$	Load-pull power
$P_{out}$	Output power
<b>RF</b>	Radio-frequency
<b>RMS</b>	Root mean square
<b>SA</b>	Spectrum analyzer
<b>SMA</b>	SubMiniature version A
<b>SNR</b>	Signal-to-noise ratio
<b>SOLT</b>	Short-open-load-thru
<b>SP</b>	Six-port
<b>TRL</b>	Thru-reflect-line
<b>VNA</b>	Vector network analyzer
<b>VSG</b>	Vector signal generator
<b>VSWR</b>	Voltage standing wave ratio



# Chapter 1

## Introduction

### 1.1 Motivation

In the last decades the radio communications industry and academic researchers have been looking for the increase of PA's output power and efficiency while maintaining linearity and broadening the operating bandwidth. The PA is the limiting performance component at any state-of-the-art mobile voice and data base-stations, which justifies the high investments in powerful systems capable of aiding the designer to get the most out of the active devices [1].

The most commonly used method in PA artful conception is the computer aided design (CAD) that provides faster and reliable simulations, which usually meet the experimentally obtained results. In some cases, the lack or inaccuracy of non-linear models makes the method unusable. Alternatively, a very attractive measurement-based method, known as load pull is typically employed, being a powerful tool in the microwave transistor and power amplifiers characterization world [1].

The term load-pull refers to the characterization of microwave transistors as a function of reflection coefficient that is seen by the device under test (DUT) at its output terminal. The traditional load-pull system is a passive technique that utilizes two mechanical tuners, one to vary the gate (input) impedance and another to vary the drain (output) impedance for a common source device [2], while accessing the DUT performance parameters.

The active technique is also commonly used in load-pull applications. It is based on signal injection, emulating the reflected travelling wave seen by the DUT. This overcomes the issues associated with the passive technique due to its inherent losses that limits the maximum achievable reflection coefficients, being capable to synthesize unit amplitude or even greater reflection coefficients. The disadvantage associated with the active technique relies on the cost of very expensive amplifiers beyond being prone to oscillations.

The hybrid load-pull system results from the combination of passive and active techniques. Although it reduces the cost of additional RF power sources or loop amplifiers, it is very expensive and hard to implement [1].

Another commonly used passive technique is the harmonic load-pull system (LPS) required to perform the characterization at the fundamental and the harmonic frequencies of a DUT. As a result of harmonic characterization through load-pull measurements, the information of the device can then be utilized for a more complex design PA architecture where efficiency and linearity are the key elements.

## 1.2 Objectives

The main objective of this work is to build a LPS based on already available mechanical tuners. Nowadays, different strategies for LPS are being employed and, because of that, it is necessary to introduce load-pull architectures applied in high-power devices characterization, allowing to understand the most suitable setup for the practical implementation of this work. That is the reason to establish the following objectives:

- Understand the LPS operation principles, measurements and techniques.
- Develop MATLAB control routines for the available tuners and system equipment.
- Test the developed routines and optimize overall performance.
- Validate the automated LPS assessing the accuracy of the characterization.

## 1.3 Organization and structure

This dissertation is organized into four chapters and have the following structure:

- **Chapter 1:** explains the context and motivation of load-pull measurements regarding the design and characterization of RF power amplifiers utilized by the radio communications industry.
- **Chapter 2:** introduces the load-pull state-of-art, addressing the main features of each topology and technique. Additionally, strategies and fundamental concepts regarding high power device characterization is given.
- **Chapter 3:** presents a concise description regarding the design, implementation and validation of the built automated tuner based load-pull system.
- **Chapter 4:** highlights the main aspects, comments the overall work and gives hints for future improvements of the developed load-pull system.

### Appendices

- **Appendix A:** MATLAB Routines conceived to enable characterization of load tuner, LPS calibration and automated load-pull measurements.
- **Appendix B:** MT981EU10\_Setup - MATLAB routine developed for the control of the tuner.
- **Appendix C:** GaN Load-Pull - List of the target impedances used in the device characterization.

# Chapter 2

## Load-Pull Systems

This chapter introduces the load-pull state-of-art explaining the most important features, measurements topologies and techniques applied to high power device characterization.

### 2.1 Introduction

The PA is designed in terms of output power, efficiency and gain. Its optimum performance is achieved when an appropriate source and load impedance are placed at its input and output terminals, respectively. Since PAs usually operate at large-signal, for exhibiting higher efficiency, linearity breaks and the microwave transistor cannot be accurately represented through linear s-parameters, justifying the usage of load-pull techniques in order to determine its optimum matching conditions [3].

Figure 2.1 shows the most commonly used techniques and applications of automated load-pull systems and the red path indicates the goal of this work.

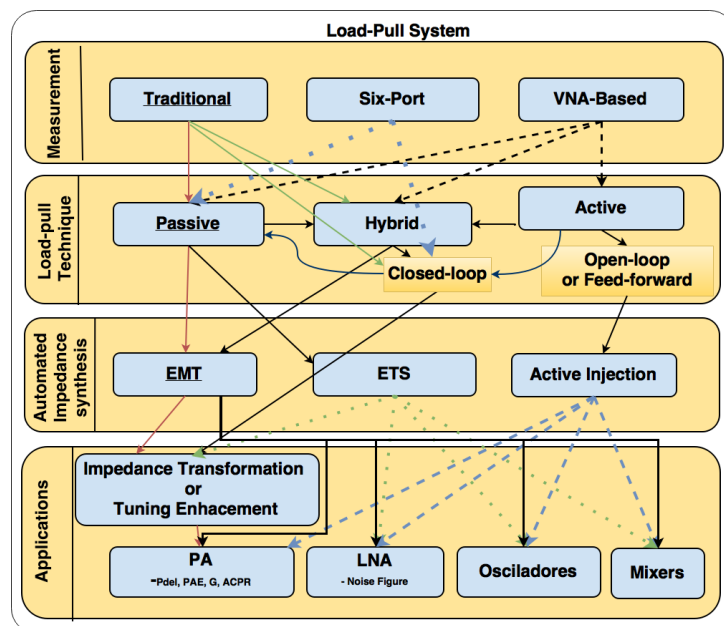


Figure 2.1: Representative diagram of load-pull and its applications.

## 2.2 Figures of Merit (FoM)

**Repeatability** - is one of the key features of an automated tuner, indicating how precisely a tuner can repeat an impedance state. The repeatability consists in the difference of s-parameters between two or more repeated mechanical positions that are measured through a calibrated vector network analyzer (VNA). The following procedure exemplifies how it can be quantified: Firstly, the measurement of the s-parameters is done for a respective chosen mechanical position and are stored in memory. Next, the tuner probe is moved to a dissimilar position, then moved back and the s-parameters are measured again. The repeatability test results are obtained by the following equations:

$$(S_{11})_{repeatability} = 20 \cdot \log_{10} |(S_{11})_{measured} - (S_{11})_{memory}| \quad (2.1)$$

**Tuning Range** - specifies the tuners maximum achievable reflection coefficient over the whole Smith chart. Usually, high power microwave transistors possess their optimum load impedances for gain, efficiency or output power at a region close to the border of the Smith chart. In addition, Tuning Range Distribution defines how the impedance points are covering the smith chart regions [4].

**Tuner Resolution** - defines how many impedances state the tuner is capable to synthesize. It is an important requisite to avoid small variations of the seen impedance by the microwave transistor that might cause significant changes in power-added efficiency (PAE) or  $P_{out}$ . Usually an impedance tuner is able to synthesize around 10.000 impedances states, which can be increased by cascading two or more tuners.

**Power Handling Capability** - describes the maximum root mean square (RMS) and the peak powers supported by the tuner without causing any significant change of the calibrated impedances. This information is specified by the manufacturer of the tuners, defining the safety limits in which it can operate without getting damaged or presenting a risk to the load-pull system.

Some tuners that in the past were poorly designed, presented large values of insertion losses, causing heat of the tuner and contributing to the corona effect. This effect causes electric discharge due to the air ionization that is surrounding the tuner conductor, damaging the DUT and system equipment.

**Tuning Speed** - is seen as the time that the tuner requires to move the probe from one position to another. Moreover, the Total time takes in consideration the tuning speed and spent time of the measurements, which is extremely important to have a fast load-pull characterization in particular, when dealing with the passive technique principle.

**Tuner Bandwidth** - is classified by the frequency range of the tuner and its instantaneous bandwidth where the specified impedances are synthesizable and the modulated bandwidth has a specified constant group delay [1].

**Tuner Size** - refers to the tuner mechanical dimensions being especially important for on-wafer applications where possible vibrations should be avoided, reducing the impact of probe movements and acoustic vibrations, as these increase the insertion losses and change the predicted impedances.

## 2.3 Load-pull measurements: Traditional, VNA and Six-Port.

The load-pull measurements are classified according to the capability of the system to determine the reflection coefficient seen by the DUT, while accessing the injected input power ( $P_{in}$ ) and the power delivered ( $P_{del}$ ) to the load. The first step in setting up a functional load-pull system is the VNA calibration performed through a standard calibration kit. This process is necessary to remove the systematic errors caused by directivity, mismatch, isolation, and cross-coupling that are associated with the VNA.

Not all load-pull systems are able to monitor in real-time the impedances seen by the DUT, unless the used topology possess waveform or vectorial capabilities such as the nonlinear vector network analyzer (NVNA). In addition, the components attached between the NVNA and the DUT reference plane must to be embedded on the calibration in order to directly measure the impedances.

Most passive setups are characterized beforehand through s-parameters measurements of tuner mechanical positions and system components. After the information of each system block is assembled and mathematically cascaded, it allows the system to predict the impedance state that is seen by the DUT based on the time-domain waveform, vectorial or scalar measurements. In case of a scalar measurements, the characterization through s-parameters provides the relation of phase and magnitude that exists between ports of the characterized network, which allows the estimation of power at the DUT reference plane as well as the seen impedance.

The power meter is never directly plugged to the DUT output terminals and because of that, the information about power is 'uncorrected', requiring a characterization of the system to mathematically remove the inherent losses of the input and output network, resulting in the effective  $P_{in}$  and  $P_{out}$ .

Because, in the passive load-pull,  $a_2$  is generated from  $b_2$  in a linear passive network (the tuner and its associated resistor termination), the synthesized reflection coefficient,  $\Gamma'_L = a'_2/b'_2$ , is independent from the absolute value of  $b_2$ . This means that, with a proper characterization of the load block, we can predict the reflection coefficient actually applied to the DUT,  $\Gamma_L = a_2/b_2$ , independently from the knowledge of  $b_2$ . Consequently, the passive load-pull technique is suitable for any of the discussed measurement topologies (Traditional, VNA Based and Six-port reflectometer). This can also be said to the closed-loop active, or hybrid closed-loop, technique, as long as all loop blocks, namely the loop amplifier, can be considered linear and perfectly characterized. This is not the case of the open-loop technique since  $a_2$  is independently generated from  $b_2$ . In such a case,  $\Gamma'_L$  or  $\Gamma_L$  can only be known after knowing  $b_2$ , and that can be obtained from its direct measurement (via a VNA or Six-port reflectometer). Otherwise, it would require the knowledge of the DUT's s-matrix and the (non assured) assumption that the DUT is linear.

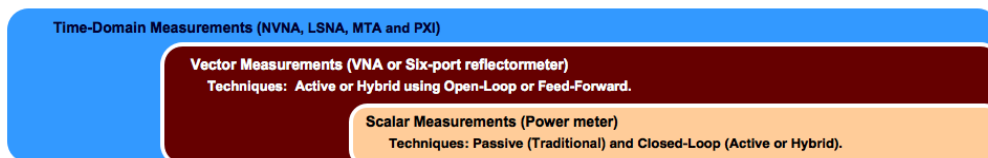


Figure 2.2: Representative diagram of the load-pull measurement capabilities.

The following subsections explain how the impedance can be predicted or measured according to the chosen topology for the passive load-pull measurements.

### 2.3.1 Traditional load-pull measurements

The traditional load-pull is based on power meter or scalar analyzer measurements, giving only the scalar information of the DUT performance. The example shown in Fig. 2.3, contains a DC power supply, an signal generator, an power meter and at least two tuners intended to control and reconfigure the input and output network through a source tuner and load tuner, respectively.

The tuner pre-characterization is a process required to determine which s-parameters corresponds to a certain mechanical position. This process plays a major role in system characterization, accounting for the s-parameters of the tuner in every used mechanical position together with the system components to properly shift the reference plane and mathematically remove the losses present at the output network of the DUT. As such, it is usually created a look up table (LUT) containing the s-parameters versus tuner mechanical position and frequency, saving time and eliminating the usage of an additional system component on the presented topology.

In order to mathematically remove the system losses from the measurements and properly assist the power at the DUT reference plane, the so-called absolute power calibration is normally used and it is well treated in Section 3.5.2. When used in passive systems, this procedure is normally followed by a  $\Delta G_t$  system verification that compares the measured transducer gain,  $G_t$ , to the one predicted through the characterization of the whole LPS.

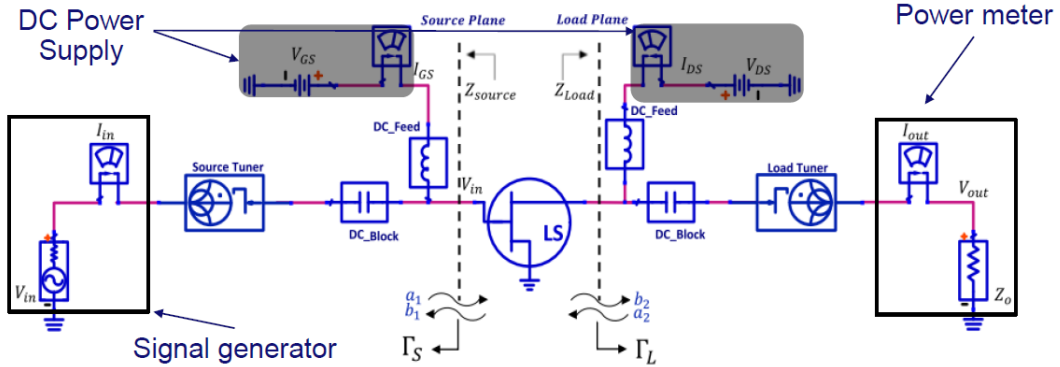


Figure 2.3: Representative schematic of a traditional automated load-pull measurement [5].

The reflection coefficients depicted in Fig.2.4, are defined by the ratio of incident travelling waves,  $a_1$ ,  $a_2$  and the reflected travelling waves,  $b_1$ ,  $b_2$ , and it is calculated by the following equations:

$$\Gamma_S = \frac{a_1}{b_1} = \frac{Z_{Source} - Z_0}{Z_{Source} + Z_0} \quad (2.2)$$

$$\Gamma_L = \frac{a_2}{b_2} = \frac{Z_{Load} - Z_0}{Z_{Load} + Z_0} \quad (2.3)$$

,where  $\Gamma_S$  is the input reflection coefficient,  $\Gamma_L$  is the output reflection coefficient,  $Z_S$  is the source impedance,  $Z_L$  is the load impedance and  $Z_0$  represents the characteristic impedance of the system.

### 2.3.2 VNA based load-pull measurements

The real-time VNA-based load-pull system shown in Fig. 2.4 is capable to monitor the four travelling waves at the DUT planes  $a_1$ ,  $a_2$ ,  $b_1$  and  $b_2$ . The VNA calibration will shift the VNA Ref and Test ports that are monitoring  $a_0$  and  $b_0$  to the DUT input plane allowing the calculation of  $\Gamma_S$  while  $a_3$  and  $b_3$  allows the access of the presented  $\Gamma_L$  at the DUT output port. The reflection coefficients  $\Gamma_S$  and  $\Gamma_L$  are defined as the previous equations 2.2 and 2.3, respectively. The system characterization is also required to assist the measurement of  $P_{in}$  and  $P_{out}$ , obtained by a proper de-embedding of the system components.

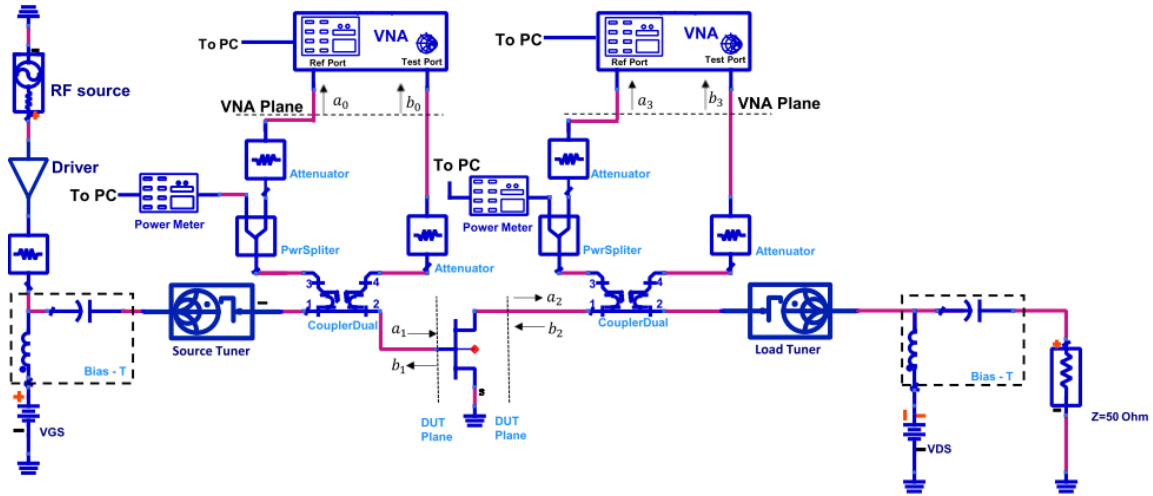


Figure 2.4: Generic block diagram of a real-time passive load-pull setup based on [6].

In VNA-based load-pull setups, the usage of attenuators are justified due to potential oscillations of the DUT that can exceed the operating power levels causing damage to the system equipment. In addition, the attenuator maintains the generated harmonic components above the levels that might interfere significantly on the measurements. Moreover, only one power sensor at each power divider termination is required. Assuming a performed pre-characterization, the tuner reflection coefficient is known and the VNA allows to check this condition [7]. The power being injected and delivered by the DUT is mathematically calculated at post processing levels, removing the losses caused by probe movements and central conductor of the tuners and the connectors. The pre-characterization of the tuners speeds up the measurement process and allows the interpolation of impedances in order to synthesize a desired reflection coefficient present in the DUT reference plane [8].

As it is known, power sensors are wide band, measuring all power including the fundamental and harmonic frequencies, which is the reason to utilize filters before the measurement reference plane to ensure that only the fundamental frequency is being monitored and no power at harmonic components is interfering on the measurements.

The presented measure topology only provides the information at real-time of the seen impedance by the DUT, it requires, in addition, an absolute power calibration in order to proper and accurately assists the power at the device input and output terminals which is a similar process utilized in the traditional technique.

### 2.3.3 Six-port based load-pull measurements

The load-pull measurement based on six-port (SP) reflectometer technique scheme is depicted in Fig. 2.5. It includes two six-port junctions, SP1 and SP2, two automated tuners, source tuner and load tuner. The SP reflectometer is a low-cost technique realized in microstrip technology, which acts as network analyser for absolute power and reflection coefficient measurement at the desired frequency [9].

This measurement topology is capable to obtain the reflection coefficient based on a circuit that possess N-port network, requiring 4N power readings [1, 10]. The information of reflection coefficient phase is directly obtained from RF signals through a proper calibration of the SP reflectometers.

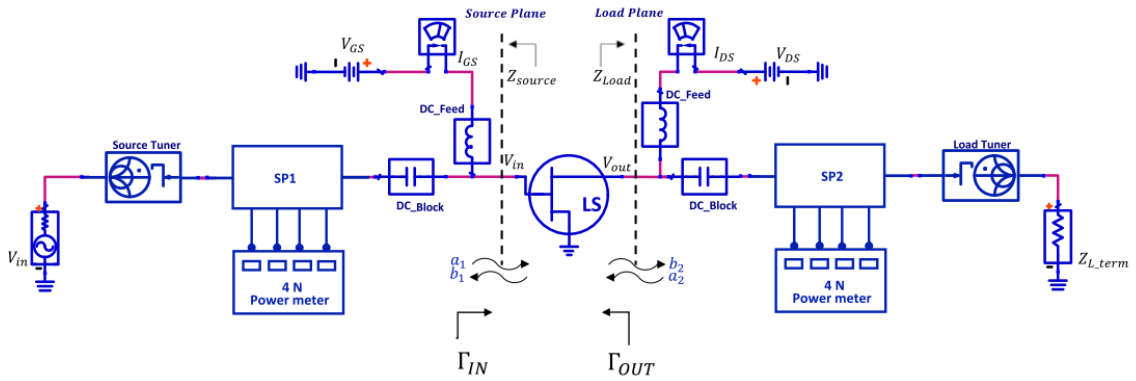


Figure 2.5: Simplified automated load-pull setup based on SP reflectometer technique.

The reflection coefficient and power that is obtained with SP reflectometer measurements is calculated the following equations:

$$\Gamma_{DUT}(f) = \frac{w(f) - e(f)}{-c(f)w(f) + d(f)} \quad (2.4)$$

$$P_{DUT}(f) = \frac{k(f)P_{Ref}(f)}{|1 + c(f)\Gamma_{DUT}(f)|^2} \quad (2.5)$$

,where  $c(f)$ ,  $d(f)$  and  $e(f)$  are the error box parameters, obtained through a proper calibration of SP junction,  $w(f)$  is the embedded reflection coefficient,  $k(f)$  is the power calibration parameter determined at each measurement frequency,  $P_{Ref}(f)$  is the power reading measurement at reference port of the SP junction and  $\Gamma_{DUT}(f)$  is the reflection coefficient measured by the SP reflectometer.

$$\Gamma_S(f) = S_{22}(f) + \frac{S_{12}(f)S_{21}(f)\Gamma_{st}}{1 - S_{11}(f)\Gamma_{st}} = \frac{\alpha(f)\Gamma_{st} + \beta(f)}{\mu(f)\Gamma_{st} + 1} \quad (2.6)$$

, where  $\alpha(f)$ ,  $\beta(f)$  and  $\mu(f)$  are directly related to the two-port network delimited by the input and output reference planes of SP junctions and  $\Gamma_{st}$  is the source tuner reflection coefficient. In a similar manner the calibration of the SP is performed at the load side of the DUT.

### 2.3.4 Comparison of the load pull measurement techniques

The major difference between the different measurement techniques is the utilized procedure for the inspection of the impedance seen by the DUT at its reference plane. The traditional method is unable to monitor, in real-time, the reflection coefficient at the DUT reference plane. On the other hand, the VNA-based technique allows the measurement of that termination at CW and multi-tones, while the six-port techniques only gives information at the fundamental frequency due to the narrowed bandwidth of the six-port fixture, which is built on microstrip lines. Modulated impedances require a more complex measurement system with time domain waveform capabilities which is not discussed in this work.

Besides the short introduction of this subsection, the main features of each system are revised in the following Table 2.1 where it is shown the main important measurements required for the characterization of microwave transistor using a load-pull application.

Table 2.1: Comparison of the load-pull measurement capabilities. Modified from [11]

<u>Measurement Parameter</u>	<u>Traditional Load Pull</u>	<u>Vector-Receiver Load Pull</u>	<u>Six-Port Load Pull</u>
Input Reflection Coefficient ( $\Gamma_{in}$ )	✗	✓	✓
Available Input Power ( $P_{in,avs}$ )	✓	✓	✓
Delivered Input Power ( $P_{in,del}$ )	✗	✓	✓
Output Power ( $P_{out}$ )	✓	✓	✓
Power Gain	✗	✓	✓
Transducer Gain ( $G_T$ )	✓	✓	✓
Power Added Efficiency (PAE)	✗	✓	✓
Drain efficiency ( $\eta_{Drain}$ )	✓	✓	✓
AM/PM	✗	✓	✓
Calibrated Harmonic Power	Spectrum analyser required	✓	✗
Multi-tone Measurements	Spectrum analyser required	✓	✗
Modulated Measurements	Spectrum analyser required	✗	✗
Power Sweep Speed (for 25 power levels)	~ 20 seconds	~ 1 second	~ 20 seconds

## 2.4 Load-pull techniques: Passive, Active and Hybrid

The load-pull techniques have been evolving in the last decades, but its classification remains organized into two categories: active and passive. These techniques of load-pull refer to how fashion impedances are synthesized, while the load-pull measurement are classified accordingly to the system capability in perform scalar, vectorial or time domain measurements.

This section explains the state-of-art of the load-pull techniques focusing on fundamental frequency characterization. In addition, it is briefly reviewed the passive harmonic load-pull techniques that might be used as future work. Moreover, due to the inherent losses existent in passive load-pull systems, it was found interesting to present some strategies adopted to increase the maximum achievable reflection coefficient in high-power microwave devices characterization.

### 2.4.1 Passive load-pull system

The traditional load-pull system is generally built around its main element, the tuner, which is usually placed between the DUT and the power meter, as shown in Fig. 2.6. The major challenge in setting up this type of load-pull system involves its characterization and calibration, required to de-embed the losses and shift reference plane from the peripheral equipment to the DUT plane, allowing to assist in measuring its performance parameters [5].

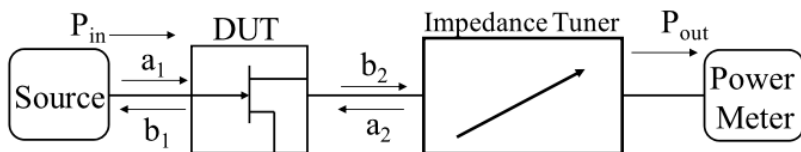


Figure 2.6: Representation of a passive load-pull system, copied from [5].

The optimum load impedance is determined by the inspection of the DUT performance parameters under different impedance states while the measurement of  $P_{in}$  and  $P_{out}$  is done through a power meter. The correct reading of  $P_{in}$ ,  $P_{out}$  and output reflection coefficient,  $\Gamma_{OUT}$  is obtained by the following equations:

$$\Gamma_{OUT} = \frac{a_2}{b_2} \quad (2.7)$$

$$P_{in} = |a_1|^2 - |b_1|^2 = |a_1|^2(1 - |\Gamma_{in}|^2) \quad (2.8)$$

$$P_{out} = |b_2|^2 - |a_2|^2 = |a_1|^2(1 - |\Gamma_{out}|^2) \quad (2.9)$$

where,  $a_n$  represents the incident travelling waves and  $b_n$ , the reflected travelling waves, where n corresponds to ports 1 and 2; There are two kinds of passive tuners: electromechanical tuner (EMT) and the electronic tuners (ETS) as is explained as follows.

## Electromechanical tuner (EMT)

The EMT is a physical mechanical structure that can be reconfigured to set some s-parameters at its ports. Generally, it is composed by probes/slug/stubs in a slotted transmission line. Figure 2.7 shows an automated EMT, composed by a slab line, two RF probes, 3 stepper motors and an electronic control board utilized to precisely control the mechanical position of the probes along the x and y axis. The precision of the motors allows the correlation between its s-parameters and respective mechanical positions, being a crucial feature of an automated load-pull system.

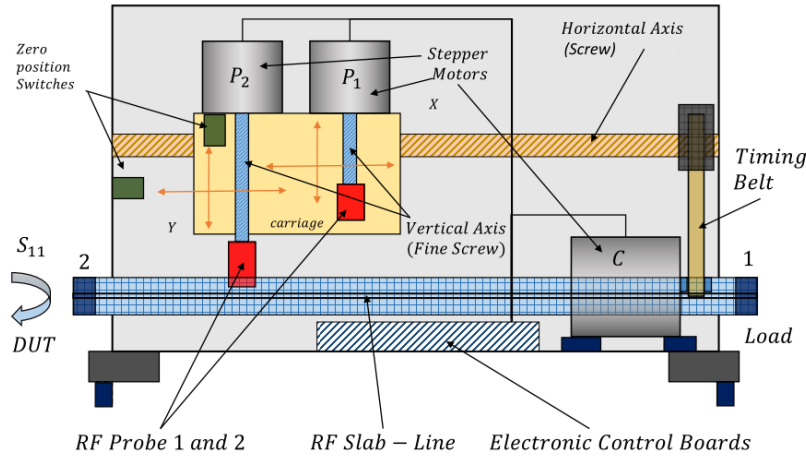


Figure 2.7: Example of an electromechanical tuner (EMT) with 2 RF probes, based on [12].

The tuner probes depicted in Fig. 2.8 illustrate the main engine utilized in the syntheses of different reflection coefficients. The probe is usually called the mismatched element, because its vertical movement over Y axis and movement along horizontal X axis, modifies the magnitude and phase of the reflection coefficient, respectively. This resonator element is specified by the manufacturer in order to cover a certain range of frequencies, which typically goes from RF up to millimeter waves [8, 13, 14].

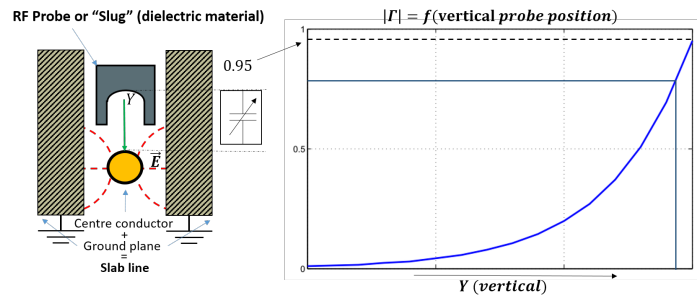


Figure 2.8: (a) Tuner RF probe. (b) Impact of parallel susceptance in the magnitude of  $|\Gamma|$  reflection coefficient.

The EMT is capable to synthesize reflection coefficients,  $\Gamma$ , normally as the order of 0.9-0.95. When it is pre-matched by the fixture or cascaded with another tuner, this range can be increased up to 0.98.

## Electronic tuners (ETS)

The ETS is a faster device fabricated with ON/OFF PIN diodes or varactors, both mounted in microstrip circuit and digitally controlled. The distribution of reflection factors over the smith chart are typically irregular due to the physical distribution of circuit elements along the microstrip line. Normally, the maximum achievable reflection coefficient of an ETS is about 0.8 enclosed in a certain range of frequencies.

A possible configuration of an ETS is depicted in Fig. 2.9, which is regularly controlling different possible ON/OFF states, through a control unit that allows the syntheses of many high-ly repeatable reflection coefficients. However, this tuner possesses a lower tuning resolution compared with the EMT, being usually cascaded with additional tuners, generating millions of impedance states, which hopefully will correspond to the desired impedance states.

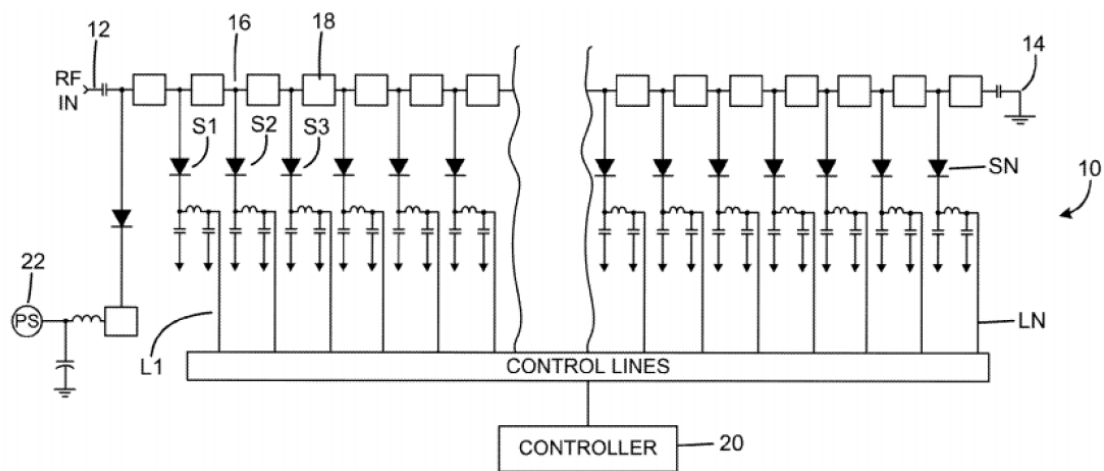


Figure 2.9: A Solid-state electronic tuner, copied from [15].

The ETS possesses higher values of loss, diminishing the maximum achievable reflection coefficient, when compared with the EMT [16]. This makes this tuner more attractive for an on-wafer characterization due to its associate smaller size and light weight, as shown in Fig.2.10.

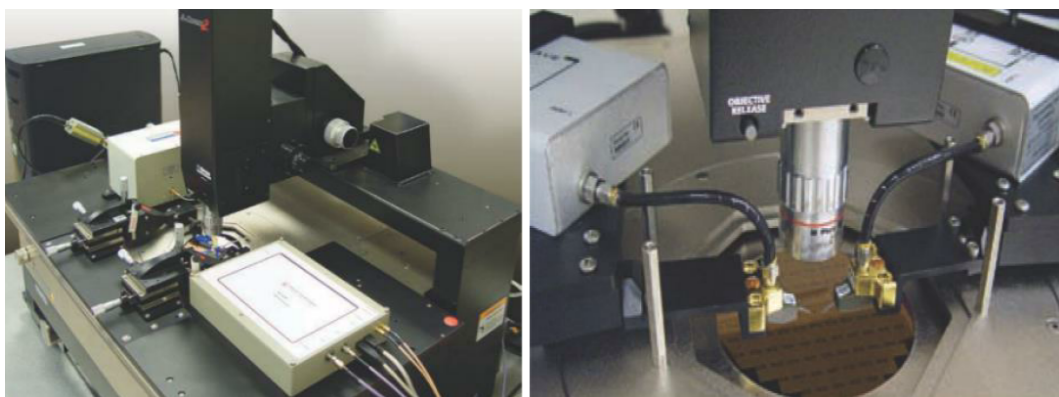


Figure 2.10: Example of an ETS assisting noise parameters in on-wafer measurements. Copied from [17].

## Comparison between EMT and ETS

The most suitable tuner for a certain load-pull application depends on its requisites. Table 2.2 shows a comparison of the main aspects of EMT and ETS utilized in designs of PAs, Low Noise Amplifier (LNA), oscillators, mixers and on-wafer tests [8].

The ETS exhibits great values of repeatability, typically -70dB, which apparently shows that the ETS is better than the EMT, which commonly presents only -60dB of repeatability. However, the EMT offers low insertion loss on the order of tenths of dB even when gamma possess high values, becoming a more attractive solution for systems requiring synthesizable load impedances near the border of the smith chart. On the other hand, the ETS operating losses can go up to 12 dB while presenting a high reflection coefficient such as  $\Gamma_L = 0.8$ , which is also one of the reasons to reduce the maximum achievable reflection coefficient once the losses can be even further making this technique inappropriate for the characterization of high power amplifiers, because of its optimum load condition of the microwave transistor is found on the edge of the smith chart.

The EMT's are relatively slower due to the time required for the measurement using general purpose interface bus (GPIB), taking a few seconds to move from one impedance state to another. On the other hand, the ETS is able to swap the impedance states faster than the EMT, which usually seems instantaneous, needing only a few milliseconds.

In case of an on-wafer device characterization, the ETS is the most suitable approach, covering a vast range of frequencies, but at low frequencies the EMT's are also used, when an appropriate vibration test is performed.

Figure 2.11 shows the comparison between the ETS and EMT, where the ETS has a fixed load distribution while ETS presents a non-uniform distribution. Due to the fact that the EMT produces a uniform distribution of generated loads, interpolation algorithms can be used to synthesize a desired reflection coefficient, while the ETS can only cascade another tuners in order to increase the number of impedances states.

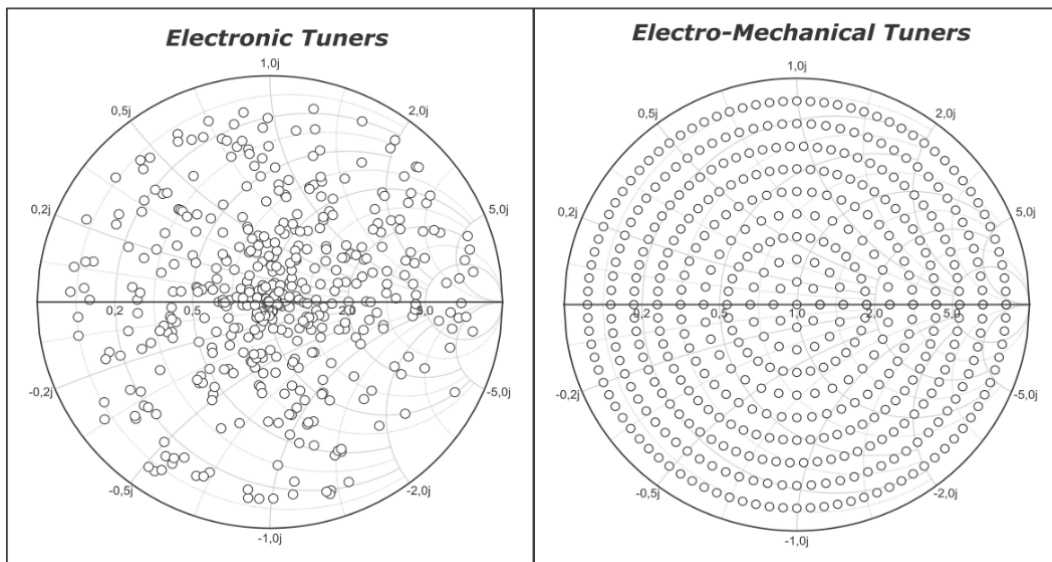


Figure 2.11: Shows the tuner distribution of ETS vs EMT. Copied from [18]

Table 2.2: Pros and Cons of ETS and EMT. Copied from [8]

Characteristic	Electronic Tuner (ETS)	Electromechanical Tuner (EMT)
<b>Reflection Factor</b>	Noise: O	++
	Load Pull: -	
<b>Number of Impedances</b>	O	++
<b>Insertion Loss</b>	-	+ / ++
<b>Tuning Resolution</b>	Noise: O	++
<b>Maximum Power</b>	O / - / --	++
	depending on DUT	
<b>Frequency Bandwidth</b>	O	++
<b>Spurious Oscillations</b>	O / -	++
<b>On Wafer operation</b>	++	O
<b>Tuner Size</b>	++	On wafer: -
		Test fixture: ++
<b>Tuner Speed</b>	++	-
<b>Test Total Speed</b>	+	+
<b>Tuner Linearity</b>	O / -	++
	depending on DUT	
<b>DSB Noise measurement</b>	--	+
<b>Temperature Drift</b>	?? /-	++

Legend: ++ Excellent; + Good; O Acceptable; - Poor/Risky; -- Unacceptable for certain tasks

## 2.4.2 Passive harmonic load-pull system

The harmonic load-pull technique is an essential tool to assist the microwave characterization and to determine the optimum fundamental and harmonic load conditions for a certain figures of merit (FoM) such as intermodulation distortion (IMD), linearity or efficiency. This information plays a major role in the design of switch-mode PAs that require specific impedances at the fundamental and the harmonic frequencies placed at DUT input and output terminal as reported in [19]. It is known that optimization of DUT harmonic impedances can improve the efficiency more 15% than a basic PA design at fundamental frequency [20].

Figure 2.12, illustrates an example of a simple harmonic load-pull system. It possesses a circulator, a low pass filter, high pass filter, and pairs of tuners, attenuators and power meters. The variable,  $b_2$  represents the total transmitted wave composed by a fundamental and harmonic travelling waves, the circulator acts as node forwarding waves from port one to port two, two to three and three to one, indefinitely. The first branch has a low pass

filter placed at port 2 of the circulator used to forward only fundamental travelling wave,  $b_2(f_0)$ , whereas at port 3 a high pass filter is forwarding the second harmonic travelling wave,  $b_2(2f_0)$ . For each of the branches a tuner is placed right after the filter allowing the control of fundamental and second harmonic components independently,  $\Gamma_L(f_0)$  and  $\Gamma_L(2f_0)$ . Thus  $a_2(f_0)$  and  $a_2(2f_0)$  are added and reflected, resulting in a  $a_2$  total reflected travelling wave seen by the DUT.

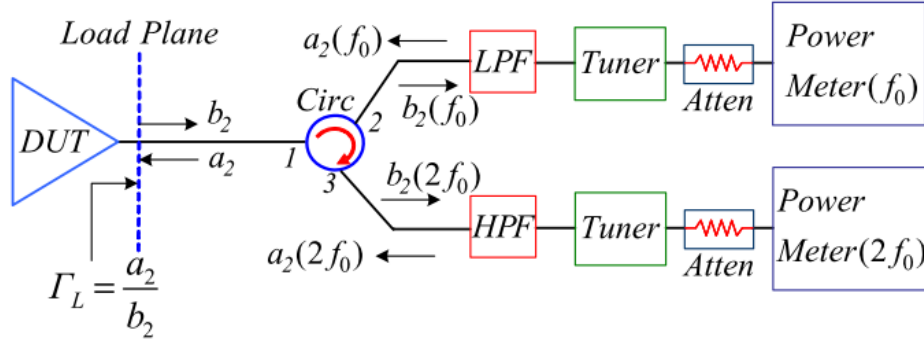


Figure 2.12: This architecture was one of the first passive harmonic load-pull setups. Copied from [22].

The reflection coefficient at fundamental and harmonic components are calculated as following equations:

$$\Gamma_L(f_0) = \frac{a_2(f_0)}{b_2(f_0)} \quad (2.10)$$

$$\Gamma_L(2f_0) = \frac{a_2(2f_0)}{b_2(2f_0)} \quad (2.11)$$

The total reflected travelling waves is obtained by the following equations:

$$a_2(f_0) = \Gamma_L(f_0)b_2(f_0) \quad (2.12)$$

$$a_2(2f_0) = \Gamma_L(2f_0)b_2(2f_0) \quad (2.13)$$

$$a_2 = a_2(f_0) + a_2(2f_0) = \Gamma_L(f_0)b_2(f_0) + \Gamma_L(2f_0)b_2(2f_0) \quad (2.14)$$

In principle this technique can be extended to a n-port wideband circulator in order to control n-1 harmonic components, requiring additionally n-2 band-pass filters for the harmonic components, a low pass filter at fundamental frequency and a high pass filter to the n-1 highest harmonic. However, this is not practicable due to reduction in the tuning range caused by the number of circulators used to deal with a vast number of harmonic frequencies.

Along the years, several variations of the presented technique were developed being nowadays classified as harmonic rejection tuner, triplex based harmonic and multi-purpose single tuner harmonic load-pull [22].

### Triplexer based harmonic load-pull setup

The triplexer based three-harmonic load-pull setup is shown in Fig. 2.13. It uses a triplexer that acts as a selective filter for the fundamental, second and third harmonic component at its respective ports, which is attached a low pass filter, a band pass filter and a high pass filter, increasing the out-of-band rejection for the undesired frequency components. As a result, the harmonic components of the incident and reflected travelling waves,  $b_2$  and  $a_2$ , are described in equations 2.12 and 2.13.

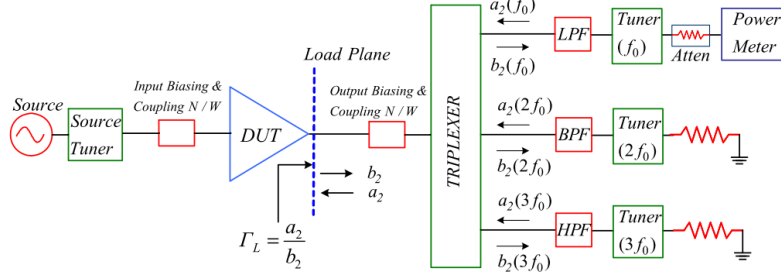


Figure 2.13: The harmonic rejection tuner based three-harmonic load-pull architecture. Copied from [5].

This setup is normally implemented with a VNA measurement system, being attached to the coupling N/W depicted in Fig. 2.13. Moreover, the input and output biasing is used to provide the gate/base bias of the transistor and feed the drain/collector power. In addition, the coupling is required to monitor the incident and reflected travelling waves at the input and output ports of the DUT, allowing to inspect which impedance is being presented at its fundamental and harmonic components. The power meter is used to access the absolute values of the output power at the carrier frequency band under different fundamental, second and harmonic load impedances.

The reflection coefficient at each respective frequency is obtained by the following eq 2.14:

$$b_2 = b_2(f_0) + b_2(2f_0) + b_3(3f_0) + \dots + b_2(nf_0) \quad (2.15)$$

$$a_2 = a_2(f_0) + a_2(2f_0) + a_3(3f_0) + \dots + a_2(nf_0) \quad (2.16)$$

$$\Gamma_{Load}(nf_0) = \frac{a_2(nf_0)}{b_2(nf_0)} \quad (2.17)$$

where,  $n = 1, 2, 3, \dots, c$

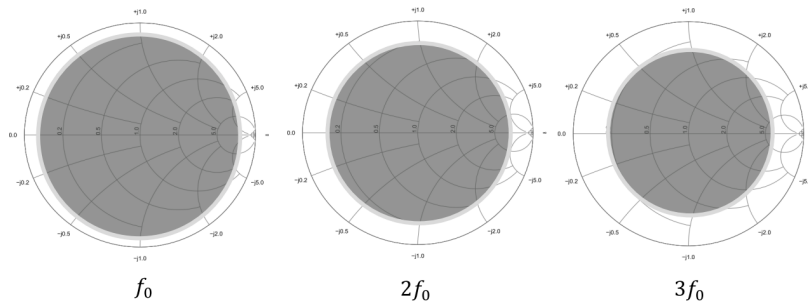


Figure 2.14: Tuning coverage at  $f_0$ ,  $2f_0$  and  $3f_0$  using the triplexer method. [23]

## Harmonic rejection tuner

The harmonic rejection tuner (HRT) is composed by a pre-match tuner cascade with a fundamental tuner. The pre-match and fundamental tuner are placed in the following manner as shown in Fig. 2.15. That is necessary to fulfill the requirements of maximum reflection coefficient at fundamental and harmonic components presented at the DUT output port due to the inherent losses of a passive system, which limits the maximum achievable reflection coefficient.

The optimum reflection coefficient at harmonic components is usually higher than fundamental. Thus, a pre-match tuner is placed as close as possible to the DUT output port, increasing the maximum achievable reflection coefficients at the harmonic components.

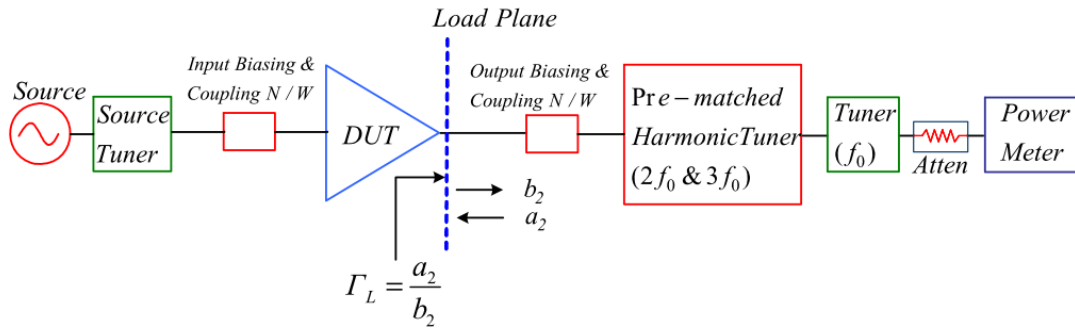


Figure 2.15: The harmonic rejection tuner based three-harmonic load-pull architecture. Copied from [5].

The setup presented in Fig. 2.15, overcomes the problem associated with the losses of the previous triplexer based technique that is shown in Fig. 2.13. The harmonic rejection technique utilizes a low loss tuner, helping the synthesis of high reflection coefficients. The major limitation of this method is that, in some applications, the DUT loads are too close to the Smith chart border aggravating the impact of even the smallest losses.

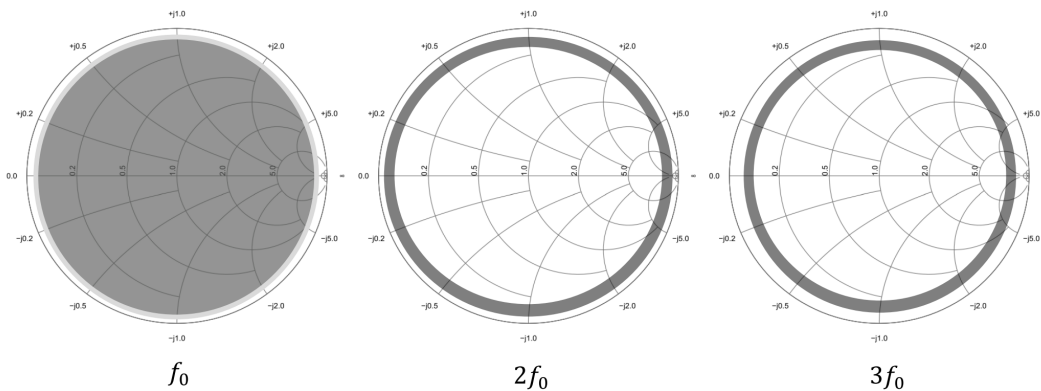


Figure 2.16: Tuning coverage at  $f_0$ ,  $2f_0$  and  $3f_0$  using a PHT and fundamental tuner.[23]

### Multi-purpose single tuner based harmonic load-pull setup

The multi-purpose single tuner (MPST) is commonly used harmonic load-pull setup, as the one depicted in Fig. 2.17, it utilizes a tuner that is capable to control fundamental and harmonic impedances at  $f_0$ ,  $2f_0$  and  $3f_0$  frequencies. This single tuner has three independent probes, which are free to move in the horizontal and vertical directions. As refer, it is a multi-purpose tuner, which drastically reduces the losses introduced by connectors and cables, achieving a greater reflection coefficient for the fundamental and harmonic components when compared with the previous techniques.

As a drawback, this technique requires an algorithm with larger computational effort to precisely monitor and control the 3 independent probes for the synthesis of fundamental and harmonic impedances due to the poor isolation.

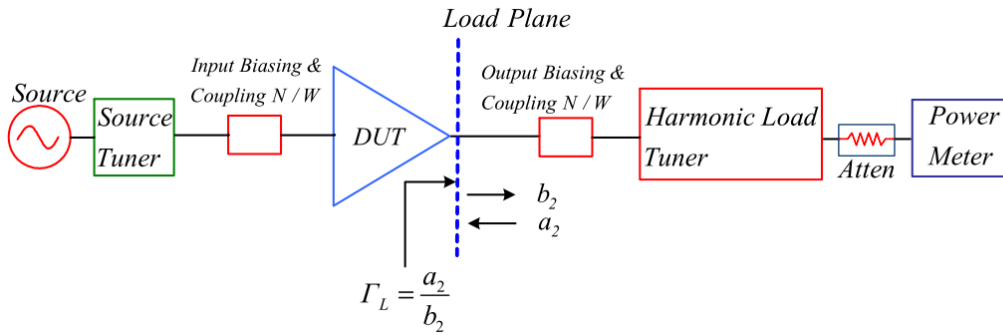


Figure 2.17: The multipurpose-single tuner based harmonic load-pull architecture. Copied from [5]

Figure 2.18 illustrates the synthesizable reflection coefficient range that is possible to obtain with the MPST technique at fundamental and harmonic components. This technique is not suitable for a applications that involves high values of voltage standing wave ratio (VSWR) at harmonic components such as power amplifiers.

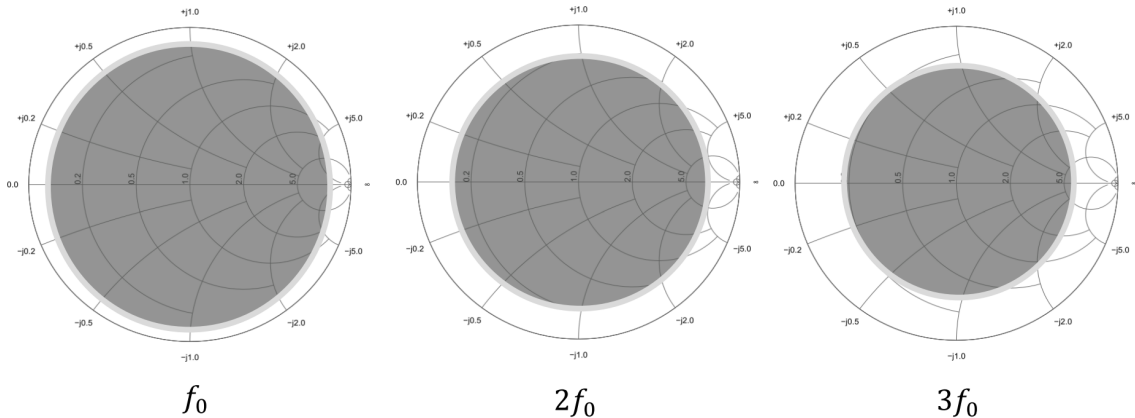


Figure 2.18: Tuning coverage at  $f_0$ ,  $2f_0$  and  $3f_0$  using the multi purpose single tuner. Based on [23]

## Comparison between the passive harmonic load-pull methods

The two main differences between the presented techniques consists in the tuning isolation and the tuning range. The isolation will directly interfere on the impedance control at fundamental and harmonic components. In HRT, the poor isolation between the rejection and fundamental tuner is around 30dB, making the fundamental and harmonic components no longer independent and requires from the system designer an additional effort to account this effect in the determination of the mechanical positions to satisfy the desired reflection coefficient synthesis [22].

On the other hand, the multi-purpose tuner possess a system that takes the effect of poor isolation repositioning the probe automatically to set the desired impedance at fundamental and harmonic components. The major drawback is the time needed to move the probes to the respective mechanical positions.

The triplex-based is the only technique that is considered to perform independent control of the fundamental and harmonic components due to the triplex isolation that is usually between 50-60dB at the fundamental and harmonic components.

The following Table 2.3 summarizes the most relevant features of the explained harmonic load-pull techniques.

Table 2.3: Characteristic of harmonic tuning methods. Copied from [23]

Tuning method	Advantages	Disvantages
<b>Triplexer based</b>	-High tuning isolation	-Unsuitable for on-wafer applications
	-Simple extension of existing setup	-Insertion loss of the triplexer at all frequencies cause a reduced tuning range
	-Very good amplitude and phase control at all the harmonic frequencies	-Out-of-band reflections in the triplexer can cause spurious oscillation
<b>Harmonic rejection tuner based (HRT)</b>	-High tuning range	-Very poor tuning isolation
	-High power handling capability	-Unsuitable for broadband application
	-Low insertion loss at fundamental frequency	-limited to only three harmonics
<b>Multi-purpose single tuner based (MPST)</b>	-High tuning range	-Slow measurement time and throughput
	-High tuning isolation	-Requires powerful computing resources
	-Ideal for on-wafer applications	
	-Appropriate for broadband applications	

### 2.4.3 Active load-pull system

The active load-pull technique is based on the principle of an active load modulation or of a split signal method, which is also known as the 'Takayama' technique [23]. In the split signal method, a signal with the same frequency of the one being injected at the DUT is created or reused. This signal acts as a reflected travelling wave and, by modifying its the magnitude and phase, results in a new reflection coefficient seen by DUT.

The active load-pull monitors, in real-time, the reflection coefficient seen at the DUT ports through a proper VNA calibration, helping to determine the forward and travelling waves, which is required by the control algorithm. The major advantage of this technique is the capability to synthesize any reflection coefficient on the smith chart, overcoming the inherent losses of the passive system.

Typically, there exists three categories of active load-pull: closed-loop, feed-forward and open-loop.

#### Closed-loop load-pull system

The closed-loop constitute the output network of this active load-pull technique, it is similar to the conventional passive LPS, where ideally the  $a_2$  is a direct function of  $b_2$  and the complex gain can modified directly the magnitude and phase of the seen reflection coefficient. If all the elements of the output network are well characterized, including the loop amplifier, this technique becomes suitable to perform the traditional measurement, which drastically reduces cost of the implemented system.

Figure 2.19 illustrates part of the block diagram that composes an ideal closed-loop active load-pull system. As it can be observed, the setup uses three-port component, e.g. circulator, for forwarding the incident travelling wave,  $b_2$ , and reflect the travelling wave,  $a_2$ . In addition, a complex variable  $\rho.e^{j\Theta}$  is used to modify the magnitude, by  $\rho$ , and the phase, by  $\Theta$ , of the incident wave,  $b_2$ , before injecting it back at the DUT reference plane as a reflected travelling wave,  $a_2$ . The reflection coefficient is synthesize as in the following equation:

$$\Gamma_{LOAD} = \frac{a_2}{b_2} = \frac{b_2 \rho.e^{j\Theta}}{b_2} = \rho.e^{j\Theta} \quad (2.18)$$

,where  $\Gamma_{LOAD}$  represents the presented reflection coefficient at the DUT plane.

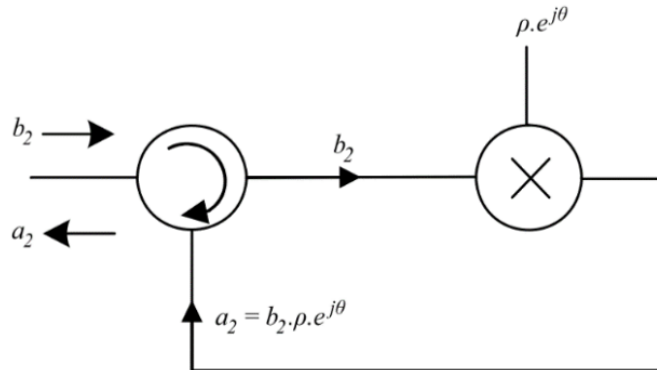


Figure 2.19: Representative loop of an ideal active closed-loop LPS. Copied from [5]

A realistic approach of a closed-loop technique requires attenuators, phase shifters, and loop amplifiers to properly control the magnitude and phase of the reflected travelling wave, as shown in Fig. 2.20

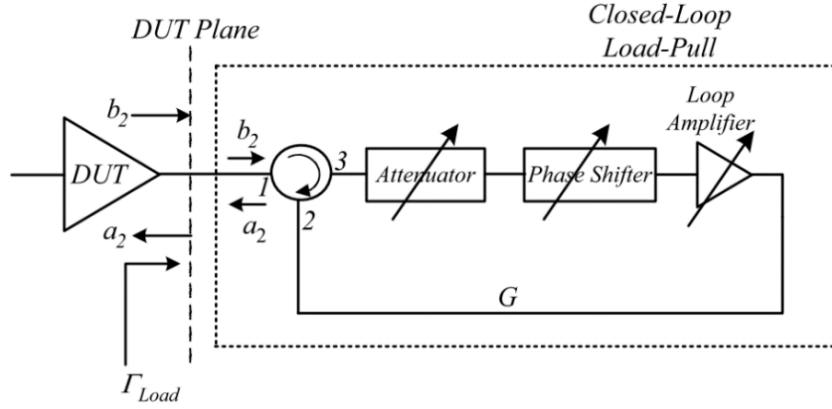


Figure 2.20: Block diagram of a realizable active closed-loop LPS. Copied from [5]

The attenuator and loop amplifier enable the changes in magnitude of the reflected travelling wave,  $a_2$ , while the phase shifter modifies the phase of  $\Gamma$ . As a result, the desired reflection factor,  $\Gamma_{LOAD}$ , can be synthesizable.

The presented closed loop shown in Fig. 2.19, assumes an ideal circulator and ignores the system losses. As a result, the travelling wave obtained at the feedback loop is given by following equation 2.19 and the  $\Gamma_{LOAD}$  at the DUT reference plane is given by equation 2.20:

$$a_2 = Gb_2 \quad (2.19)$$

$$\Gamma_{LOAD} = \frac{a_2}{b_2} = G \quad (2.20)$$

, where  $G$  is the complex gain of the feedback loop controlling the magnitude and phase of the synthesized reflection coefficient. Notice that  $G$  can assume any value and can be even greater than one causing unwanted oscillations due to the closed-loop network, which can possibly damage the DUT and the system equipment.

The closed-loop technique is a more attractive solution for the on-wafer devices characterization, excluding the unavoidable mechanical movements of the EMT that reduces the needed tuning range of impedances. Despite the ETS also avoid the movements on the measure system, it possess a limited tuning range of reflection coefficient that can be overcome with the closed-loop technique. On the other hand, this technique is prone to oscillates due to the leakage existent in the passive components, which can be reduces with the usage of filters that consequently makes this approach narrow band.

### Feed-forward load-pull system

The active feed-forward load-pull system is considered to be stable contrary to what happens in the closed-loop technique. In Fig. 2.21 it is shown an example of this setup that is composed by a simple active tuning chain, a signal source, a variable phase shifter, an attenuator, a variable gain stage and one isolator. The incident travelling wave at the output port of DUT,  $b_2$ , is typically given by following equation:

$$b_2 = S_{21}a_1 + S_{22}a_2 \quad (2.21)$$

If we assume that the components are ideal,  $a_2$ , the reflected travelling wave presented at the output port of the DUT is obtained with the following equation:

$$a_2 = Ga_1 \quad (2.22)$$

The  $\Gamma_{Load}$  represents the ratio of  $a_2$  over  $b_2$ , where the  $a_2$  is generated from the incoming wave,  $a_1$ , and then adjusted by the phase shifter, attenuator, loop amplifier and isolator. Consequently, the  $\Gamma_{Load}$  results from the combination of Eq. 2.21 and Eq. 2.22 yielding the following equation:

$$\Gamma_{Load} = \frac{a_2}{b_2} = \frac{1}{\frac{S_{21}}{G} + S_{22}} \quad (2.23)$$

,where  $G$  represents the complex gain introduced by the loop amplifier of the feed-forward load-pull network and  $S_{21}$  and  $S_{22}$  represents the unknown DUT large signal s-parameters.

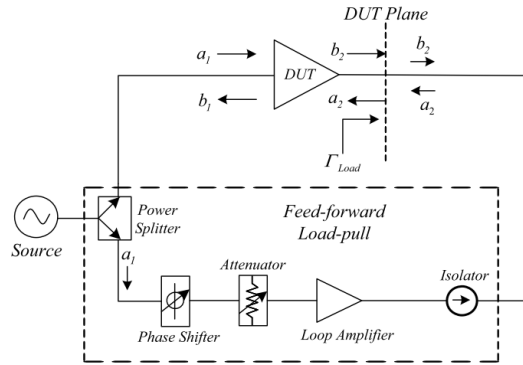


Figure 2.21: A generic schematic of feed-forward active load-pull architecture [5]

Accordingly to Eq. 2.23, it is important to notice the dependence of the reflection coefficient with the complex gain  $G$  and the DUT large signal s-parameters  $S_{21}$  and  $S_{22}$ . Consequently, the synthesis of  $\Gamma_{Load}$  becomes unpredictable due to unknown large-signal s-parameters exhibited by the DUT. In order to obtain a desired reflection coefficient, it is necessary to use convergence techniques to get a certain reflection coefficient. Moreover the complex loop gain,  $G$ , must be bounded between  $G = 0$ , and  $G = 1/S_{22}$ . Corresponding to no operating feed-forward load and the case where it presents the maximum reflection coefficient,  $\Gamma_{Load}$ , at DUT plane. Thus, if the  $G$  is bounded, the attenuator and isolator will prevent the loop amplifier to oscillate. Moreover, while the DUT operates at its stable region the  $S_{22} \leq 1$  and the Eq. 2.23 keeps its usefulness for the calculation of  $\Gamma_{Load}$ .

### Open-loop load-pull system

The open-loop is very similar to the feed-forward technique, its difference consists basically in the addition of external sources utilized in the creation of the reflected travelling wave,  $a_2$ , as shown in Fig. 2.22. The loop amplifier and phase shifter will control the magnitude and phase of the reflected travelling wave,  $a_2$ . In addition, the isolator will guarantee safe operation range of the loop amplifier preventing it to get damaged.

The two sources 1 and 2, shown in Fig. 2.22, are responsible for the incident travelling waves injected at the DUT reference planes, namely  $a_1$  and  $a_2$ . Being the reflected travelling wave  $b_1$  caused by the  $\Gamma_{IN}$  of the DUT and the feed-back of the device,  $b_2$  as shown in the denominator of Eq. 2.24. Consequently, the usage of an external signal of 10 MHz will maintain the phase coherence between the incident and reflected waves  $a_2$  and  $b_2$ , once  $b_2$  is created as a function of the source 1, and  $a_2$ , as a function of source 2.

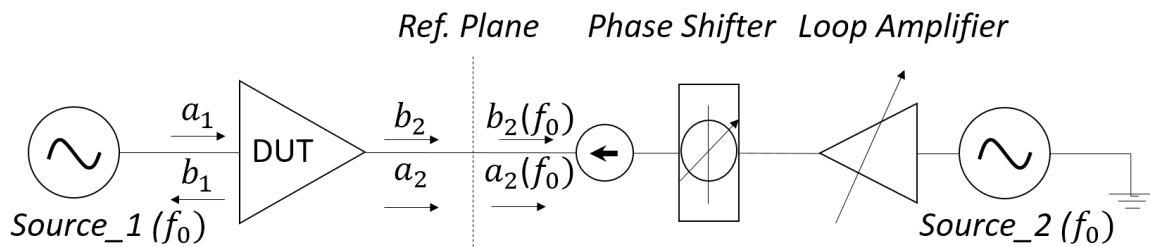


Figure 2.22: Functional diagram of an active open-loop load-pull system.

The load reflection coefficient synthesized with the open-loop technique is given by the following equation:

$$\Gamma_{Load} = \frac{a_2}{b_2} = \frac{a_2}{S_{21}a_1 + S_{22}a_2} = \frac{1}{S_{21}\frac{a_1}{a_2} + S_{22}} \quad (2.24)$$

,where  $S_{21}$  and  $S_{22}$  are the large-signal s-parameters of the DUT at the fundamental frequency.

An notable point in equation (2.24) is that the value of the load reflection coefficient,  $\Gamma_L$ , can vary from 0 to  $\infty$ , only by modifying the magnitude of the reflected travelling wave,  $a_2$ . The major drawback of this technique is the necessity of an expensive external source. In the case of active harmonic load-pull applications, a power divider with frequency multiplier can be used with additional loop amplifiers and phase shifters, or adding an external source at each harmonic component.

The equation 2.23 and 2.24 presents a theoretical point of view for the feed-forward and open-loop, respectively. In both cases it is assumed that s-matrix of the DUT is known, although it still valid only if the DUT operates in small signal where its behaviour is linear. Alternatively, for the large-signal characterization the information of the unknown  $b_2$  is necessarily obtained through a measure equipment, helping in the determination of the reflection coefficient based on the characterization of the system. Moreover, helping in this task, it is also used a convergence algorithm such as Newton-Raphson [5] to properly set the desired reflection coefficient at the DUT's port, which is usually achieved with 5-10 iteration.

For a more detailed information about the open-load pull technique the reader is referred to [24, 25, 26].

### 2.4.4 Hybrid load-pull system

The hybrid load-pull system is normally recommended for highly reflective load-pull applications, it combines the passive and active techniques in order to overcome the associated problems of both, despite increasing its complexity.

In Fig. 2.23, it is shown an example of the hybrid load-pull application that combines the passive tuners with active open-loop load-pull setup, the VNA based approach allows to monitor not only the fundamental but also the harmonic components of the microwave transistor if the case.

Moreover, the passive part of the system is composed by a source and load impedance tuner that is normally used to reflect the high power at the fundamental frequency and therefore requires a smaller signal to be injected, i.e, it acts as pre-match network of the DUT. In addition, the active part, in this particular case, is composed by an additional signal source and amplifier which is placed at the tuner output port, supporting the needed amount of power that is necessary to overcome the inherent losses of the passive network and synthesize the desired load impedance.

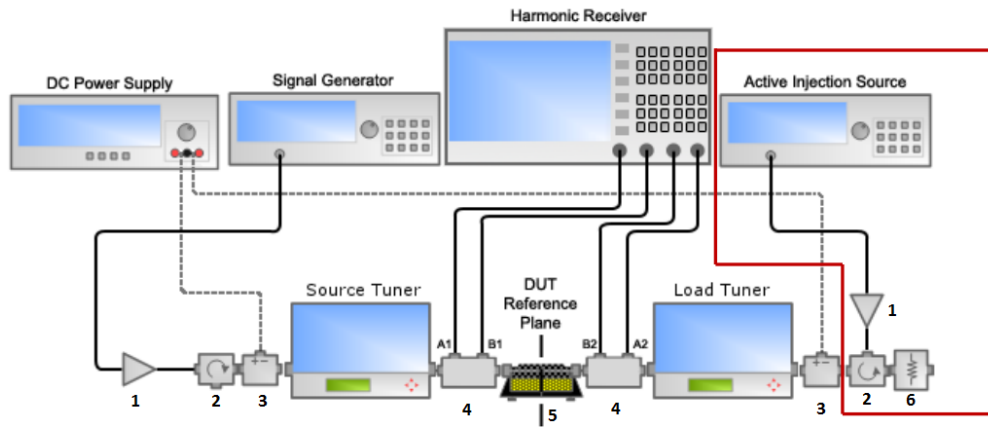


Figure 2.23: Hybrid-Active fo load-pull system copied from [28]

- | 1 - amplifier | 2 - isolator | 3 - bias tee | 4 - dual coupler | 5 - fixture | 6 - attenuator|

In the hybrid technique, the passive and fundamental load tuner is augmented by an active source, while the mechanical positions of the tuner are used as a pre-match decreasing the required load-pull power ( $P_{LP}$ ). The requisite of an external high-power amplifier is diminished, maintaining the needed high reflection coefficient.

This setup is cheaper than an active open-loop load-pull system, once it requires less  $P_{LP}$  to be injected at the DUT output port in order to emulate the desired load impedance, while accessing the DUT performance parameters.

## 2.5 Comparison of the different kinds of load-pull setups

Table 2.4, summarizes the main characteristics of the active and passive method, not covering the hybrid load-pull due to the vast possible sets that can be obtained with this technique.

The closed-loop technique possess the lowest reflection coefficient range, when compared with any active technique, as it requires a flat gain of the loop amplifier to avoid oscillations. On the other hand, the feed-forward and the open-loop techniques are not restricted to a flat gain condition, however the feed-forward technique might oscillates under some conditions, which makes the open-loop the most robust active technique in terms of oscillation.

Table 2.4: Comparison between the passive and active techniques. Based on [5].

	<b>Passive</b>	<b>Active (Closed-Loop)</b>	<b>Active (Feed-Forward)</b>	<b>Active (Open-Loop)</b>
<b>Load-Pull Reflection Coefficient Range</b>	$ \Gamma  < 0.98$	$ \Gamma_{max}  = 1$ $ \Gamma_{min}  = Limited$	$ \Gamma_{max}  = 1$ $ \Gamma_{min}  = 0$	$ \Gamma_{max}  = 1$ $ \Gamma_{min}  = 0$
<b>VSWR Range</b>	100:1	Active (Lowest)	Active (Middle)	Active (Highest)
<b>Power Range (CW)</b>	500 W	400 W	350 W	200 W
<b>Possibility of the System Oscillates</b>	None	High	Low	None
<b>Bandwidth</b>	Narrow band	Narrow-band	Broader band	Broader band
<b>Modulation Bandwidth</b>	300 MHz	Not supported	---	120 MHz
<b>Harmonic Control</b>	Easy	Easy	Difficult	Difficult
<b>On-Wafer Measurements</b>	The vibration of probes causes additional losses	Easier	Easier	Easier
<b>Major Drawback. Hard at ...</b>	High frequency	High Power	High Power	High Power
<b>Relative System Cost</b>	1	1.5	1.5	3
<b>Measurement Speed</b>	200 ms/point	1 ms/point	1 ms/point	1 ms/point

## 2.6 Reflection coefficient enhancement techniques

The traditional LPS is a reliable and low cost setup that uses mechanical tuners for the high-power device characterization. However, it typically possess a limited range of reflection coefficient due to the inherent losses of the system caused by the couplers, cables and fixture that exists between the DUT and tuners. It delimits the maximum achievable VSWR requiring large amounts of power to properly characterize the DUT.

This section presents the most common techniques used to overcome the already mentioned problems associated with the passive load-pull system. A short description of the pre-matched tuning enhancement, the enhanced loop, the quarter-wave impedance transformation and the broadband impedance transformation is presented, allowing to increase the maximum achievable reflection coefficient at the same time that it reduces the needed  $P_{LP}$  to assist the DUT performance parameters [5].

### 2.6.1 Pre-matched

The pre-matching technique utilizes two independent RF probes that are inside of the same tuner, being usually called the pre-matching and tuning probes. The probes are placed side-by-side on a central conductor as the equivalent representation shown in Fig. 2.24.

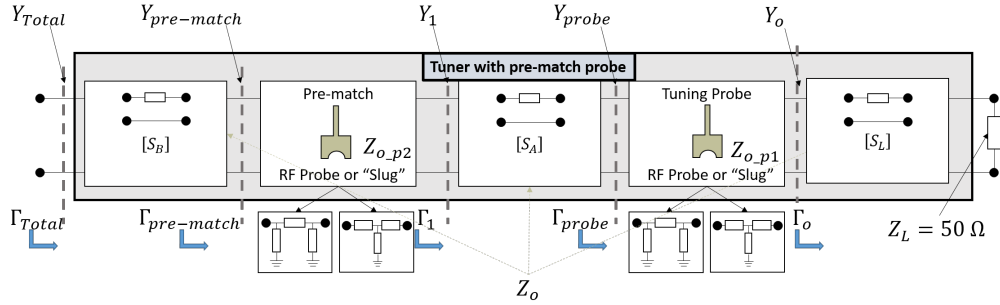


Figure 2.24: Circuit model of a mechanical tuner with pre-match and tuning probe.

In this type of tuner to enhance the tuning range, the two RF probes are combined to produce high levels of reflection coefficients, when compared with a single tuner. Its mathematical formulation of how the reflection coefficients are normally synthesized is shown in the following equations.

$$\Gamma_{total} = S_{11}^B + \frac{S_{21}^B S_{12}^B \Gamma_{pre-match}}{1 - S_{22}^B \Gamma_{pre-match}} \quad (2.25)$$

$$\Gamma_{pre-match} = \frac{Y_0 - Y_{pre-match}}{Y_0 + Y_{pre-match}} \quad (2.26)$$

$$Y_{pre-match} = Y_{probe} + Y_0 \left( \frac{1 - \Gamma_1}{1 + \Gamma_1} \right) \quad (2.27)$$

$$\Gamma_1 = S_{11}^A + \frac{S_{21}^A S_{12}^A \Gamma_{probe}}{1 - S_{22}^A \Gamma_{probe}} \quad (2.28)$$

$$\Gamma_{probe} = \frac{Y_0 - (Y_{probe} + Y_0)}{Y_0 + (Y_{probe} + Y_0)} = \frac{-Y_{probe}}{Y_{probe} + 2Y_0} \quad (2.29)$$

## 2.6.2 Enhanced loop

The enhanced loop setup is a simple passive load-pull system that additionally possess a circulator and an cable with a certain length  $L_2$ , as shown in the example presented in Fig. 2.25 (a).

The loop is attached to a low-loss impedance tuner and the reflection coefficient present at the DUT plane, can be obtained from simplification of the signal flow graph shown in Fig. 2.25 (b), which results in Eq. 2.27 [28].

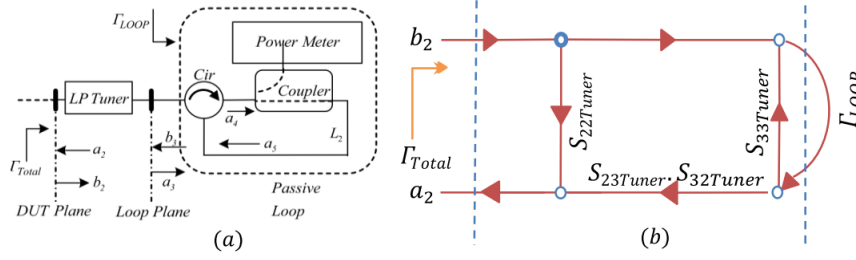


Figure 2.25: Functional diagram (a) and the signal flow of an enhanced load-pull setup (b) copied from [29].

$$\Gamma_{Total} = \frac{a_2}{b_2} = S_{22Tuner} + \frac{S_{23Tuner}S_{32Tuner}\Gamma_{Loop}}{1 - S_{33Tuner}\Gamma_{Loop}} \quad (2.30)$$

where

$$\Gamma_{Loop} = \frac{a_3}{b_3} = |\Gamma_{Loop}|e^{-2j\beta L_2} \quad (2.31)$$

The  $\Gamma_{Loop}$  is the reflection coefficient generated by the passive loop presented at the output port of the tuner that is successively transformed in the  $\Gamma_{Total}$ , being this the impedance seen by the DUT at its output port. Figure 2.6 shows a comparison between an pre-matched tuner, as blue circles, and the low loss tuner using the tuning enhanced loop, represented as a the red circles. Notice that the maximum reflection coefficient is increased with the tuning enhancement technique.

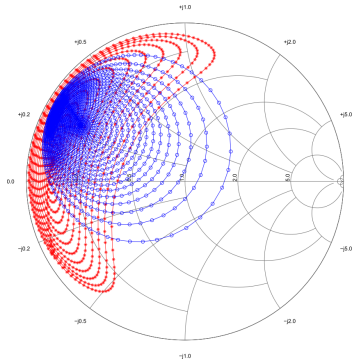


Figure 2.26: Comparison of the maximum achievable reflection coefficient between a commercial pre-matched tuner and a loop enhanced tuner at 1.8 GHz base on [29].

### 2.6.3 Quarter-wave impedance transformation

The quarter-wave impedance transformation is a technique used to increase the accuracy and the maximum achievable reflection coefficient, as shown in Fig. 2.27. The enhanced loop and pre-match techniques are limited in terms of accuracy due to its reference characteristic impedance that is typically 50 Ohms. In addition, the employment of this technique allows to diminish the uncertainty on VNA measurements performed at the border of the Smith chart.

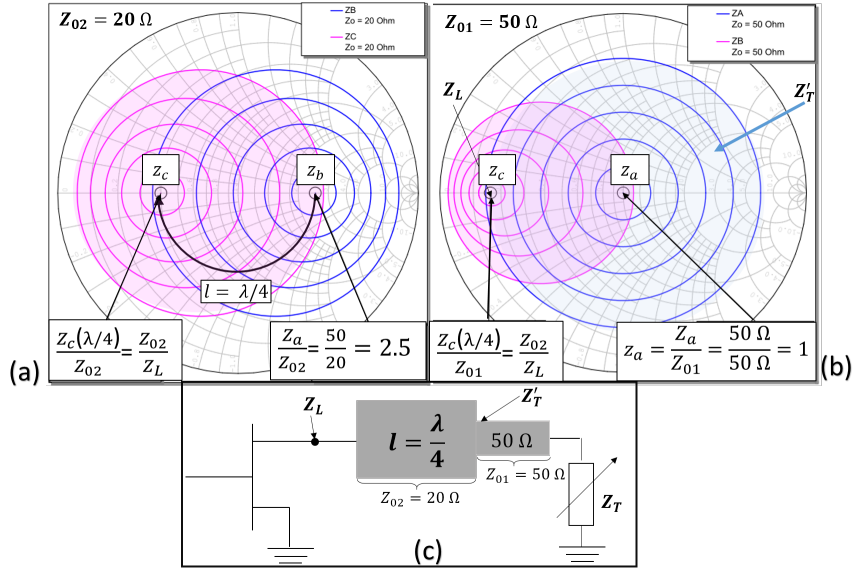


Figure 2.27: Illustration of the quarter-wave transformer technique in (c). The  $Z'_T$  represents the synthesizable loads that are inside of the light blue circles. Moreover, the  $Z_L$  are the loads presented after the quarter-wave transformation that are inside of the light purple circles. Those ones that possess a characteristic line impedance of 50  $\Omega$  are depicted in (a) and those ones that possess a characteristic line impedance of 20  $\Omega$  are represented in (b).

The major benefit of the quarter-waver transformation technique is the modification of the reference impedance, which consequently reduces VSWR for the synthesis of a desired reflection coefficient. In addition, the chances of potential damage to the DUT, tuner and measurement equipment are diminished, since the required  $P_{LP}$  to operate the load pull system for the same target impedance have also been reduced.

Figure 2.28 shows two fixtures with  $\lambda/4$  transformers, the (a) without biasing and (b) with the drain biasing. The purpose of (b) is to accelerate the design process.

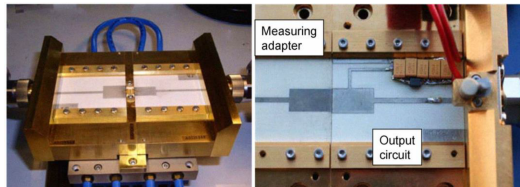


Figure 2.28: Fixtures with  $\lambda/4$  - transformers for load-pull measurements (a) no-bias (b) bias. Copied from [30].

#### 2.6.4 Broadband impedance transformer

The broadband impedance transformation overcomes the very narrow bandwidth characteristic associated with the quarter-wave transformer which is only 5 to 10 percent of the carrier frequency. Consequently, the quarter-wave transformer technique is unusable in applications that involve harmonic characterization.

The also called multi-section impedance transformation allows the synthesis of fundamental and harmonic impedances with an appropriated tuning range that also reduces  $P_{LP}$  required for the high reflective load-pull applications.

The tapers are multi-section transformers, which possess different characteristic impedance in each section. In theory, the infinite series of sections form a continuously tapered line, being the most commonly used linear, triangular, exponential and Klopfenstein. The criterion of choice mainly depends on the impedance transformation, which, for some applications, cannot exceed an established length of the transformer [30].

The linear taper is the simplest one and its design is rapidly obtained but its disadvantage is the required length for its implementation. The triangular and exponential taper are slightly complex but present a better response in impedance transformation, being the presented reflection coefficient lower than the one of the linear transformer, for the same correspondent length.

The best taper is undoubtedly the Klopfenstein once it possess the shortest taper length for the maximum reflection coefficient specification, presenting the lowest in band reflection coefficient. However, its formulation and design relies on the more complex Bessel functions.

Figure 2.29 shows an example from Maury microwave test fixture that utilizes Klopfenstein



Figure 2.29: Maury load pull low-loss test fixture. [32]

taper, using APC 7 mm connector, which presents a good repeatability. In addition, coolers are used to stabilize the DUT temperature. More information about this type of structures and related theory about multi-section transformers can be found in the Pozar book [33].



## Chapter 3

# Design and implementation of an automated tuner-based load-pull system

This chapter presents a concise description of the built setup and all steps regarding the design, implementation and validation of the automated load-pull system.

### 3.1 Introduction

The load-pull system is an essential tool utilized to assist power amplifier design, in particular to determine the ideal matching impedance for gain, efficiency or power.

The built passive tuner-based setup consists of one fundamental load tuner, one signal source, a test fixture, a dual channel power meter, a power supply, a spectrum analyzer, a RF test set (including cables, attenuator, filter, couplers and power dividers) and a VNA.

The tuner is selected based on its FoM such as repeatability, resolution and tuning range and distribution of the synthesizable reflection coefficients. This helps to achieve high levels of impedance accuracy, to obtain a vast number of impedances states and synthesize high levels of reflection coefficients covering, in this way, the whole Smith chart.

The implementation of this load-pull system involved 4-four steps described as follows:

- Characterization - to find out the s-parameters of each system component, including the tuner for a wide range of mechanical positions.
- Assembly of the system components - to establish a load-pull measurement setup.
- Calibration of the load-pull measurement setup - to find out, based on the characterization files, the inherent losses of the system and to shift the reference plane to the device packaging ports.
- Measurement of relevant data at the calibrated reference planes - gives us the  $P_{in}$  and  $P_{out}$  after de-embedding the losses that are associated to the measured data.

Then, knowing the DC supplied ( $P_{DC}$ ),  $P_{in}$  and  $P_{out}$  the PA FoM such as gain, PAE and drain efficiency ( $\eta_D$ ) can be easily calculated.

## 3.2 Diagram of the automated load-pull system

Figure 3.1 presents a diagram of the whole implementation process of the automated load-pull setup. First, a calibration of the VNA is performed and then a characterization of each passive system component is done. This procedure is treated in the upcoming subsections, specifically 3.3 and 3.4.

Furthermore, it is necessary to check the repeatability of the automated load-pull system under two different scenarios to prove its accuracy and viability. The first test is necessary to verify the tuner repeatability, where the results should correspond to the data sheet of the tuners manufacturer, which states that the tuner should present at least a repeatability of -50 dB at a certain range of frequencies. Afterwards, in the second test a fixture and a load block are attached to the port 1 and 2 of the tuner, respectively, as it can be seen in Subsection 3.6 and in Fig. 3.12.

The used methodology allows to systematically track and identify the sources of error, along each step of the system characterization that is indicated in the diagram of Fig. 3.1. A more detailed information regarding the load-pull system verification will be given in the following sections.

The last routine is responsible to perform the measurements and store all the relevant information. This load-pull data is saved in three different directories and forms. The first directory contains the figures of each saved load characterization, the second is a file that contains all the relevant data regarding the measurements. Finally, the third directory stores a file with the AWR/MWO file format containing the DUT load-pull characterization which includes all the tested load impedances.

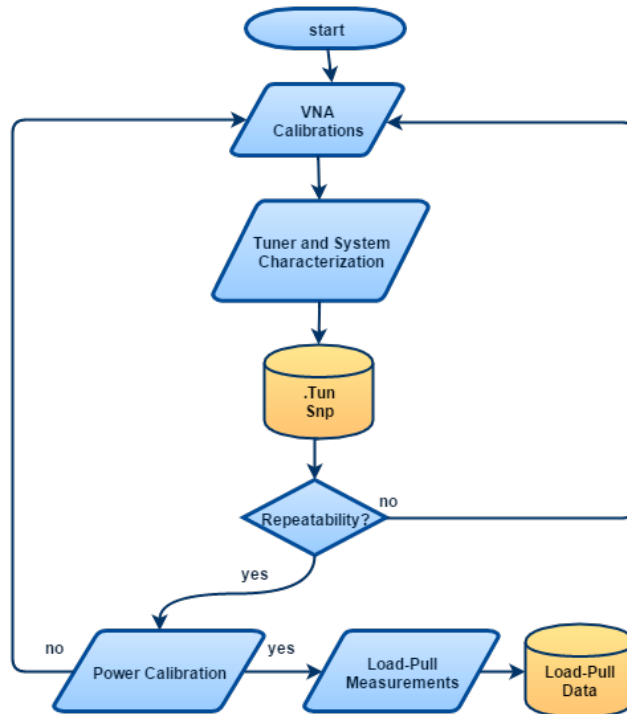


Figure 3.1: Automated load-pull system implementation flow chart.

### 3.3 System description

The built load-pull system is composed by 3 fundamental blocks: Source Block, Load Tuner, and Output Block. Moreover, four additional instruments are required: power meter, DC power analyzer, PC control and the VNA.

A block diagram of the automated load-pull system is shown in Fig. 3.2. The DUT is fed from a high-power microwave source, which is achieved combining the signal generator and driver amplifier. The load impedance is controlled by an automated mechanical tuner and the measurement data is generated by using a dual channel power meter. The DC power supply is necessary to provide the gate/base bias of the transistor and feed the drain/collector power.

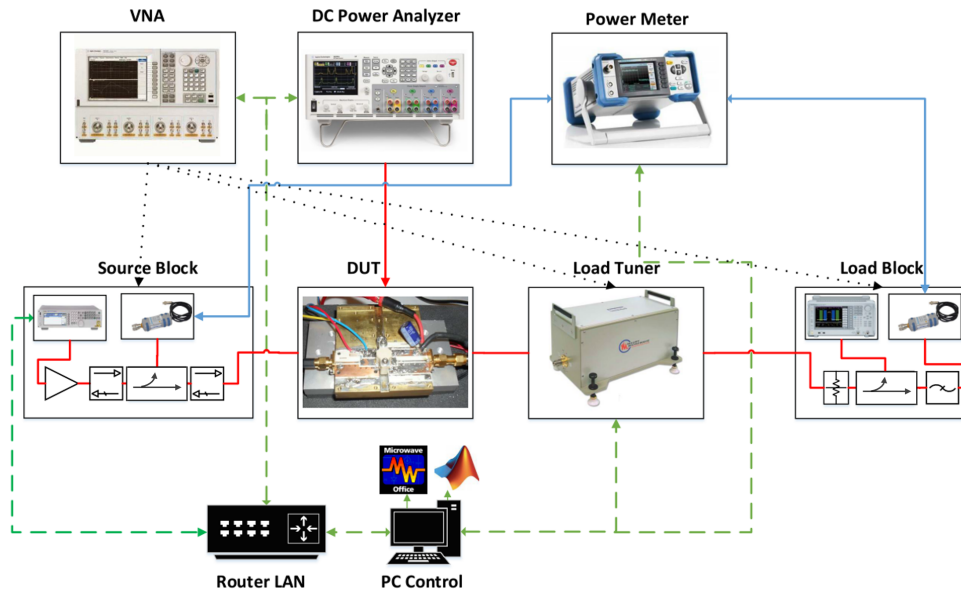


Figure 3.2: Scheme of the built automated load-pull system.

An additional external trigger connection, not displayed on the Fig. 3.2, guarantees a synchronous measurement.

- The black dotted lines denote the calibrated VNA characterized blocks.
- The green dashed lines indicate the LAN connection utilized to remotely control the de-vices.
- The red full lines are the illustrative flow of DC and RF power.
- The blue full lines are used to represent the physical interconnection of the power sensor and power meter.

It is important to notice that the power meter is only monitoring the (uncorrected) power at each system block where it is placed. The s-parameters obtained from the characterization are then used to determine and correct the measured power of the amplifier, via the available, absolute power calibration and transducer gain formula to effectively measure the power being injected and delivered by the DUT.

### 3.3.1 Source block

The source block is composed by a vector signal generator (VSG) used for generating the signal and driver for adjusting the power level. This input network is composed by the following instruments and components:

- Signal Generator enables the performance assessment of the amplifier under a specific type of stimuli.
- Driver Amplifier is utilized to boost the RF signal, once it is necessary to supply the needed amount of power that leads the DUT to the desired compression gain.
- Isolator at port 1 is used to guarantee that the driver right after the VSG sees a matched load, regardless on the input impedance of the DUT.
- Coupler allows to sample part of the incident wave that is travelling into the DUT.
- Power sensor A is part of the measurement system that provides the uncorrected information about the  $P_{in}$  magnitude.

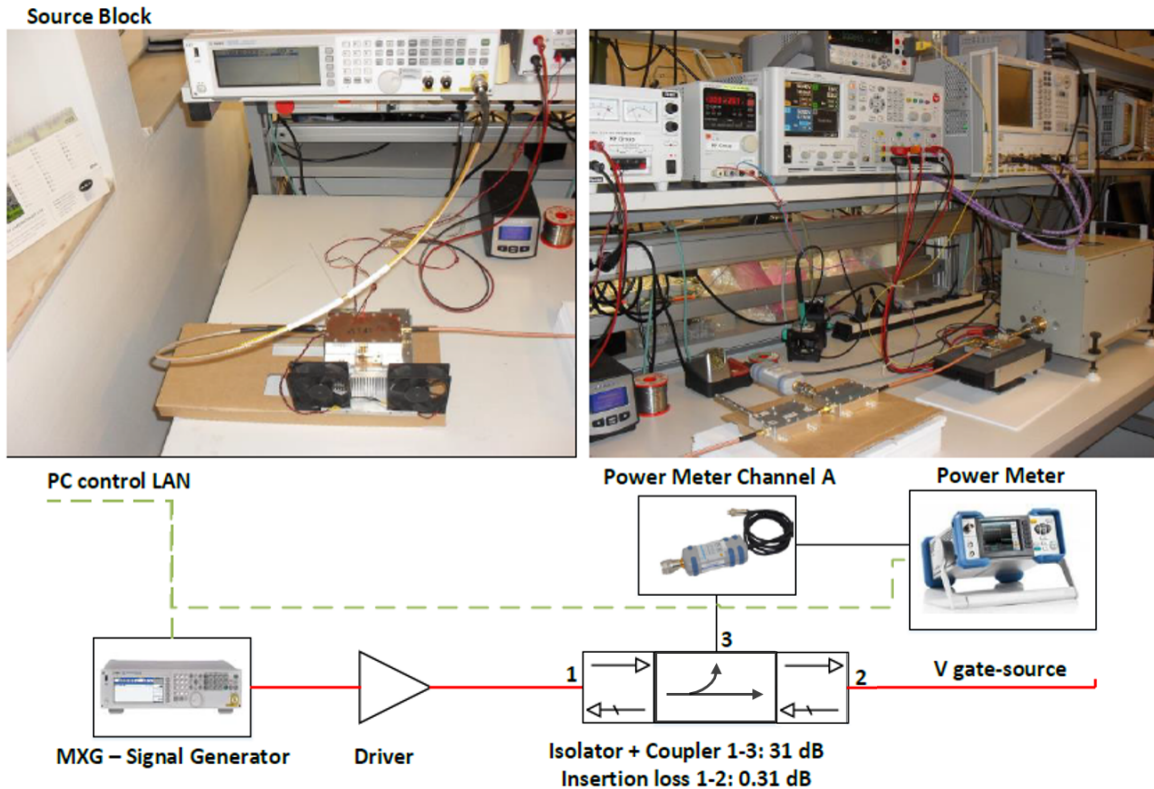


Figure 3.3: Functional diagram of the system source block.

This kind of application dissipates a lot of heat, which justifies the usage of cooler units to maintain an average temperature of the DUT and driver.

### 3.3.2 Load block

The load block is composed by an attenuator, a coupler, a low pass filter and a power sensor B. Additionally, a spectrum and time domain analyzer allows to visually inspect the waveform of the incoming signal. The output network is placed after the tuner and is comprised by:

- Attenuator is used to ensure that less power flows to the power sensor preventing the instrument from being damaged and allowing the performance assessment of the amplifier.
- Coupler is an additional component, utilized to sample part of the signal that is going to be measured by the power meter at the same time the waveform is being monitored.
- Low pass filter is here used to ensure that only the fundamental component is being measured by the power sensor.
- Spectrum and time domain analyzer is used to check if the desired stimuli of the DUT has the correct waveform, guaranteeing that no waveform distortion is caused by the automatic leveling control (ALC) of the Signal Generator.
- Power sensor B is part of the measurement system that provides the uncorrected information about the  $P_{out}$ , magnitude.

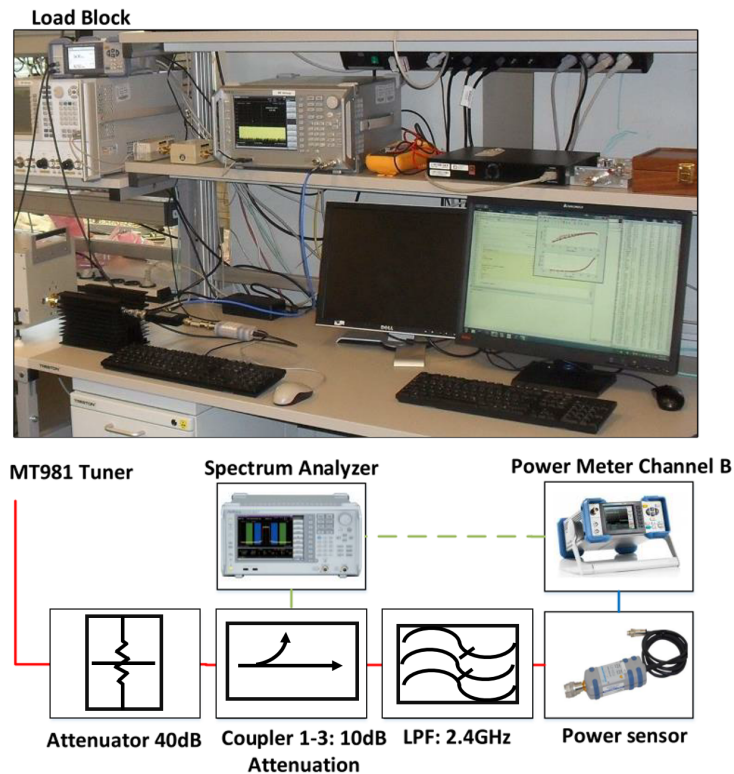


Figure 3.4: Functional diagram of the system load block.

### 3.3.3 Load tuner

The passive tuners are typically of the slide screw type. They are usually composed by a slab line enclosed by two parallel ground planes with a centred main line and a reflective element (a conductive 'probe') [32]. When this probe is fully retracted the tuner presents an line impedance of approximately  $50 \Omega$ .

Likewise a stub, when the probe moves closer to the line, a capacitive effect is inserted. As a result the impedance presented by the tuner is modified, corresponding to the length of line between the probe and the tuner input.

As the probe position changes along the vertical direction, it modifies the presented reflection coefficient magnitude. Alternatively, any movement along the longitudinal axis modifies the presented phase of the reflection coefficient.

The load tuner is the element present in the output matching network that is responsible to its reconfiguration. This makes the  $\Gamma_L$  controllable, only by setting the tuning probe position along the longitudinal and vertical axes of the slab line.

The tuner model MT981EU has a carriage structure that supports 2 probes, allowing a vertical movement of this reflective element along the line, which is automatically controlled by precise stepper motors.

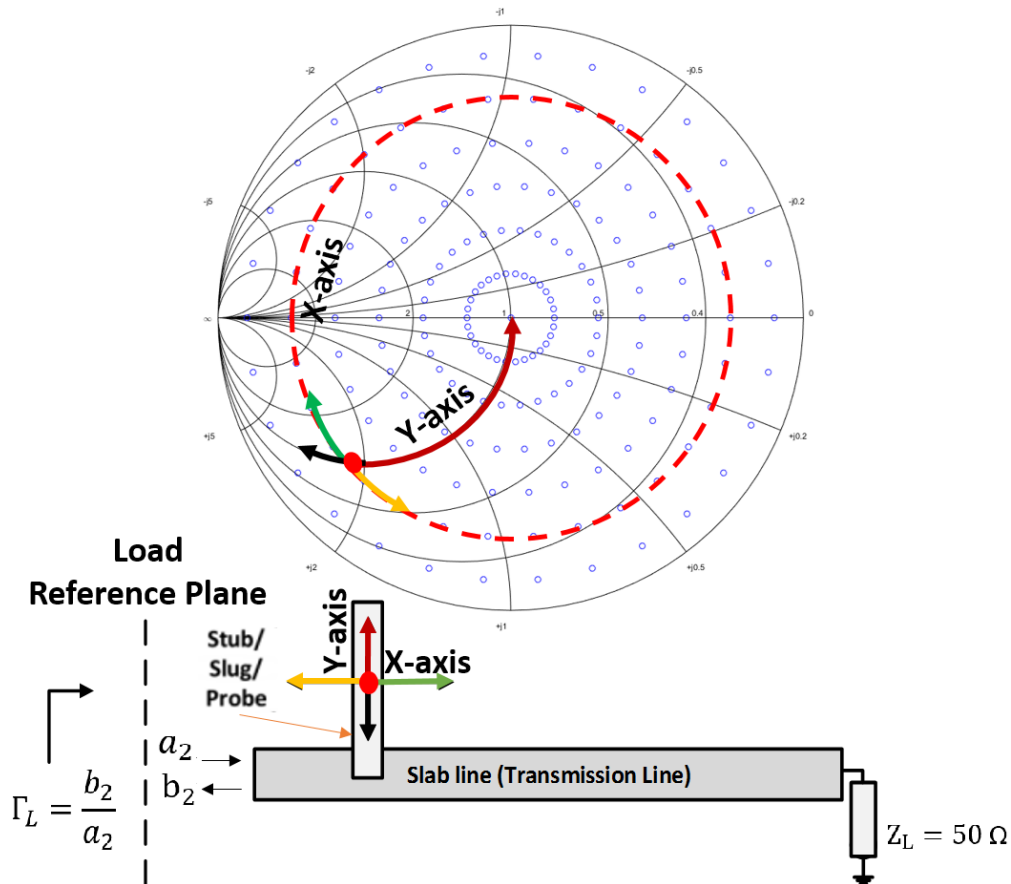


Figure 3.5: Illustrate how the reflection coefficient of a slide screw tuner change, with a conductive probe moving in two directions within a slab line, being represented on the admittance smith chart.

### 3.4 Characterization of the load-pull system

The characterization of the load-pull system consists in creating one-port or two-port s-parameter files of each passive element presented in the source and load blocks. As a result, a file with .tun extension, is created. This file contains the tuner characterization, which is composed by the set of s-parameters for each of the tuner mechanical positions and frequencies, respectively.

During the measurements it is known that information about the power is 'uncorrected', requiring a characterization of the system to mathematically remove the inherent losses of the input and output network. As a result the effective  $P_{in}$  and  $P_{out}$  are achieved. For such purpose, a proper calibration of the VNA is required before any system component characterization. It removes all systematic errors arising from the inherent directivity, mismatch and cross-coupling of the measurement equipment.

For this reason, I decided to explain how the s-parameters of system components, tuner and fixture are obtained. In conclusion, the VNA calibration and system verification are described, where all the passive elements indicated by the dotted arrow in Fig. 3.2 were characterized by the short-open-load-thru (SOLT) VNA Calibration method.

### 3.5 Characterization of the system components

The reference planes of the characterized source block are shown in Fig. 3.3, by the ports 1, 2 and 3. The reference planes of the load block are the input port of the attenuator, output port of the coupler and the output filter port, shown in Fig. 3.4.

Each passive element of the source and load blocks were individually characterized, allowing them to be integrated in their respective blocks. As an implementation tool, the microwave office (MWO) was utilized to cascade the obtained s-parameter blocks, resulting in a new block for the input network and another for the output network.

The s-parameters shown in Fig. 3.6 are the result of a 3-port conversion into a 2-port of the input network characterization, which the conversion of output and input network are explained in Appendix D.1 and D.2, respectively.

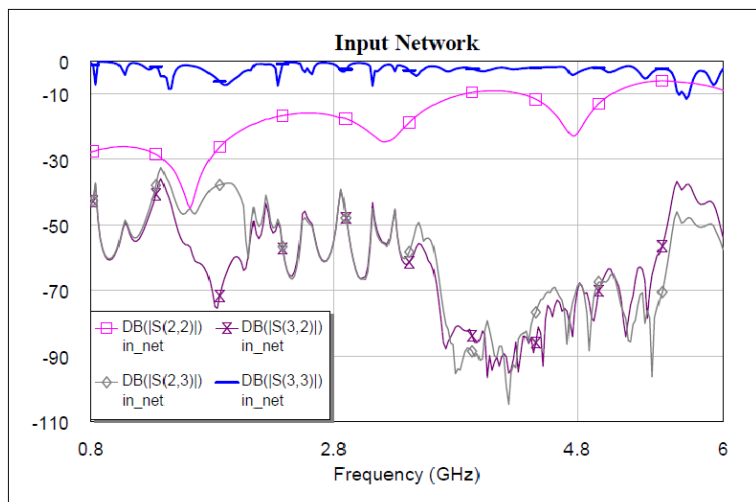


Figure 3.6: Equivalent 2-port of the input network of the LPS.

### 3.6 Characterization of tuner

The tuner characterization is performed to determine a set of s-parameters, respectively to each of its mechanical positions at each particular frequency. This information is later on utilized by interpolation routines in order to synthesize the desired new reflection coefficient.

When a certain target impedance is chosen to characterize the amplifier, it might happen that this load the impedance falls between pre-calibrated states, as shown in Fig. 3.7. In order to achieve such level of accuracy, a dynamic-link library (DLL) function is used to interpolate between the closest pre-characterized impedances and determine the new physical X and Y mechanical position of the desired impedance and its respective s-parameters. In order to improve the accuracy, it is necessary to increase the numbers of pre-characterized positions.

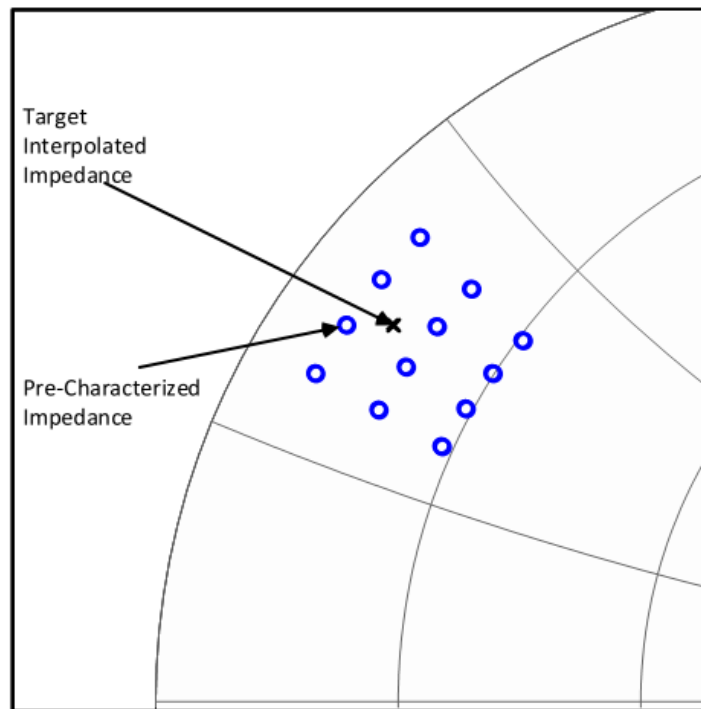


Figure 3.7: Interpolation result based on the pre-characterized load impedances.

The replacement of any adapter will require a new tuner characterization. Thus, it is highly recommended to characterize the tuner without any additional component attached, such as any bias tee, giving more flexibility for future changes on the system topology.

Furthermore, the characterization precision is verified by setting the tuner for an arbitrary impedance near to the centre and then near to edge of the Smith chart over the whole range of  $2\pi$  radians phase. This procedure must satisfy the condition in which the error is less than 0.2% in the magnitude and 0.1 deg in the phase. Any value worse than that indicates a problem in the calibration and the characterization procedure must be repeated. The goal of this requirement is to ensure a level of precision around -50dB, which corresponds to a worst case deviation in the real and/or imaginary part of the reflection coefficient of less than 0.003.

### 3.6.1 Characterization of the fixture

When dealing with high-power device characterization the load-pull system must possess a mechanism that minimizes the VSWR and, at the same time, enables to synthesize high reflection coefficients, without any risk of damage for the instruments or even the DUT. The used quarter-wave transformer technique satisfies these requirements allowing to 'pre-match' the device nearly to its optimum impedance region over the Smith chart.

The thru-reflect-line (TRL) method of VNA calibration is used for non-coaxial reference planes such as the DUT microstrip test fixture. This method presents a better effective directivity, source match and load match compared with the SOLT calibration and helps to acquire the needed information about s-parameters of each fixture halves.

The TRL standards are generally easy to fabricate requiring only to know the impedance, approximately the electrical length of the line standard and the reflect standard that can be any high reflection devices like shorts or opens [33].

### 3.6.2 VNA calibration and verification

The VNA calibration is a procedure necessary to remove errors presented on the measurement system which are repeatable and usually predictable over time and temperature.

The standard calibration kit utilized in this work, the Agilent 85031B 7mm and the E-Cal N4431-60008, are only responsible to remove the systematic errors. They allow to perform a complete SOLT calibration when they are combined with the Unknown-thru calibration, since some connectors might differ from each other, as is the case, for example, of the APC 7 mm and a TYPE(N) 50 connector types. There are three types of measurement errors:

- The **systematic errors** occur due to imperfections of the test equipment, those errors are caused by directivity, crosstalk, source and load impedance mismatches and frequency response. The **directivity and crosstalk** exist due to signal leakage. The **source and load impedance mismatches** are directly related with the unavoidable reflections in the test set. In addition the **frequency response** is caused by the deficient reflection and transmission tracking of the test receivers over frequency.
- The **random errors** presented in the measurement system are usually generated by the instrument noise (e.g. intermediate frequency (IF) noise floor, and the sampler noise), connector and switch repeatability. The presented noise errors can be reduced by narrowing the IF bandwidth, increasing source power, or even using trace averaging.
- The **drift errors** are not removable but still possible to minimize, only by setting a stable ambient temperature for the test environment.

The **verification** is performed after the calibration is done, in order to observe if the s-parameters correspond to the expected ones. As a practical rule, a good calibration holds the following condition: when a thru connection is tested, the measured magnitude of  $S_{21}$  and  $S_{12}$  must to be as close as possible to 0 dB and the phase of  $S_{11}$  should be at a mili-degree of resolution, meaning that the ports 1 and 2 are matched to 50 Ohms.

The  $S_{21}$  isolation is obtained by connecting two loads, one on port 1 and one on port 2. Next, it is measured the magnitude of  $S_{21}$  and check if it is less than the specified isolation (typically less than  $-80$  dB). Another typical procedure is to leave the source port 1 open and verify if the  $S_{11}$  magnitude is near to 0 dB (within about  $\pm 1$ dB) [34].

## 3.7 MATLAB routines

In this section I will explain the main details regarding the MATLAB routines implementation. The source code developed in this work can be found in the Appendix A.

### 3.7.1 Pre-characterization

This routine is responsible to store in memory the s-parameters, X and Y mechanical positions and frequency at a user-defined number of points. Another important requisite for this routine is to have an even distribution of characterized impedances over the Smith chart, so that the future interpolated impedances exhibit similar accuracies.

### 3.7.2 Absolute power calibration

The absolute power calibration routine is mainly used to correct the removal of the inherent losses of the LPS from the measured data, but it is also used as a resource to determine the driver gain and, thus, control the available source power.

The so-called  $\Delta G_t$  factor is utilized to account for the error in the predicted losses, consisting in the comparison between measured and predicted transducer gain,  $G_t$ . This method involves measuring the gain of our system with all LPS components including the DUT microstrip fixture as thru connection, where the centre of the fixture is used as reference plane while the tuner is swept through a load-pull [35].

The prediction of  $G_t$  is based on the s-parameters that constitute the input and output network of the load-pull system characterization, including the DUT test fixture, and is given by the following equation [36].

$$G_t = \frac{P_L}{P_{avs}} = \frac{1 - |\Gamma_S|^2}{|1 - \Gamma_{IN}\Gamma_S|^2} |S_{21}|^2 \frac{|\Gamma_L|^2}{|1 - S_{22}\Gamma_L|^2} \quad (3.1)$$

where, the  $\Gamma_S$  and  $\Gamma_L$  are the respectively source and load blocks that are seen by the DUT microstrip fixture at its centre. The shown s-parameters belongs to the DUT fixture, and the  $\Gamma_{IN}$  input reflection coefficient is obtained with the following equation:

$$\Gamma_{IN} = S_{11} + \frac{S_{21}S_{12}\Gamma_L}{1 - S_{22}\Gamma_L} \quad (3.2)$$

The used DUT test fixture for the absolute power calibration is a thru connection and its s-parameters are represented by the following expression.

$$S_{THRU} = \begin{pmatrix} S_{11} & S_{12} \\ S_{21} & S_{22} \end{pmatrix} = \begin{pmatrix} 0 & 1 \\ 1 & 0 \end{pmatrix} \quad (3.3)$$

by replacing the terms of the equation 3.3 into 3.2 results in

$$\Gamma_{IN} = \Gamma_L \quad (3.4)$$

and consequently it simplifies the equation 3.1, where  $G_t$  becomes

$$G_t = \frac{(1 - |\Gamma_S|^2)(1 - |\Gamma_L|^2)}{|1 - \Gamma_L\Gamma_S|^2} \quad (3.5)$$

Furthermore, the  $P_{out}$  is determined through a proper calculation of the incident and reflected travelling waves at the DUT reference plane that is obtained through a proper characterization of each of the shown blocks represented in Fig. 3.8. In addition,  $\Gamma_{pwr}$  represents the reflection coefficient imposed by the power meter B, acting as a load termination of the total two-port network. This network and its characterized s-parameters provide the relation between the power that is being read by the power meter and the  $P_{out}$  of the device as shown in the following equations.

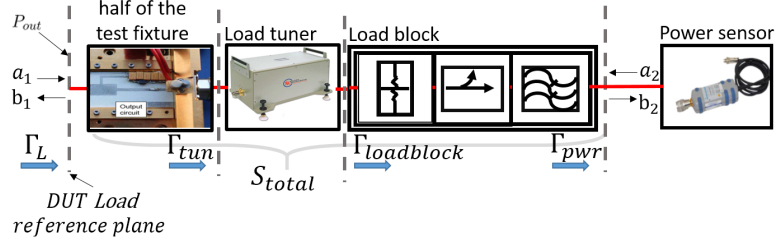


Figure 3.8: Representation of the output network of the developed load-pull system.

The power meter readings correspond to the reflected travelling wave seen by the output network,  $b_2$ .

$$\begin{bmatrix} S_{11_{total}} & S_{12_{total}} & -1 & 0 \\ S_{21_{total}} & S_{22_{total}} & 0 & -1 \\ 0 & \frac{-1}{\Gamma_{pwr}} & 0 & 1 \\ 0 & 0 & 0 & 1 \end{bmatrix} \begin{bmatrix} a_1 \\ a_2 \\ b_1 \\ b_2 \end{bmatrix} = \begin{bmatrix} 0 \\ 0 \\ 0 \\ K \end{bmatrix} \quad (3.6)$$

$$\underbrace{\begin{bmatrix} S_{21_{total}} & S_{22_{total}} & 0 & -1 \\ 0 & \frac{-1}{\Gamma_{pwr}} & 0 & 1 \\ S_{11_{total}} & S_{12_{total}} & -1 & 0 \\ 0 & 0 & 0 & 1 \end{bmatrix}}_A \underbrace{\begin{bmatrix} a_1 \\ a_2 \\ b_1 \\ b_2 \end{bmatrix}}_{\Theta} = \underbrace{\begin{bmatrix} 0 \\ 0 \\ 0 \\ K \end{bmatrix}}_B \quad (3.7)$$

The coefficients represented by  $\Theta$  are obtained by the ratio of A/B, which is presented by the following equations:

$$a_1 = K \frac{1 - S_{22_{total}} \Gamma_{pwr}}{S_{21_{total}}} \quad (3.8)$$

$$a_2 = K \Gamma_{pwr} \quad (3.9)$$

$$b_1 = K \frac{(S_{11_{total}} - \Gamma_{pwr} \Delta)}{S_{21_{total}}} \text{ where, } \Delta = S_{11_{total}} S_{22_{total}} - S_{21_{total}} S_{12_{total}} \quad (3.10)$$

$$b_2 = K = \sqrt{20 \frac{pwr_{meas} - 30}{10}}, \text{ where } \phi = 0. \quad (3.11)$$

Thus, the  $P_{out}$  at the output of the DUT reference plane is given by following equation :

$$P_{out}(dBm) = |a_1|^2 - |b_1|^2 = 10 \log_{10} \left( \frac{1}{2} |a_1|^2 (1 - |\Gamma_L|^2) \right) + 30 \quad (3.12)$$

,where  $\Gamma_L$  is given by Eq. 2.16 and its deduction is presented in the next section as well.

### 3.7.3 Load-pull measurements

Firstly, the tuner moves to the desired impedance, next the power supply is switched on feeding the DUT. Soon after, the RF output power of the VSG is turned on and, finally, the measurements are performed.

In the load-pull measurements, it was extracted absolute values of gain and efficiency, but it is simply presented its normalized values, because the absolute values are confidential. Moreover, the type of stimuli is classified, highlighting that is not the conventional CW.

Before the gallium nitride (GaN) microwave transistor characterization no matter which target impedance is chosen, a  $P_{in}$ , that conducts the device to its compression region is unknown. For this reason, it is necessary to utilize a safe level of  $P_{in}$ , commonly known as input back-off, in order to guarantee that the device does not go directly to its compression region, which can damage the DUT instantaneously.

One of the 114 loads utilized in the DUT characterization is the  $Z_L = 6.8895 + j2.8285 \Omega$ . A  $V_{GS} = -2.66$  V,  $V_{DS} = 50$  V,  $I_{DS} = 1.395$  mA at the frequency of 1800 MHz gives the result shown in Fig. 3.9 that is normalized by its maximum gain and drain efficiency.

Moreover, the RF output power is swept, step-by-step, recording a user-defined number of data points at each iteration. The routine is responsible to change the maximum peak power of the signal until the device meets a gain compression value of 3dB. In case this desired gain compression is not achieved, the MATLAB routine is prepared to store null values for the FoM where the desired compression is not achieved. Next, the tuner moves to another mechanical position and this same measurement procedure is repeated.

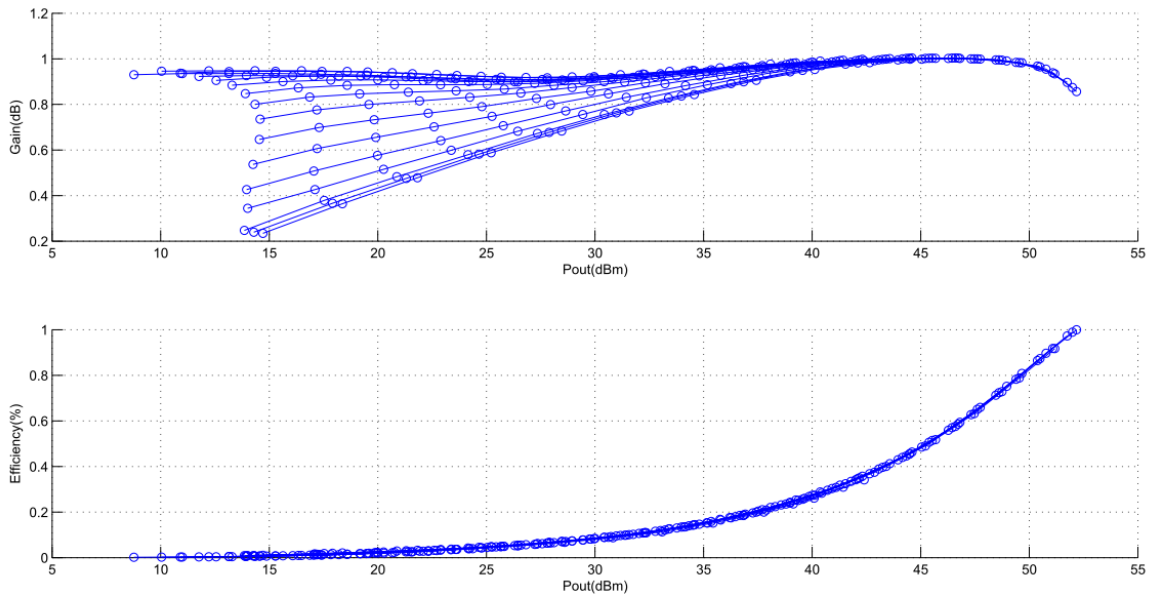


Figure 3.9: Normalized load-pull results obtained in the characterization of one load impedance, displaying the achieved gain(dB) and efficiency as function of  $P_{out}$ .

The other loads utilized in the DUT measurements can be found in Appendix C.

## 3.8 Automated load-pull system verification

The system verification is systematically performed and repeated, until the desired precision is achieved. The flow-chart in Fig. 3.1 illustrates how the tuning setup must be done. This section is dedicated to prove the reliability of this setup and present the achieved results.

The verification process starts with the tuner repeatability check, whose achieved results go down to around -50dB, which guarantees a precision of at least 3 decimal places.

Moreover, the system components were assembled and tested in two steps. First, only the tuner and then the load block and test fixture were tested. In addition, a prediction test is performed, which is similar to the repeatability test. This process consist in cascading the system s-parameter blocks and calculating what is going to be the  $\Gamma_L$  seen by the DUT.

For the prediction check, a test fixture was designed and created using a SubMiniature version A (SMA) connector at the input and the output. The fixture is composed by a  $50 \Omega$  line with a capacitor placed in middle of the line. This fixture will cause an impedance transformation, shifting the reference plane, which allows to understand and verify how precisely the impedance transformation can be done and how well the impedances can be measured by the VNA. In order to prove the reliability of this system, the impact of precision measurements and load-pull data results are also shown.

### 3.8.1 Repeatability test

As mentioned before in this work, the repeatability test is performed under two different scenarios. The first one is only intended for the tuner alone and its results can be seen in Fig. 3.10. The last repeatability test, which has all the output network elements assembled, is already a prediction test. The  $\Gamma_{Total}$  is the input impedance present at the transistor output terminal and results from the cascaded test fixture, tuner and load block. For the device characterization and prediction test the selected frequency was 1.8GHz.

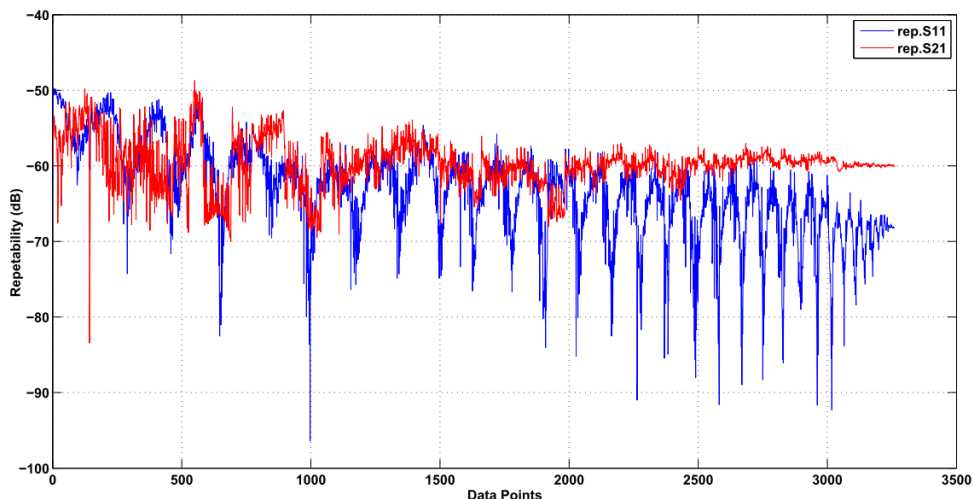


Figure 3.10: Obtained results of the repeatability check test at 1.8 GHz.

- $\Gamma_{TUN}$  Repeatability - Tuner

The calculation of  $\Gamma_{TUN}$  is equal to the  $\Gamma_{IN}$  of equation 3.2, it is verified that  $\Gamma_{TUN} \approx S_{11}$  when the VNA is calibrated. The VNA ports placed at the tuner reference plane acts as  $50\Omega$  source and load impedances, respectively. Thus, the  $\Gamma_{load_{block}}$  shown in Fig. 3.11 is approximately zero,  $\Gamma_{load_{block}} \approx 0$ .

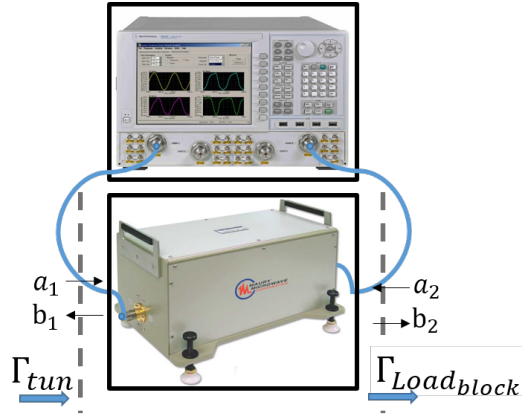


Figure 3.11: Characterization and tuner repeatability setup.

The high density of impedance states is required to achieve a good accuracy level, when using the impedance interpolation functions.

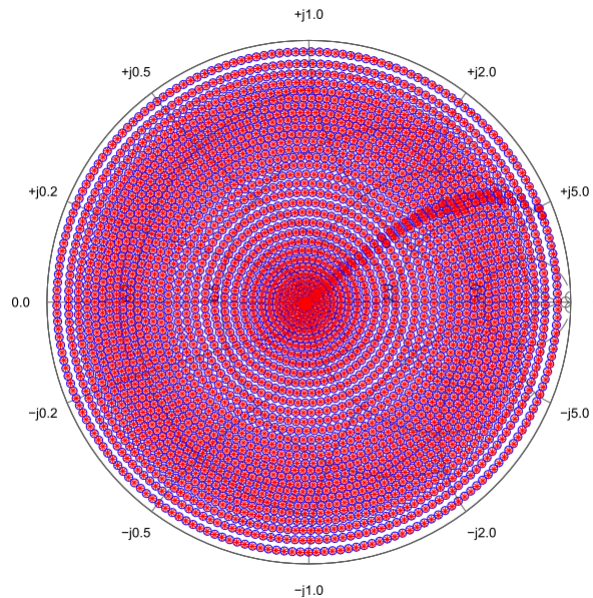


Figure 3.12: Displayed repeatability test over the Smith chart.

Figure 3.12 shows the repeatability results displayed over the Smith chart, where the red symbol '\*' indicates the second measurement and the blue 'o' indicates the first measurements. As can be observed, both symbols overlap, which graphically represent an achieved accuracy of at least -50dB, using  $50\Omega$  as reference impedance.

- $\Gamma_{TUN}$  Repeatability - Output Network

For the prediction test it is necessary beforehand to cascade all the s-parameters of the output network. As such, the following steps are described.

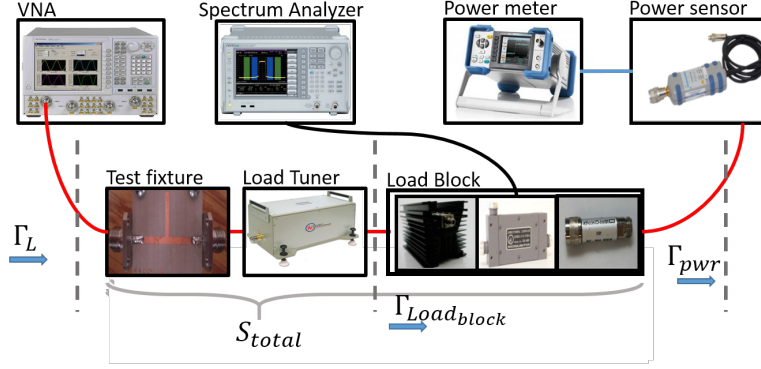


Figure 3.13: Scheme of the output network repeatability test.

First, the S-matrix of each element of the output network is transformed to a ABCD-matrix, as shown below:

$$\begin{bmatrix} A & D \\ B & C \end{bmatrix} = \begin{bmatrix} \frac{(1+S_{11})(1-S_{22})+S_{12}S_{21}}{2S_{21}} & Z_O \frac{(1+S_{11})(1+S_{22})-S_{12}S_{21}}{2S_{21}} \\ \frac{1}{Z_O} \frac{(1-S_{11})(1-S_{22})-S_{12}S_{21}}{2S_{21}} & \frac{(1-S_{11})(1+S_{22})+S_{12}S_{21}}{2S_{21}} \end{bmatrix} \quad (3.13)$$

Then, the DUT test fixture, the tuner and load block are cascaded by a simple matrix multiplication, resulting in a new ABCD-matrix.

$$\begin{bmatrix} A_{total} & D_{total} \\ B_{total} & C_{total} \end{bmatrix} = \begin{bmatrix} A_{fix} & D_{fix} \\ B_{fix} & C_{fix} \end{bmatrix} \cdot \begin{bmatrix} A_{tuner} & D_{tuner} \\ B_{tuner} & C_{tuner} \end{bmatrix} \cdot \begin{bmatrix} A_{loadblock} & D_{loadblock} \\ B_{loadblock} & C_{loadblock} \end{bmatrix} \quad (3.14)$$

Next, this ABCD-matrix is converted back to an S-matrix that contains the whole output network, as shown in the example below.

$$\begin{bmatrix} S_{11_{total}} & S_{12_{total}} \\ S_{21_{total}} & S_{22_{total}} \end{bmatrix} = \begin{bmatrix} \frac{A_{total}+B_{total}/Z_O-C_{total}Z_O-D_{total}}{A_{total}+B_{total}/Z_O+C_{total}Z_O+D_{total}} & \frac{2(A_{total}D_{total}-B_{total}C_{total})}{A_{total}+B_{total}/Z_O+C_{total}Z_O+D_{total}} \\ \frac{2}{A_{total}+B_{total}/Z_O+C_{total}Z_O+D_{total}} & \frac{-A_{total}+B_{total}/Z_O-C_{total}Z_O+D_{total}}{A_{total}+B_{total}/Z_O+C_{total}Z_O+D_{total}} \end{bmatrix} \quad (3.15)$$

As a result, a new 2 port s-parameters block is obtained and by using it in the  $\Gamma_{IN}$  formula, the presented  $\Gamma_L$  at the output terminal of the amplifier can be properly calculated as follows.

$$\Gamma_L = S_{11_{total}} + \frac{S_{12_{total}}S_{21_{total}}\Gamma_{pwr}}{1 - S_{22_{total}}\Gamma_{pwr}} \quad (3.16)$$

This  $\Gamma_{tun}$  is the required  $\Gamma$  at the tuner reference plane as shown in Fig. 3.8. It is typically used by the MLibTuners library functions in order to predict the  $S_{tun}$ -parameters and estimate the new mechanical positions required to synthesize a certain target impedance.

The  $S_{Total}$  parameters are utilized to de-embed the output network from the measurements. A given example is shown in Fig. 3.17 where the red '\*' represents  $\Gamma_{tun}$  and the blue 'o' circles the  $\Gamma_L$ , in this case, the target impedances.

### 3.8.2 Impact of precision measurements

This section reveals the matter of a pre-matching technique and how it contributes to the maximum achievable reflection coefficient. As it can be seen in Fig. 3.12, the tuner exhibits a good repeatability for the first 3000 load impedances, once the  $VSWR > 1.5:1$ .

For the loads closer to  $50 \Omega$ , the presented signal-to-noise ratio (SNR) required to a proper measurement of the reflected power wave is diminished, due to the match conditions, existing between the VNA ports and DUT. Both the noise floor and the sampler noise contribute to this degradation. In order to diminish, or possibly overcome, this problem, it is normal to use a lower IF, to use averaging or to increase the VNA source power.

Another important constraint regarding the imprecision of the VNA measurements is due to the very low-loss reactive elements, such as the tuner, being less accurate for the load which exhibits a maximum reflection coefficient greater than 0.8. These problems can be overcome by using some impedance technique transformation that enables the synthesis of the same desired impedance requiring a low VSWR.

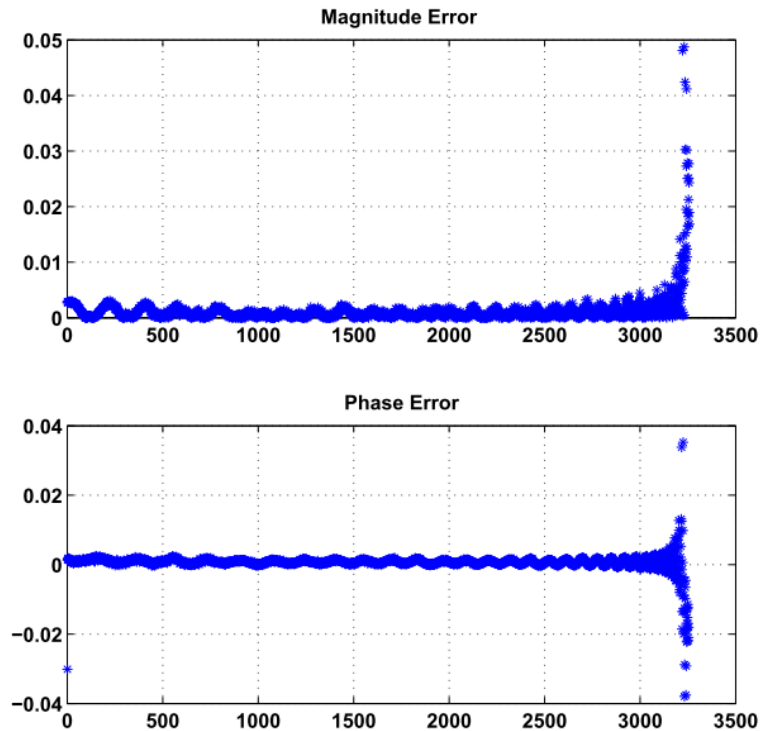


Figure 3.14: Pre-characterization magnitude and phase error results.

The next two figures reveal how important it is the VNA calibration performance. As it can be seen in Fig. 3.15, the black dotted loads exhibit low values of repeatability approximately -45dB. Since these loads at the tuner reference plane are mostly closer to  $50 \Omega$ , this usually occurs when the calibration is not properly performed and becomes even worse after usage of a test fixture. As such the capability to predict load impedances is lost, and the corresponding load-pull results become meaningless.

Another important aspect related to the non-uniform repeatability distribution is that the interpolation algorithm will not preserve the same performance as the repeatability, even if the number of pre-characterized states increases, as the example shown in Fig. 3.15.

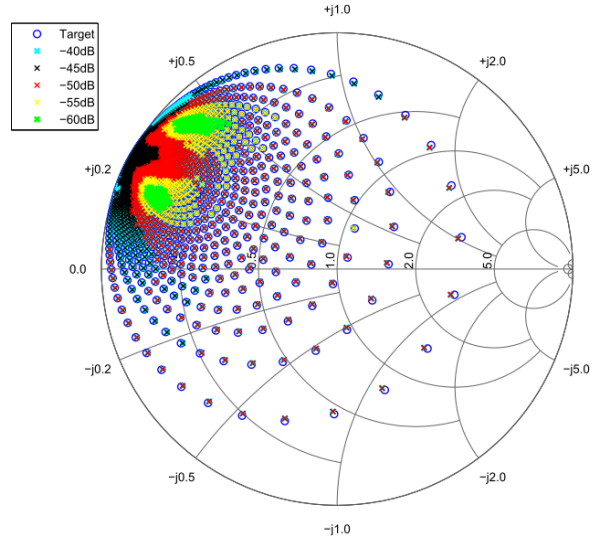


Figure 3.15: Precision of poorly calibrated prediction loads.

For the second test displayed in Fig. 3.15, the required corrections on the VNA calibration process were applied and the target loads exhibit almost the same accuracy as the tuner repeatability, which is around -50 dB. This result will guarantee a correct and precise impedance seen by the DUT, and so it is the one that I decided to use in the load-pull measurements, which shows a uniformly accurate load characterization that provides meaningfully interpolated target results with a desired fidelity.

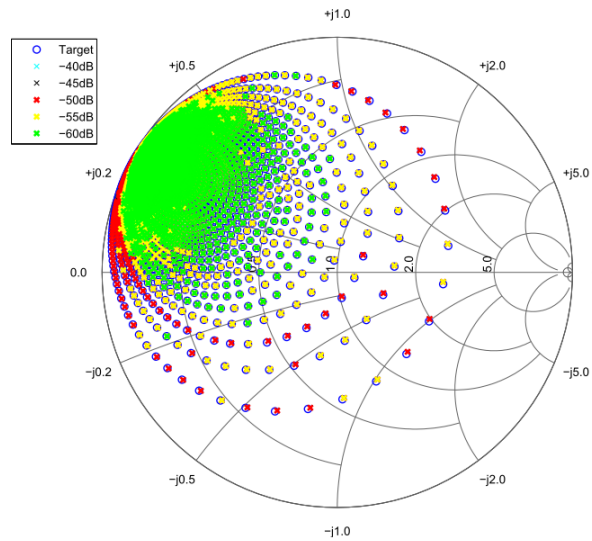


Figure 3.16: Precision of the well performed prediction loads.

### 3.8.3 Target impedances

For a chosen set of target load impedances, the interpolation algorithm determines a new set of mechanical positions and their respective s-parameters based on already characterized output network shown in Fig. 3.8, taking also into account half of the test fixture of the DUT and output block. In the Fig. 3.17, target loads at the fixture flange plane are represented by blue 'o' points while the red '\*' ones represent the required impedances at the tuner flange plane.

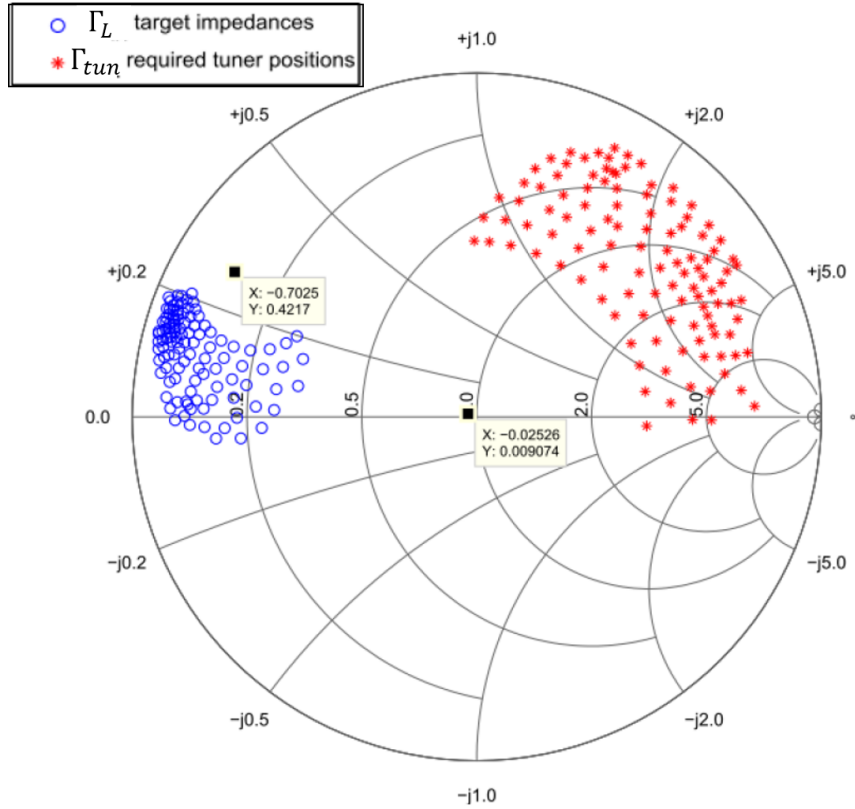


Figure 3.17: Estimated tuner impedances based on target impedances for the DUT characterization.

The new mechanical positions are obtained by inverting the similar input reflection coefficient formula shown in equation 3.16 so that  $\Gamma_{tun}$  becomes a function of  $\Gamma_L$ :

$$\Gamma_{tun} = \frac{\Gamma_L - S_{11_{fix}}}{\Gamma_L S_{22_{fix}} - S_{11_{fix}} S_{22_{fix}} + S_{12_{fix}} S_{21_{fix}}} \quad (3.17)$$

It is important to notice that  $\Gamma_{IN}$  corresponds to the  $\Gamma$  at the DUT output, the s-parameters are the test fixture ones and the  $\Gamma_L$  is the equivalent  $\Gamma_{IN}$  at the tuner reference plane which is attached to the fixture.

### 3.8.4 Load-pull results

After the proper absolute power calibration and system characterization are discussed, the achieved results of the load-pull measurements of a certain GaN microwave transistor is shown in Fig. 3.18. They contain the contours of load-pull displayed over the Cartesian plane, also called Z-plane, in Fig. 3.18 and Fig. 3.19 presents these same results on the Smith chart.

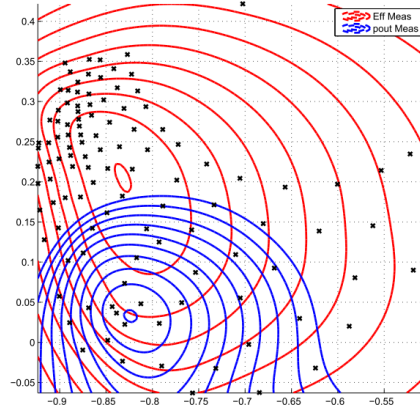


Figure 3.18: Load-Pull contours at the Z-plane.

The obtained load-pull contours are displayed over the Smith chart, where the black symbols 'x' indicate the target impedances, the blue contours denote  $P_{out}$ , at 3dB gain compression point and the red curves  $\eta_D$ . The information presented in Fig. 3.16 shows the load-pull amplifier characterization at the  $50\Omega$  reference plane.

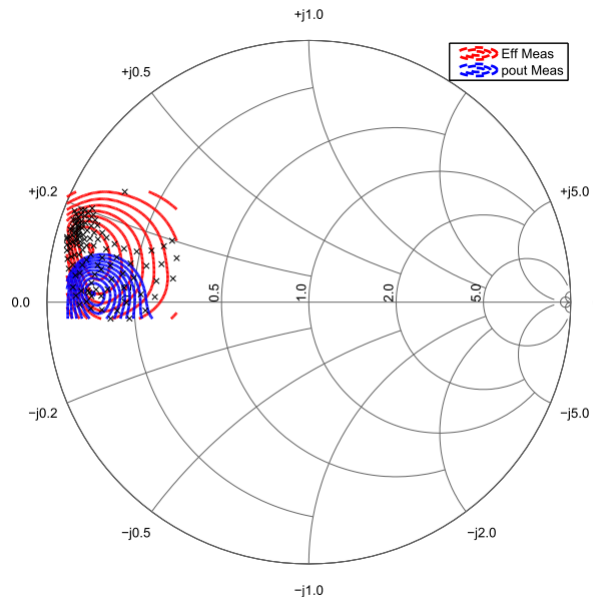


Figure 3.19: Load-Pull contour at 3dB gain compression point.

By inspecting the load-pull results the optimum load impedances in terms of efficiency and power at 3dB of gain compression are the following:

$$Z_L = 4.1459 + j1.0265\Omega, P_{out3dB} \quad (3.18)$$

$$Z_L = 3.299 + j6.270\Omega, Drain_{eff3dB} \quad (3.19)$$

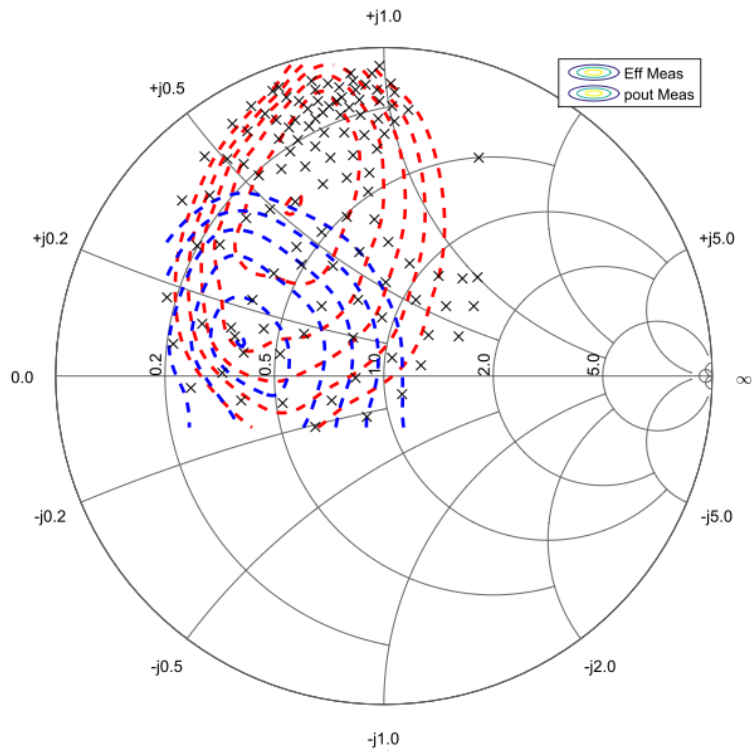


Figure 3.20: Load-Pull contour at 3dB gain compression point where  $Z_0 = 10 \Omega$ .



Figure 3.21: Final bench at Huawei Sweden of an automated tuner based load-pull system.

## Chapter 4

# Conclusion and Future Work

This chapter presents the main important aspects of this dissertation as well as its conclusions. In addition, some ideas are given that might be used as future work.

### 4.1 Conclusion

The strong motivation of this dissertation consists in the fact that, along the years, the industry of telecommunications has found the necessity to optimize the time spent in the microwave transistor characterization process in order to quickly and accurately design a PA that meets the next generation requirements of power, linearity and efficiency. That is required due to the data traffic, user capacity and base station covering range, which is intensively increasing from one generation of a cellular base station to another. Thus, the main objective of this dissertation was to build an automated load-pull systems at HUAWEI Technologies AB, similar to the one that was previously manually performed. In this sense, a concise study about the load-pull methods and techniques was given, which was further utilized in the system design.

After getting the knowledge about the most important concepts, regarding load-pull theory, an automated load-pull system was built, implemented and validated. The design allows to understand the role played by each component of the load-pull system and how to proceed the characterization and integration of the whole system. Therefore, a systematic procedure was established using applied wave research (AWR)/MWO to support the developed MATLAB routines utilized in the characterization, absolute power calibration and load pull measurements.

The traditional load-pull technique implemented in this work utilizes a routine for the tuner characterization, besides of dedicated DLL for the control of the step motors and interpolation algorithms of the MT981EU. This makes possible to reconfigure the output network based on the characterization beforehand of the system, which enables the prediction of the seen impedance by the DUT and to accurately read the power at the DUT input and output ports.

During the practical tests, it was found that the presented repeatability of the MT981EU was about - 60dB and even when attached with the rest of the system components it was maintained. This fills the requirement of accuracy to reproduce precisely a certain impedance state at the DUT reference plane, while assisting its performance assessment [37].

It was understood that a proper absolute power calibration and system verification ensure that most of the loss deviation on the predicted network losses is fixed, avoiding possible

discrepancies in the presented drain efficiency.

As a final result, the load-pull measurements of the developed systems needs only 2 hours to measure 114 loads of a certain transistor, being not even comparable to the manual system that was built in Aveiro Univeristy which needs about 14 hours of handwork to measure a similar device with the same quantity of target impedances.

The main goal of this work was successfully achieved where a well-defined procedure for a system characterization and calibration was done, as well as the load-pull measurement routines. Once all calibrations were finished, it was only necessary to introduce the target parameters for a certain DUT such as  $V_{GS}$ ,  $V_{DS}$ , frequency, desired compression and a set of target reflection coefficients that should be used for its characterization. The routine performs the measurements automatically saving the results in a proper manner for a future post processing, PA design and non-linear model validation.

## 4.2 Future work

As a future work, it is recommended to utilize a source tuner in addition to the already presented topology that was developed in this work. It has the purpose to optimize the overall performance of the implemented traditional load-pull system allowing a proper power gain verification that is increased due to the connectors and tuner repeatability.

Another advice would be the change from the traditional to the VNA measurement based topology granting the correct reading of the presented impedance and  $P_{in}$  being injected at the DUT input, enhancing the accuracy of the obtained results in terms of PAE and Power Gain.

Moreover, the harmonic characterization can be added to the system in two different forms using additional tuners for the second and third harmonics as needed, or through the active injection of the signal that is going to emulate the harmonic reflection coefficient. This active injection might require less power at the harmonic than at the fundamental, which reduces the cost of power amplifiers with high power capabilities.

In addition, the strategy to record the generated data can be optimized, providing an easier access to the result and it can be integrated in the MWO/AWR scripts speeding up the process of the artful conception of a PA, reducing the time to design an PA and avoiding extensive search of the recorded data.

# Bibliography

- [1] G. Simpson, *A Beginner's Guide To All Things Load Pull or Impedance Tuning 101 (5A-062)*. Maury Microwave Corporation, March, 2015.
- [2] J. Hoversten, M. Roberg, and Z. Popović, "Harmonic load pull of high-power microwave devices using fundamental-only load pull tuners," in *Microwave Measurements Conference (ARFTG), 2010 75th ARFTG*. IEEE, 2010, pp. 1–4.
- [3] Z. Wang, *Envelope Tracking Power Amplifiers for Wireless Communications*. Artech House, 2014.
- [4] J. Sevic, "Introduction to tuner-based measurement and characterization," *Maury Technical Data 5C-054*, 2004.
- [5] F. M. Ghannouchi and M. S. Hashmi, *Load-pull techniques with applications to power amplifier design*. Springer Science & Business Media, 2012, vol. 32.
- [6] R. S. Tucker and P. D. Bradley, "Computer-aided error correction of large-signal load-pull measurements," *IEEE transactions on microwave theory and techniques*, vol. 32, no. 3, pp. 296–300, 1984.
- [7] P. D. Bradley and R. Tucker, "Computer-corrected load-pull characterisation of power mesfet's," in *1983 IEEE MTT-S International Microwave Symposium Digest*, 1983, pp. 224–226.
- [8] F. Microwave, "Computer controlled microwave tuner," - *CCMT, Product Note 41*, Jan, 1998.
- [9] S. Bensmida, E. Bergeault, G. I. Abib, and B. Huyart, "Power amplifier characterization: An active load-pull system based on six-port reflectometer using complex modulated carrier," *Microwave Theory and Techniques, IEEE Transactions on*, vol. 54, no. 6, pp. 2707–2712, 2006.
- [10] D.-L. Lê and F. M. Ghannouchi, "Source-pull measurements using reverse six-port reflectometers with application to mesfet mixer design," *Microwave Theory and Techniques, IEEE Transactions on*, vol. 42, no. 9, pp. 1589–1595, 1994.
- [11] R. Tuijtelaars, H. Westra, and G. Sutorius, "Power amplifier design and load-pull measurements in practice." in *Agilent technologies and BSW*, 2013.
- [12] F. Microwave, "Tuner operation basics," Dec. 23 2010. [Online]. Available: <http://www.focus-microwaves.com/sites/default/files/TunerOperationBasics.pdf>

- [13] M. M. Corporations, "Slide screw tuner," *Technical Data*, 2G-035A, Feb, 1998.
- [14] F. Microwave, "Electronic tuners (ets) and electromechanical tuner (emt) – a critical comparison," *Technical Note*, Aug, 1998.
- [15] C. Woodin and D. Wandrei, "High power solid state programmable load," Jan. 4 1994, uS Patent 5,276,411. [Online]. Available: <https://www.google.com.ar/patents/US5276411>
- [16] R. Tuijtelaars, "Overview of device noise parameter measurement systemse." in *BSW TestSystems & Consulting bv*. VDE/ITG, Dec, 2001.
- [17] M. Microwave, "Measurement and modeling device characterization solutions," Dec. 23 2015. [Online]. Available: <https://www.maurymw.com/pdf/MAURY-CATALOG-COMPONENTS.pdf>
- [18] P. Colantonio, F. Giannini, and E. Limiti, "High efficiency rf and microwave solid state power amplifiers," 2009.
- [19] R. Hajji, F. M. Ghannouchi, and R. G. Bosisio, "Large-signal microwave transistor modeling using multiharmonic load-pull measurements," *Microwave and Optical Technology Letters*, vol. 5, no. 11, pp. 580–585, 1992.
- [20] S. C. Cripps, *Advanced techniques in RF power amplifier design*. Artech House, 2002.
- [21] R. B. Stancliff and D. Poulin, "Harmonic load-pull," in *1979 IEEE MTT-S International Microwave Symposium Digest*, 1979, pp. 185–187.
- [22] F. Microwave, "Comparing harmonic load-pull techniques with regards to power-added efficiency (pae)," Application Note 58, May, Tech. Rep., 2007.
- [23] B. Hughes, A. Ferrero, and A. Cognata, "Accurate on-wafer power and harmonic measurements of mm-wave amplifiers and devices," in *Microwave Symposium Digest, 1992., IEEE MTT-S International*. IEEE, 1992, pp. 1019–1022.
- [24] C. Arnaud, J.-L. Carbonero, J.-M. Nebus, and J.-P. Teyssier, "Comparison of active and passive load-pull test benches," in *ARFTG Conference Digest-Spring, 57th*, vol. 39. IEEE, 2001, pp. 1–4.
- [25] M. S. Hashmi, A. L. Clarke, S. P. Woodington, J. Lees, J. Benedikt, and P. J. Tasker, "An accurate calibrate-able multiharmonic active load-pull system based on the envelope load-pull concept," *Microwave Theory and Techniques, IEEE Transactions on*, vol. 58, no. 3, pp. 656–664, 2010.
- [26] A. P. Ferrero and V. Teppati, "Experimental comparison of active and passive load-pull measurement technologies," -, 2000.
- [27] S. Dudkiewicz, "Hybrid-active load pull with pna-x and maury microwave," *Agilent Technologies*, Inc 2012.
- [28] F. M. Ghannouchi, M. S. Hashmi, S. Bensmida, and M. Helaoui, "Loop enhanced passive source-and load-pull technique for high reflection factor synthesis," *Microwave Theory and Techniques, IEEE Transactions on*, vol. 58, no. 11, pp. 2952–2959, 2010.

- [29] J. Flucke, P. Heymann, A. Liero, and W. Heinrich, "Rf-measurements of packaged broadband power transistors," *ITG-Fachbericht-GeMIC 2008*, 2008.
- [30] W. Sha, W. Xianliang, H. Zhixiang, C. Mingsheng, and V. Zhurbenko, "The high-order symplectic finite-difference time-domain scheme: Passive microwave components and antennas," 2010.
- [31] M. Microwave, "Mt964 load pull test fixtures," [Accessed 23 12 2015]. [Online]. Available: <https://www.maurymw.com/pdf/datasheets/4T-005.pdf>
- [32] V. Teppati, A. Ferrero, and M. Sayed, *Modern RF and microwave measurement techniques*. Cambridge University Press, 2013.
- [33] J. Fleury and O. Bernard, "Designing and characterizing trl fixture calibration standards for device modeling," *Applied Microwave and Wireless*, vol. 13, no. 10, pp. 26–55, 2001.
- [34] A. technologies, "Agilent 10 hints for making better network analyzer measurements," 25 Oct 2001. [Online]. Available: <http://cp.literature.agilent.com/litweb/pdf/5965-8166E.pdf>
- [35] B. D. Huebschman, "Calibration and verification procedures at army research laboratory (arl) for the focus microwaves load pull system," *ARL-TR-3985*, Nov 2006.
- [36] M. Microwave, "Theory of load and source pull measurement," *Maury Microwave Corporation*, vol. 27, 1999.
- [37] J. Sevic, "Basic verification of power load-pull systems," *Maury Microwave Corp., Application Note 5C-055, Ontario, CA*, 2004.



# Appendix A

## MATLAB Routines

### A.1 Pre-Characterization

```
%%%%%%%%%%%%%%%%%%%%%%%%%%%%%%%%%%%%%%%%%%%%%%%%%%%%%%%%%%%%%%%%%%%%%%%%
%% Thesis: "Fully-Automated Load-Pull System Based on Mechanical Tuners" %%
% HUAWEI / IT / University of Aveiro %
%-----%
% Description : Main script of tuner characterization %
% Tuner Model : MT981EU10:3170 (Maury) %
%-----%
% Creator : Alison Willian Pereira (awx281679) %
%-----%
% Revision History: %
% Name Date Description %
% awx281679 20150412 Created and initial Revision. %
% awx281679 20150521 Version 2.0 %
%-----%
% Freq_start: 1.8 GHZ Freq_stop: 1.8 GHZ N_points 3000 Cal_set: 1 %
%%%%%%%%%%%%%%%%%%%%%%%%%%%%%%%%%%%%%%%%%%%%%%%%%%%%%%%%%%%%%%%%%%%%%%%%
main_dir = 'D:\ALPS\Routines\';
cd( strcat(main_dir,'MT981EU10_characterization\') )
lp_func = strcat('D:\ALPS\Routines\','aux_tun_charac\')
addpath(genpath(lp_func ))
addpath(genpath( strcat(main_dir,'\Driversdir_drivers\') ))
config = fg_getconfig_v3
handle_pna = config.Instruments.Vector_Analyzer.handle

%% Calibration setup
AgN5230C_Setup( handle_pna,'system','delete_all_measurements',' ') ;
AgN5230C_Setup( handle_pna,'system','preset',' ') ;
clrdevice( handle_pna ) ;
fg_pna_user_setup( handle_pna ) ;
ocs_callset = 'cset1.cst' ;
AgN5230C_Setup( handle_pna,'memory','load',ocs_callset) ;
pause(3) ;
AgN5230C_conf_read_maury(handle_pna) ;
%% Set the storage directory folder
is_filename_tun = strcat(lp_func,'\dir_tun\8CELL_Last_shot.tun') ;
share_path = strcat('\dir_load_pull\dir_measurements',...
'\AWPTST5152015_tun\HUAWEI_MT981EU10_CAL_MEAS\') ;
```

```

is_fname_vna      = '\dir_load_pull\dir_measurements\AWPTST5152015_tun\' ;
i_call_set       = 1 ;
%% Tuner initialization - MT981EU10
MT981EU10_Setup('MLibTuners','load_libraries','') ;
MT981EU10_Setup('MLibTuners','init_setup','') ;
MT981EU10_Setup('MLibTuners','init','') ;
%% Load-Tun File
oct_tunf         = tun_to_mat(is_filename_tun) ;
freqs           = oct_tunf.data.freq ;
%% Set Paths
shareDay_path    = strcat(share_path,datestr(now,'yyyy-mm-dd')) ;
file_out        = strcat(shareDay_path,'\',datestr(now,'yy-mm-dd'),...
                        '- ',datestr(now,'HH-MM'),'_TChar_OUT') ;
%% Create Paths
if(~exist(shareDay_path,'dir'))
    mkdir(shareDay_path);
end
%% Short test of single frequency characterization
.
for freq_sel = 1:size(freqs,2)
    [oct_measured_data] = ... % OUTPUT: pre_characterization tun structure .
    f_tun_characterization_v2( ... % FUNCTION NAME .
    handle_pna          ,... % INPUT: ih_vna object used during the process .
    is_filename_tun     ,... % INPUT: fullpath and name of the tun file .
    freqs(freq_sel)    ,... % INPUT: target frequency for characterization .
    freq_sel           ) ;

    freq               = freqs(1,freq_sel) ;
    line               = sprintf('%1gMHz_ws.mat',round(1000*freq)) ;
    save(              = strcat(file_out,line) ;
    disp('Pre-Characterization complete! saving ...') ;
    f_write_tun_file( = strcat(main_dir,...
    strcat(file_out(3:end),line(1:end-4),'.tun')),...
    oct_measured_data) ;
end
%-----Auxiliar pre-characterization function-----%

function ...
    [oct_tunfile] = ... % OUTPUT: pre_characterization tun structure.
    f_tun_characterization_v2( ... % FUNCTION NAME.
    handle_pna    ,... % INPUT: ih_vna object used during the process.
    is_filename_tun ,... % INPUT: fullpath and name of the tun file.
    ic_sel_freq   ,... % INPUT: target frequency for characterization.
    freq_sel      )

%% 1~ Load .tun file with the mechanical position data.
fct_tundemo = tun_to_mat(is_filename_tun) ;

%% 2~ Load the mech_pos of the frequency to be pre-characterized.
crv_mechpos = fct_tundemo.data.mec_pos(1,freq_sel).data(:,1:3) ;

%-----
SmithChart(0); hold on;
%-----
set(gcf,'units','normalized','outerposition',[0 0 1 1]) ;

oct_tunfile.info.Method = fct_tundemo.info.Method ;

```

```

oct_tunfile.info.Name      = fct_tundemo.info.Name      ;
oct_tunfile.info.Model    = fct_tundemo.info.Model    ;
oct_tunfile.info.Date_Time = strcat('Date: ', sprintf(date), ...
                                     'Time: ', datestr(now, 'HH:MM:SS')) ;
oct_tunfile.info.Embedding = fct_tundemo.info.Embedding ;
oct_tunfile.info.start    = fct_tundemo.data.freq(1, freq_sel) ;
oct_tunfile.info.stop     = fct_tundemo.data.freq(1, freq_sel) ;
oct_tunfile.info.numfreq  = 1 ;

%% Creates xxx.Data branch of the structure
oct_tunfile.data.freq      = ic_sel_freq ;
oct_tunfile.data.def_gamma = fct_tundemo.data.def_gamma ;
oct_tunfile.data.positions = fct_tundemo.data.positions(freq_sel) ;
AgN5230C_Setup(handle_pna, 'system', 'delete_all_measurements', ' ') ;
AgN5230C_Setup(handle_pna, 'system', 'preset', ' ') ;
pause(3) ;
%% Load call set of the VNA calibration.
ocs_callset                = 'cset1.cst' ;
AgN5230C_Setup( handle_pna, memory', 'load', ocs_callset) ;
AgN5230C_conf_read_maury(handle_pna) ;
%% Set a desired frequency
AgN5230C_Setup( handle_pna, 'user', 'f_sel_freq', ic_sel_freq) ;
%% Wait the VNA be read
for ind = 1:oct_tunfile.data.positions
MT981EU10_Setup('MLibTuners', 'move_tuner' , crv_mechpos(ind,1:3)) ;
SPM                = AgN5230C_s2p_read(handle_pna) ;
s11_cp             = SPM(1)+1i.*SPM(2) ;
plot(s11_cp , '*r') ;
legend(            sprintf('s11: %1.4g j%1.4g ', SPM(1), SPM(2)) , ...
                    sprintf('s21: %1.4g j%1.4g ', SPM(3), SPM(4)) , ...
                    sprintf('s12: %1.4g j%1.4g ', SPM(5), SPM(6)) , ...
                    sprintf('s22: %1.4g j%1.4g ', SPM(7), SPM(8))) ;
drawnow ;
crv_spm_total(ind, :) = SPM ;
end
%% Creates xxx.Info branch of the structure
oct_tunfile.data.mp_sparam = [crv_mechpos(:, :) crv_spm_total] ;
%% End
disp('Measurement finished !!!') ;
figure(1) ;
pause(2) ;
close(figure(1)) ;
end
%-----%

```



## A.2 Power Calibration

```

%%%%%%%%%%%%%%%%%%%%%%%%%%%%%%%%%%%%%%%%%%%%%%%%%%%%%%%%%%%%%%%%%%%%%%%%
%% Thesis: "Fully-Automated Load-Pull System Based on Mechanical Tuners" %%
% HUAWEI / IT / University of Aveiro %
%
% Description: wb_pwr_calibration v1.0 - Power Calibration %
%
% Revision History: %
% Name Date Description %
% awx281679 2015\06\25 First run. %
%%%%%%%%%%%%%%%%%%%%%%%%%%%%%%%%%%%%%%%%%%%%%%%%%%%%%%%%%%%%%%%%%%%%%%%%
main_dir = 'D:\ALPS\Routines\' ;
cd( strcat(main_dir,'MT981EU10_pwr_cal\')) ;
addpath(genpath( strcat(main_dir,'MT981EU10_pwr_cal\')) ) ;
%%
% Loading all the instruments %%
%
config = fg_getconfig_v4 ;
tpwm = config.Instruments.Power_Meter.handle ;
tdca = config.Instruments.Power_Supply.handle ;
tmxg = config.Instruments.Signal_Generator.handle ;
handle_pna = config.Instruments.Vector_Analyzer.handle ;

AgN5230C_Setup( handle_pna,'system','delete_all_measurements' , ' ' ) ;
AgN5230C_Setup( handle_pna,'system','preset', ' ' ) ;
clrdevice( handle_pna ) ;
ocs_callset = 'cset1.cst' ;
AgN5230C_Setup( handle_pna,'memory','load',ocs_callset) ;
pause(3);
AgN5230C_conf_read_maury( handle_pna ) ;
ic_sel_freq = 1.8 ;
AgN5230C_Setup( handle_pna,'user','f_sel_freq',ic_sel_freq) ;
%%
% Tuner initialization setup %%
%
MT981EU10_Setup( 'MLibTuners','load_libraries','' ) ;
MT981EU10_Setup( 'MLibTuners','init_setup','' ) ;
MT981EU10_Setup( 'MLibTuners','init','' ) ;
%
% Loading characterization and system s-parameters %
%
filename = strcat(main_dir,'dir_load_pull\dir_loads\8cell_eff.txt') ;
data = f_read_load_awr_llparam(filename) ;
ZLoad = data.R + 1i.*data.jX ;
sloads = z_to_s(ZLoad,50) ;
fix_fname = 'fixture_8cells.s2p' ;
[~,X.sfix] = f_awr_get_s2p_at_freq_sel( fix_fname,ic_sel_freq ) ;
X.sfix_11 = X.sfix(1,1) ;
X.sfix_21 = X.sfix(1,2) ;
X.sfix_12 = X.sfix(1,3) ;
X.sfix_22 = X.sfix(1,4) ;
gin_fix_to_tun = (-X.sfix_11 + sloads)./ ...
((-X.sfix_11.*X.sfix_22)+sloads.*X.sfix_22+X.sfix_12.*X.sfix_21);
sbfix_s2p = 'sma_male_emb_p1.s2p' ;
[~,X.sbfix ] = f_awr_get_s2p_at_freq_sel( sbfix_s2p ,ic_sel_freq ) ;

```

```

X.sbfix_11      = X.sbfix(1,1)                                ;
X.sbfix_21      = X.sbfix(1,2)                                ;
X.sbfix_12      = X.sbfix(1,3)                                ;
X.sbfix_22      = X.sbfix(1,4)                                ;
loads           = gamma_x + 1i.*gamma_y                       ;
gin_f_fix_2_tun = (-X.sbfix_11 + loads)./ ...
                ((-X.sbfix_11.*X.sbfix_22)+loads.*X.sbfix_22+X.sbfix_12.*X.sbfix_21);
gin_dut         = X.sbfix_11 + ((X.sbfix_21*X.sbfix_12.*gin_f_fix_2_tun )./ ...
                (1-X.sbfix_11.*gin_f_fix_2_tun))                ;
gamma_x         = real(gin_f_fix_2_tun)                       ;
gamma_y         = imag(gin_f_fix_2_tun)                       ;
filename        = '15_06_28-18_50_Tchar_OUT1800MHz_ws.tun'   ;
meas_dir        = '...\AWPTST5152015_tun\HUAWEI_MT981EU10_CAL_MEAS' ;
MT.tuner_number = 0                                           ;
MT.fname        = strcat(main_dir,meas_dir,'\2015_06_28\',filename) ;
MT.tuner_model  = 'MT981EU10'                                 ;
MT.freq         = ic_sel_freq                                  ;
MT.mec(1:3)     = 9500                                        ;
MT.interp_mode  = 1                                           ; KEY is required.
gamma_out_slp   = 'gamma_out_slp.slp'                         ;
[~,X.gamma_out_slp] = f_awr_get_slp_at_freq_sel( gamma_out_slp , ic_sel_freq ;
MT.gamma_x_termination = (16.4*10^-3)                         ;
MT.gamma_y_termination = (-5.23*10^-3)                       ;
MT981EU10_Setup( 'MLibTuners','free_tuner_data' ,MT)         ;
MT981EU10_Setup( 'MLibTuners','read_tuner_data_file',MT)     ;
% -----
%           Estimating the Mechanical position and s2p for the loads
% -----

SmithChart(2);hold on;
for k = 1:size(sloads,1)
    MT.gamma_x      = gamma_x(k)                                ;
    MT.gamma_y      = gamma_y(k)                                ;
    mpos            = MT981EU10_Setup('MLibTuners', 'get_tuner_refl_posn',MT) ;
    mp(k,1:3)       = [mpos.carr mpos.p1 mpos.p2]              ;
%plot target imp
    plot( gin_fix_to_tun(k), 'o');
%plot (tst.data.mec_pos.data(k,4) +1i.*tst.data.mec_pos.data(k,5), 'o');
    MT981EU10_Setup( 'MLibTuners','move_tuner', [ mp(k,1) mp(k,2) mp(k,3) ]) ;
    s_aux          = AgN5230C_s_read(handle_pna)                ;
    s_pchar_11(k)  = s_aux(1)+1i.*s_aux(2)                      ;
    s_pchar_21(k)  = s_aux(3)+1i.*s_aux(4)                      ;
    s_pchar_12(k)  = s_aux(5)+1i.*s_aux(6)                      ;
    s_pchar_22(k)  = s_aux(7)+1i.*s_aux(8)                      ;
                    plot( s_pchar_11(1,k) , 'r*' ); drawnow
    err(k)         = 20.*log10(abs(( gin_fix_to_tun(k) ...
                    - s_pchar_11(1,k)))                        ;
    gin(k)         = X.sfix_11 + (X.sfix_21.*X.sfix_12.*s_pchar_11(1,k))./ ...
                    (1 - X.sfix_22.*s_pchar_11(1,k))          ;
    plot(sloads(k), 'bo');
    plot(gin(k), 'r*');
end
err2              = err                                        ;
sgoal             = [ s_pchar_11' s_pchar_21' s_pchar_12' s_pchar_22'] ;
% -----
%           Power Calibtraion                                %%
% -----

```

```

addpath('D:\ALPS\fpwr_swp_signals' );
fps_lps_signal_fname = 'fps_15_p_30dB' ;
ot_cal = fpwr_swp_pwr_cal_ldmos_config_v4(config,ic_sel_freq,fps_lps_signal_fname);
%
% s-parameters of system components %%
%
gspec_out_slp = 'gspec_out.slp' ;
[~,X.gspec_out]= f_awr_get_slp_at_freq_sel( gspec_out_slp , ic_sel_freq);
gpwr_b_slp = 'gpwr_b.slp' ;
%Power_meter
[~,X.gpwr_b] = f_awr_get_slp_at_freq_sel( gpwr_b_slp , ic_sel_freq);
gamma_out_s2p = 'gamma_out_s2p.s2p' ;
[~,X.gamma_out_s2p ]= f_awr_get_s2p_at_freq_sel( gamma_out_s2p , ic_sel_freq);
gamma_c_pwrc_f_t_tun = 'conector_pwr_cal_b_fix_tuner.s2p' ;
[~,X.gamma_c_pwrc_f_t_tun ] = f_awr_get_s2p_at_freq_sel(gamma_c_pwrc_f_t_tun,...
ic_sel_freq);
X.abcd_gamma_c_pwrc_f_t_tun = s_to_abcd([X.gamma_out_s2p(1,1) X.gamma_out_s2p(1,3);
X.gamma_out_s2p(1,2) X.gamma_out_s2p(1,4)],50);
X.abcd_gamma_out = s_to_abcd([X.gamma_c_pwrc_f_t_tun(1,1) X.gamma_c_pwrc_f_t_tun(1,3);
X.gamma_c_pwrc_f_t_tun(1,2) X.gamma_c_pwrc_f_t_tun(1,4)],50);
MT_pcharc = tun_to_mat(MT.fname) ;
X.mp = MT_pcharc.data.mec_pos.data(:,1:3) ;

for k = 1:size(X.s11_t,1)
X.abcd_t(:, :,k) = s_to_abcd([X.s11_t(k,1) X.s21_t(k,1) ;
X.s12_t(k,1) X.s22_t(k,1)],50) ;
X.abcd_gamma_out_total(:, :,k) = X.abcd_gamma_c_pwrc_f_t_tun * X.abcd_t(:, :,k)*...
X.abcd_gamma_out ;
X.gamma_out_total(:, :,k) = abcd_to_s(X.abcd_gamma_out_total(:, :,k),50) ;

X.gin(k) = X.gamma_out_total(1,1,k) +(( X.gamma_out_total(1,2,k).* ...
X.gamma_out_total(2,1,k).*X.gpwr_b)...
./(1- X.gamma_out_total(2,2,k).*X.gpwr_b)) ;

Gp_lin(k) = (1/(1-(abs(X.gin(k))^2))) .* ...
(abs(X.gamma_out_total(2,1,k).^2) .* ...
(( 1- abs(X.gpwr_b).^2) ./ ...
(abs(1-X.gamma_out_total(2,2,k).*X.gpwr_b).^2))) ;

Gp_dB(k) = 10.*log10(Gp_lin(k)) ;

end
figure(2); plot(Gp_dB, '-o');grid on;
SmithChart(0); plot(X.gin, 'o');
close all ;
%
% ----- WARNING THIS UPPER IS USED ONLY TO POWER CAL -----
%
ot_cal.max = 10.1 ;
PAInputLoss = 31.33 ;
OutputLosses_array = -Gp_dB ; %G21_dB_out;% -41.5702 ;

%
% Freescale driver
%

```

```

Gain_driver_offset = 5.67;
PeakPower          = 42;
steps              = [PeakPower-15:15/2:PeakPower]-36.251496748344728-0.35      ;
OBO_in_pts        = 11                                                         ;
dB_comp           = 1                                                           ;
max_peak_after_backoff = 0.01                                                 ;

for k = 72:10

    OutputLosses = OutputLosses_array(k)                                       ;
    MT981EU10_Setup( 'MLibTuners', 'move_tuner', [ mp(k,1),mp(k,2),mp(k,3) ])  ;
    MT981EU10_Setup( 'MLibTuners', 'move_tuner', [ 100 ,9500,9500])           ;
% -----
aux = 1;
for j = 1:size(steps,2)
    ot_cal.AvgPower = steps(j)                                                 ;
    ot_flps_pcal    = fpwr_swp_ldmos_fetch_load( con-fig,ot_cal,PAInputLoss,OutputLosses);
    Pout_peak(:,aux)= ot_flps_pcal.PoutdBm                                     ;
    A(j)            = max(Pout_peak(:,j))                                       ;
    aux             = aux +1                                                    ;
    s               = input('Next','s')                                        ;
end
end
% -----%

```

## A.3 Load-Pull Measurements

```

%%%%%%%%%%%%%%%%%%%%%%%%%%%%%%%%%%%%%%%%%%%%%%%%%%%%%%%%%%%%%%%%%%%%%%%%
%% Thesis: "Fully-Automated Load-Pull System Based on Mechanical Tuners" %%
% HUAWEI / IT / University of Aveiro %
%
% Description: wb_alps.m - Automated Load-Pull System - PA Measurements %
%
% Revision History: %
%
% Name Date %
% awx281679 2015\04\25 First run. %
% awx281679 2015\06\18 Updated. %
%%%%%%%%%%%%%%%%%%%%%%%%%%%%%%%%%%%%%%%%%%%%%%%%%%%%%%%%%%%%%%%%%%%%%%%%
clear all; close all; clc;

%%
% set main path %%
%
config = fg_getconfig_v4 ;
main_dir = 'D:\Tese\Desktop\Msc_LPS\MATLAB_V2\' ;
cd( main_dir );
addpath( strcat(main_dir, '\wb_flps') );
addpath( '\workbenchs' );
addpath(genpath('D:\Tese\Desktop\Msc_LPS\MATLAB_V2\wb_pwr_calibration\' ));
addpath('D:\Tese\Desktop\Msc_LPS\MATLAB_V2\dir_load_pull\dir_func\f_flps\' );
addpath('D:\Tese\Desktop\Msc_LPS\MATLAB_V2\dir_load_pull\dir_func\f_r_awr\' );
addpath('D:\Tese\Desktop\Msc_LPS\MATLAB_V2\dir_load_pull\dir_func\AgN5230C\'',...
'D:\Tese\Desktop\Msc_LPS\MATLAB_V2\dir_load_pull\dir_func\'',...
'D:\Tese\Desktop\Msc_LPS\MATLAB_V2\dir_load_pull\dir_tun\'',...
'D:\Tese\Desktop\Msc_LPS\MATLAB_V2\dir_load_pull\dir_drivers\' ');

%%
% LPS User Setup %%
%
% filename of the setup. ex: target is the load's to be measured
dut_loads_fname = strcat(main_dir, 'dir_load_pull\dir_loads\8cell_eff.txt' );
fixture_fname = 'fixture_8cells.s2p' ;
signal_fname = '1800MHz_ws_v2' ;
fps_lps_signal_fname = 'fps_15_p_30dB' ;

% Folder of the fpwr_swp_directory:
trans = 'G068_8Cell' ;

%% Dut Bias
Vds = 50 ;
Vgs = -2.66 ;
Ids = 1.395 ;
Imax = 2 ;
ic_sel_freq = 1.8 ;

%%
% Loading all the instruments %%
%
% Init. instr. & load libraries
config = fg_getconfig_v4 ;
tpwm = config.Instruments.Power_Meter.handle ;

```

```

tdca          = config.Instruments.Power_Supply.handle      ;
tmxg          = config.Instruments.Signal_Generator.handle  ;

%% Tuner initialization setup
MT981EU10_Setup( 'MLibTuners','load_libraries','')        ;
MT981EU10_Setup( 'MLibTuners','init_setup','')            ;
MT981EU10_Setup( 'MLibTuners','init','')                  ;

%% -----
%               Creating file directories to save data      %%
% -----

dir           = 'flps_data\'                                ;
path          = main_dir                                    ;
share_path    = strcat(path,dir)                           ;
shareDay_path = strcat(share_path,trans,'\','...',
    strcat(datestr(now,'yyyy-mm-dd'))                       );

file_out      = strcat(shareDay_path,'\','...',
    datestr(now,'yy-mm-dd'),'\'','...',
    datestr(now,'HH-MM'),trans,'_lpfs_','\' ');
file_out2     = strcat(file_out,trans,'_figures\'          );
file_out3     = strcat(file_out,trans,'_swp_load_data\'    );

if(~exist(file_out,'dir'))
    mkdir(file_out)                                        ;
end

if(~exist(file_out2,'dir'))
    mkdir(file_out2)                                      ;
end

if(~exist(file_out3,'dir'))
    mkdir(file_out3)                                      ;
end
%% -----
%               Estimating the Mechanical position and s2p  %
% -----

data          = f_read_load_awr_1lparam(dut_loads_fname)  ;
ZLoad         = data.R + 1i.*data.jX                       ;
sloads        = z_to_s(ZLoad,50)                           ;
[~,X.sfix]    = f_awr_get_s2p_at_freq_sel(fixture_fname,...
    ic_sel_freq                                           );

X.sfix_11     = X.sfix(1,1)                                ;
X.sfix_21     = X.sfix(1,2)                                ;
X.sfix_12     = X.sfix(1,3)                                ;
X.sfix_22     = X.sfix(1,4)                                ;

gin_f_fix_to_tun1 = (-X.sfix_11 + sloads)./((-X.sfix_11.*X.sfix_22) ...
    +sloads.*X.sfix_22+X.sfix_12.*X.sfix_21)              ;

fix_conec_s2p = 'fix_and_connector.s2p'                   ;
[~,X.sfix_conec] = f_awr_get_s2p_at_freq_sel( fix_conec_s2p , ic_sel_freq );

X.sfix_conec_11 = X.sfix_conec(1,1)                        ;
X.sfix_conec_21 = X.sfix_conec(1,2)                        ;
X.sfix_conec_12 = X.sfix_conec(1,3)                        ;

```

```

X.sfix_conec_22 = X.sfix_conec(1,4) ;

gin_f_fix_to_tun = (-X.sfix_conec_11 + sloads)./ ...
                  ((-X.sfix_conec_11 .* X.sfix_conec_22) ...
                  +sloads.*X.sfix_conec_22+ X.sfix_conec_12 .* X.sfix_conec_21 );

X.gamma_x      = real(gin_f_fix_to_tun) ;
X.gamma_y      = imag(gin_f_fix_to_tun) ;

%% -----
%                               Tuner pre-characterization setup                               %
% -----
MT.tuner_number = 0 ;
filename        = '15_06_28-18_50_TChar_OUT1800MHz_ws.tun' ;
meas_dir        = 'dir_load_pull\dir_measurements' ;
meas_dir2       = '\AWPTST5152015_tun\HUAWEI_MT981EU10_CAL_MEAS' ;
MT.tuner_number = 0 ;
MT.fname        = strcat(main_dir,meas_dir,meas_dir2,'\2015_06_28\',filename);
MT.tuner_model  = 'MT981EU10' ;
MT.freq         = ic_sel_freq ;
MT.mec(1)       = 9500 ;
MT.mec(2)       = 9500 ;
MT.mec(3)       = 9500 ;
MT.interp_mode  = 1 ;
MT.gamma_x_term = 0 ;
MT.gamma_y_term = 0 ;
MT981EU10_Setup( 'MLibTuners','free_tuner_data' , MT ) ;
MT981EU10_Setup( 'MLibTuners','read_tuner_data_file', MT ) ;

%% -----
%                               Load-Pull full characterization                               %%
% -----
%                               Gamma_out                                                  %
% -----

fix_and_conec   = 'fix_and_connector.s2p' ;
[~,X.fix_and_conec]= f_awr_get_s2p_at_freq_sel( fix_and_conec, ic_sel_freq ) ;
gamma_out_s2p    = 'gamma_out_s2p.s2p' ;
[~,X.gamma_out_s2p ]= f_awr_get_s2p_at_freq_sel( gamma_out_s2p,ic_sel_freq ) ;
gspec_out_slp    = 'gspec_out.slp' ;
[~,X.gspec_out] = f_awr_get_slp_at_freq_sel( gspec_out_slp,ic_sel_freq ) ;
gpwr_b_slp       = 'gpwr_b.slp' ;
[~,X.gpwr_b]     = f_awr_get_slp_at_freq_sel( gpwr_b_slp,ic_sel_freq ) ;

% -----
%                               ABCD -MATRIX                                               %
% -----
X.abcd_fix_and_conec = s_to_abcd([X.fix_and_conec(1,1) X.fix_and_conec(1,3);
                                X.fix_and_conec(1,2) X.fix_and_conec(1,4)],50) ;

X.abcd_gamma_out      = s_to_abcd([X.gamma_out_s2p(1,1) X.gamma_out_s2p(1,3) ;
                                X.gamma_out_s2p(1,2) X.gamma_out_s2p(1,4)],50) ;

MT_pcharc             = tun_to_mat(MT.fname) ;
X.mp                  = MT_pcharc.data.mec_pos.data(:,1:3) ;

```

```

X.s11      = MT_pcharc.data.mec_pos.data(:,4) + ...
            1i.*MT_pcharc.data.mec_pos.data(:,5)      ;

X.s21      = MT_pcharc.data.mec_pos.data(:,6) + ...
            1i.*MT_pcharc.data.mec_pos.data(:,7)      ;

X.s12      = MT_pcharc.data.mec_pos.data(:,8) + ...
            1i.*MT_pcharc.data.mec_pos.data(:,9)      ;

X.s22      = MT_pcharc.data.mec_pos.data(:,10) + ...
            1i.*MT_pcharc.data.mec_pos.data(:,11)     ;

% -----
% Remove the losses and shift the reference plane to properly read out_pwr_b
% -----

idx        = NaN.*ones(size(gin_f_fix_to_tun,1),1)    ;
for k = 1:size(gin_f_fix_to_tun,1)
    [~,idx(k)] = min(20.*log10(abs( gin_f_fix_to_tun(k)-X.s11))) ;
end

X.s11_t    = X.s11(idx)                               ;
X.s21_t    = X.s21(idx)                               ;
X.s12_t    = X.s12(idx)                               ;
X.s22_t    = X.s22(idx)                               ;

% -----
%                               Post processing awr s2p files
% -----

MT.gamma_x_term = (16.4*10^-3)                        ;
MT.gamma_y_term = (-5.23*10^-3)                      ;
MT981EU10_Setup( 'MLibTuners','free_tuner_data'      ,MT) ;
MT981EU10_Setup(  MLibTuners','read_tuner_data_file',MT) ;

%% Generating mechanical positions
SmithChart(0);hold on;

for k = 1:size(X.gamma_x,1)
    MT.gamma_x = X.gamma_x(k)                          ;
    MT.gamma_y = X.gamma_y(k)                          ;
    mpos       = MT981EU10_Setup('MLibTuners','get_tuner_refl_posn',MT) ;
    mp_t(k,1:3) = [mpos.carr mpos.p1 mpos.p2]           ;
    plot(      gin_f_fix_to_tun(k), 'o')               ;
    drawnow                                         ;
    plot(      loads(k), 'bo')                        ;
end

for k = 1:size(X.s11_t,1)
    X.abcd_t(:, :, k) = s_to_abcd([X.s11_t(k,1) X.s21_t(k,1)
                                X.s12_t(k,1) X.s22_t(k,1)], 50) ;

    X.abcd_gamma_out_total(:, :, k) = X.abcd_fix_and_connec * X.abcd_t(:, :, k) * X.abcd_gamma_out ;
    X.gamma_out_total(:, :, k) = abcd_to_s(X.abcd_gamma_out_total(:, :, k), 50) ;

    X.gin(k) = X.gamma_out_total(1,1,k) + (( X.gamma_out_total(1,2,k).* ...

```

```

X.gamma_out_total(2,1,k).*X.gpwr_b)...
./(1- X.gamma_out_total(2,2,k).*X.gpwr_b)) ;

Gp_lin(k) = (1/(1-(abs(X.gin(k))^2))).*(abs(X.gamma_out_total(2,1,k).^2).*...
((1- abs(X.gpwr_b).^2) ./ ...
(abs(1-X.gamma_out_total(2,2,k).*X.gpwr_b).^2))) ;

Gp_dB(k) = 10.*log10(Gp_lin(k)) ;

end

close all ;
SmithChart(0); plot(sloads,'o'); hold on; plot(X.gin,'*r') ; pause(1) ;
close all ;

%% -----
% Fast power sweep config %%
% -----
dos('start http://10.202.8.222/web.exe?file=FrontPanel.html') ;
pause(2) ;
addpath('\wb_fast_pwr_swp_lps\') ;

%% -----
% function fpwr_swp_gan_config_v4 confidential %%
% -----
ot_flps = fpwr_swp_gan_config_v4( config,ic_sel_freq,...
fps_lps_signal_fname,Vds,Imax ) ;

% -----
%% -----
% FPSWP measurements %%
% -----close all
;-----
% Header

filename = strcat(file_out,sprintf('f_%dMHz_G068.txt',ic_sel_freq*1000) ) ;
fid = fopen(filename,'w','n','US-ASCII');
fprintf(fid,'! Load Pull Measurement Data\n');
fprintf(fid,'!-----\n') ;
fprintf(fid,(sprintf('! Frequency = %.3f GHz \n',ic_sel_freq)) ) ;
fprintf(fid,'! Char.Impedances = Source: 1 + 0j Ohm Load: 1 + 0j Ohm \n') ;
fprintf(fid,(sprintf('! Source Frequencies = %.3f GHz \n',ic_sel_freq)));
fprintf(fid,'! Source Impedances F0: 1 - 0j Ohm \n') ;
fprintf(fid,'!----- \n') ;
fprintf(fid,'Point \t R \t\t jX \t Gain[dB] \t EffP3dB[%] \t'
);
fprintf(fid,'P3dB[dBm] \t EffP1dB[%] \t'
);
fprintf(fid,'P1dB[dBm] \t Eff47R0dBm[%]\t'
);
fprintf(fid,'Eff49R0dBm[%] \t Eff50R0dBm[%]\n'
);
fprintf(fid,'!-----'
);

% -----
% Generating the Look-up table for the at the plan of the device power levels %%
% -----
PAInputLoss = 31.33 ;
% ----- WARNING THIS UPPER VALUE WAS USED ONLY FOR THE POWER CAL -----
ot_flps.max = 6.1 ;
% -----

```

```

%                               Freescale driver

PeakPower      = 38.2-3                                     ;
SigPAR         = 12.27                                     ;
Power_cal_corrections = -36.251496748344728-0.35+5.6      ;
steps          = [PeakPower-SigPAR]+Power_cal_corrections ;
OBO_in_pts     = 11                                       ;

% It's a index that decide from 10 points
dB_comp       = 3                                         ;

% use the 10 pts to start the calculation.
X.Zloads      = s_to_z(sloads,50)                         ;
for k =1:size(mp_t,1)
ot_flps.AvgPower = steps                                   ;
OutputLosses    = -Gp_dB(k)                               ;
MT981EU10_Setup( 'MLibTuners','move_tuner', [ mp_t(k,1) mp_t(k,2) mp_t(k,3)] ) ;
pause(0.3)                                             ;
j              = 1                                         ;
aux_max        = 0                                         ;
filename       = strcat(file_out3,sprintf(...
    '%.2dMHz_Vgs_%.3fV_Ids_%.3fmA_ZL_%.4f+j_%.4f_Ohm.txt',...
    ic_sel_freq*1000,Vgs,Ids,real(X.Zloads(k)),imag(X.Zloads(k))));
mdat_file     = fopen(filename,'wt')                     ;

fprintf(mdat_file, '! FPS Load Pull Measurement Data\n'   );
fprintf(mdat_file, '!-----\n');
fprintf(mdat_file,sprintf('! OutputLosses: %.3d dB \t PAInputLoss: %.3d dB \n',...
    OutputLosses,PAInputLoss));
fprintf(mdat_file, '!Efficiency\tGain[dB]\tPoutdBm\tPdc\tPindBm\tPinW\t PoutW\n');
fprintf(mdat_file, '!-----\n');

while (aux_max < dB_comp)
ot_flps.k = k;
%% -----
%                               function fpwr_swp_gan_fetch_loadconfidential
% -----
ot_flps_pswp    = fpwr_swp_gan_fetch_load(config,ot_flps,PAInputLoss,OutputLosses);
% -----
minv            = min(ot_flps_pswp.PoutdBm)               ;
maxv            = max(ot_flps_pswp.PoutdBm)               ;

pout_x         = ot_flps_pswp.PoutdBm                    ;
gain_y         = ot_flps_pswp.Gain_data                  ;
eff_y          = ot_flps_pswp.Eff_data                   ;

pout_xx        = minv:0.1:maxv                            ;
gain_yy        = pchip(pout_x,gain_y,pout_xx)            ;
eff_yy         = pchip(pout_x,eff_y ,pout_xx)            ;

figure(k);      hold on; subplot(2,1,1)                  ;
plot(           pout_x,gain_y, '-ro' ,pout_xx,gain_yy);  grid on      ;
subplot(2,1,2)
plot(           pout_x,eff_y, '-ro' ,pout_xx,eff_yy );  grid on      ;

Gmax           = max(gain_yy)                             ;
idx            = find( gain_yy == max(gain_yy))           ;

```

```

PoutdBm_at_Gmax = pout_xx(idx) ;
RT.Avgpower = ot_flps.AvgPower ;
j = j+1 ;

Pmin_after_pk = min(gain_yy(idx:end)) ;
comp_meas = Gmax - Pmin_after_pk ;
RT.Point = k ;

RT.comp_meas = comp_meas ;
if ot_flps.AvgPower > 5.67 ;
    aux_max = 100 ;
end

if comp_meas > dB_comp ;
    aux_max = comp_meas ;
end

if comp_meas <1 && comp_meas<(dB_comp* 0.8) ;
    ot_flps.AvgPower = ot_flps.AvgPower + 1 ;
    RT.inc_step = '+1' ;
end

if comp_meas > (dB_comp* 0.8) ;
    ot_flps.AvgPower = ot_flps.AvgPower + 0.1 ;
    RT.inc_step = '+0.1' ;
end

if comp_meas >1 && comp_meas<(dB_comp* 0.8) ;
    ot_flps.AvgPower = ot_flps.AvgPower + 0.5 ;
    RT.inc_step = '+0.5' ;
end

% -----
%                               Write the file with the load-pull data
% -----

if aux_max > dB_comp ;
    wr_awr.point = k ;
    wr_awr.R = real(X.Zloads(k)) ;
    wr_awr.jX = imag(X.Zloads(k)) ;
    dBcomp_find = 1 ;
    idx_1dB_comp = idx + find( (abs(Gmax-gain_yy(idx:end)- dBcomp_find )) ...
    == min((abs(Gmax-gain_yy(idx:end)- dBcomp_find )) ) -1 ;

    dBcomp_find = 3 ;
    idx_3dB_comp = idx + find( (abs(Gmax-gain_yy(idx:end)- dBcomp_find )) ...
    == min((abs(Gmax-gain_yy(idx:end)- dBcomp_find )) ) -1 ;

    wr_awr.gain = pchip(pout_x,gain_y,45) ;
    wr_awr.gain_1dB = gain_yy(idx_1dB_comp) ;
    wr_awr.gain_3dB = gain_yy(idx_3dB_comp) ;

    wr_awr.eff_1dB = eff_yy(idx_1dB_comp) ;
    wr_awr.eff_3dB = eff_yy(idx_3dB_comp) ;

    wr_awr.P1dB = pout_xx(idx_1dB_comp) ;
    wr_awr.P3dB = pout_xx(idx_3dB_comp) ;
    ot_flps = f ;
end

```

```

% Set condition around 1dB for extrapolate if the max pout measure goes behind so it' set 0.
if maxv < 47
    wr_awr.eff47ro = 0 ;
    wr_awr.eff49ro = 0 ;
    wr_awr.eff50ro = 0 ;
end
if maxv > 47
    wr_awr.eff47ro = pchip(pout_x,eff_y,47) ;
    wr_awr.eff49ro = 0 ;
    wr_awr.eff50ro = 0 ;
end
if maxv > 49
    wr_awr.eff47ro = pchip(pout_x,eff_y,47) ;
    wr_awr.eff49ro = pchip(pout_x,eff_y,49) ;
    wr_awr.eff50ro = 0 ;
end
if maxv > 50
    wr_awr.eff47ro = pchip(pout_x,eff_y,47) ;
    wr_awr.eff49ro = pchip(pout_x,eff_y,49) ;
    wr_awr.eff50r = pchip(pout_x,eff_y,50) ;
end
if k < 9
    fprintf(fid_awr, sprintf('\n%i\t%.4f\t%.4f\t%.1f\t%.1f\t%.1f\t%.1f\t%.1f\t%.1f\t%.1f', ...
        k, wr_awr.R, wr_awr.jX, wr_awr.gain, wr_awr.eff_3dB, wr_awr.P3dB, ...
        wr_awr.eff_1dB, wr_awr.P1dB, wr_awr.eff47ro, wr_awr.eff49ro, ...
        wr_awr.eff50ro
        ));
else
    fprintf(fid_awr, sprintf('\n%i\t%.4f\t%.4f\t%.1f\t%.1f\t%.1f\t%.1f\t%.1f\t%.1f\t%.1f', ...
        k, wr_awr.R, wr_awr.jX, wr_awr.gain, wr_awr.eff_3dB, wr_awr.P3dB, ...
        wr_awr.eff_1dB, wr_awr.P1dB, wr_awr.eff47ro, wr_awr.eff49ro, ...
        wr_awr.eff50ro
        ));
end
end
% -----
% Saving alldata_pts
% -----
fetch_m = [ot_flps_pswp.Eff ot_flps_pswp.Gain_data ot_flps_pswp.PoutdBm ot_flps_pswp.Pdc' ...
    ot_flps_pswp.PindBm ot_flps_pswp.PinW ot_flps_pswp.PoutW ] ;
for idx_w_file=1:size(fetch_m,1)
    fprintf(mdat_file, '%.5f\t%.5f\t %.5f\t %.5f\t %.5f\t %.5f\t %.5f\n',...
        fetch_m(idx_w_file,:)) ;
end
fprintf(mdat_file, '!\n');
end
fclose(mdat_file);
% -----
% Saving figures
% -----
plot = figure(k) ;
figure_name = strcat(file_out2,...
    printf('GO68_%.2dMHz_Vgs_%.3fV_Ids_%.3fmA_ZL_%.4f+j%.4f_Ohm.fig',...
        ic_sel_freq*1000,Vgs,Ids,real(X.Zloads(k)),imag(X.Zloads(k))));
saveas(plot,figure_name); clearvars plot; clear l; close all; clc ;
end
% -----

```

## Appendix B

# MT981EU10\_Setup - HUAWEI

The MATLAB requires an lcc or a equivalent c++ compiler in order to enable the communication with the Maury tuner (MT981EU) performed through a DLL. In addition, it is also necessary to add a piece of code to the file named 'MLibTuners.h',as shown in the following:

```
// At the begin
#ifdef __cplusplus
    extern "C" {
#endif

...

// At the end
#ifdef __cplusplus
    }
#endif

function [ocr_data] = MT981EU10_Setup(current,cmd,val)
%MT981EU10_SETUP Control routine
switch lower(cmd)
%% ----- First step load tuner library -----
case 'load_libraries'
    flag = libisloaded('MLibTuners' );

    if flag == 0
        addpath('C:\Program Files (x86)\Maury\MLibV04\' );
        loadlibrary('MLibTuners','MLibTuners.h' );
        ocr_data = 1;
    end
case 'show_functions'
    libfuncions('MLibTuners');
    ocr_data = 1 ;

case 'view_all_func'
    libfuncions('MLibTuners');
    ocr_data = 1 ;

%-----
[current,ctrl_exe,model,error] = calllib('MLibTuners','add_controller',0,...
    TunHubMech','MT981EU10',250,11,0,3170,...
```

```

                                'error'                                );
[current,model,num_axis,tun_step_limits,...
fmin,fmax,freq_to_change_probe] = calllib('MLibTuners','add_tuner',0,'MT981EU10',...
                                3170,0,1,3,[0 0 0],0,0,0,...
                                'error'                                );
ocr_data      = [current,ctrl_exe,model,error,...
                current,model,num_axis,tun_step_limits,fmin,fmax,...
                freq_to_change_probe]
;
case 'init'
ocr_data      = calllib('MLibTuners','init_tuners','error'      );
case 'get_tuner_pos'
[flag,carr,p1,p2,error] = calllib(current,'get_tuner_position',0,0,0,0,'error');
ocr_data.flag      = flag                                        ;
ocr_data.carr      = carr                                        ;
ocr_data.p1        = p1                                        ;
ocr_data.p2        = p2                                        ;
ocr_data.error     = error                                       ;

case 'get_tuner_refl_data'

                s11_x = 0;    s21_x = 0;    s12_x = 0;    s22_x = 0        ;
                s11_y = 0;    s21_y = 0;    s12_y = 0;    s22_y = 0        ;

[tuner_number,carr,p1,p2,s11_x, ...
s11_y,s21_x,s21_y,s12_x,s12_y, ...
s22_x,s22_y,error] = calllib(current,'get_tuner_refl_data',
                val.tuner_number,val.interp_mode,
                val.freq,
                val.gamma_x_termination,
                val.gamma_y_termination, ...
                val.gamma_x,val.gamma_y,9500,9500,9500,
                s11_x,s11_y,
                s21_x,s21_y,
                s12_x,s12_y,
                s22_x,s22_y,                                'error' );
ocr_data.tuner_number = tuner_number                            ;
ocr_data.carr         = carr                                    ;
ocr_data.p1           = p1                                    ;
ocr_data.p2           = p2                                    ;
ocr_data.error        = error                                  ;
ocr_data.s11          = s11_x + 1i.*s11_y                     ;
ocr_data.s21          = s21_x + 1i.*s21_y                     ;
ocr_data.s12          = s12_x + 1i.*s12_y                     ;
ocr_data.s22          = s22_x + 1i.*s22_y                     ;

case 'free_tuner_data'
[ocr_data.error] = calllib(current,'free_tuner_data',val.tuner_number) ;
case 'move_tuner'
[flag,error]     = calllib(current,'move_tuner',0,.val(1),val(2),val(3),...
                                'error'                                );
ocr_data         = [flag,error]                                     ;

case 'get_tuner_refl_posn'
[tuner_number,carr,p1,p2,error] = calllib(current,'get_tuner_refl_posn',
                val.tuner_number, val.interp_mode,val.freq,...
                val.gamma_x_termination,...
                val.gamma_y_termination,

```

```

        val.gamma_x, val.gamma_y, 9500, 9500, 9500,
            'error' );

ocr_data.tuner_number = tuner_number ;
ocr_data.carr = carr ;
ocr_data.p1 = p1 ;
ocr_data.p2 = p2 ;
ocr_data.error = error ;

case 'read_tuner_data_file'
[tuner_number, fname, tuner_model, error] = calllib(current, 'read_tuner_data_file',
            val.tuner_number, val.fname,
            val.tuner_model, 'error' );

ocr_data.tuner_number= tuner_number ;
ocr_data.tuner_model = tuner_model ;
ocr_data.fname = fname ;
ocr_data.error = error ;

case 'get_tuner_position_mode'
[tuner_number, mode, error] = calllib(current, 'get_tuner_position_mode',
            val.tuner_number, val.freq, val.mec(1), ...
            val.mec(2), val.mec(3), val.interp_mode, ...
            'error' );

ocr_data.tuner_number = tuner_number ;
ocr_data.mode = mode ;
ocr_data.error = error ;

end

```

## Appendix C

# GaN Load-Pull - Target impedances

The following table C.1 shows the used target impedances in the characterization of the GaN microwave transistor.

Point	R	jX	Point	R	jX	Point	R	jX
1	4.3658	1.0801	39	1.8616	6.24	77	7.1276	5.6441
2	1.9708	7.9461	40	1.6419	6.9399	78	5.6567	6.3424
3	1.9033	8.1284	41	1.4958	7.4572	79	4.4331	7.2359
4	1.7479	8.5786	42	1.4023	7.817	80	3.8085	7.8454
5	1.6448	8.9053	43	1.2444	8.4911	81	3.2771	8.4813
6	2.0668	7.6982	44	1.0699	9.3828	82	2.8394	9.1205
7	2.1563	7.4778	45	12.975	0.79843	83	2.5018	9.7199
8	2.275	7.1999	46	10.91	1.1077	84	14.176	9.8952
9	2.3832	6.9591	47	8.583	1.9	85	13.18	8.7106
10	2.6029	6.5013	48	6.8896	2.8285	86	11.552	7.5769
11	2.7828	6.1532	49	5.5093	3.8692	87	9.5463	6.9506
12	3.051	5.671	50	5.0274	4.3093	88	7.803	6.9241
13	3.6741	4.6855	51	4.0398	5.3748	89	6.5033	7.2073
14	4.8518	3.1813	52	3.3755	6.255	90	5.3553	7.7024
15	6.5044	1.5816	53	2.99	6.8501	91	4.7002	8.1116
16	8.9611	-0.089002	54	2.7309	7.2959	92	3.916	8.7616
17	11.551	-1.2091	55	2.396	7.9439	93	3.4794	9.2258
18	7.7304	-1.0806	56	2.2379	8.2855	94	3.0879	9.731
19	9.2796	-2.1989	57	2.0924	8.6264	95	2.7065	10.343
20	5.778	0.73636	58	1.8496	9.2682	96	4.5696	-0.69713
21	5.136	1.4644	59	1.6916	9.7545	97	4.107	0.078137
22	4.5564	2.1944	60	15.619	3.888	98	3.4822	1.234
23	3.3183	4.0644	61	13.065	3.2137	99	2.731	2.8445
24	2.7688	5.0887	62	9.7496	3.3128	100	2.2995	3.9246
25	2.3146	6.0758	63	8.235	3.7254	101	2.0069	4.749
26	2.1685	6.4298	64	6.5366	4.5083	102	1.7634	5.5121
27	2.0662	6.6912	65	5.407	5.2608	103	1.6034	6.0635
28	1.9166	7.0963	66	4.1362	6.4119	104	1.4374	6.6902
29	1.8026	7.4263	67	3.539	7.1099	105	1.263	7.4288
30	1.5822	8.1318	68	2.9989	7.8693	106	3.3278	-0.27019
31	1.4675	8.5446	69	2.5822	8.5747	107	2.9219	0.68894
32	1.3159	9.1588	70	2.2333	9.287	108	2.5737	1.588
33	6.8518	-2.0368	71	2.001	9.8568	109	1.9429	3.4642
34	5.8504	-0.91733	72	5.3408	13.708	110	1.6667	4.4304
35	4.6435	0.66886	73	15.653	7.3474	111	1.4474	5.2918
36	4.2166	1.3096	74	13.463	5.9009	112	1.319	5.8483
37	3.1535	3.1592	75	11.273	5.2456	113	1.1595	6.6122
38	2.3246	4.9777	76	9.0511	5.1969	114	1.1926	6.4457

Table C.1: Target impedances of the used microwave transistor.

## Appendix D

# 3-port to 2-port network conversion

### D.1 LPS - Output Network

In this work the placed spectrum/time-domain analyzer at output network of the built load-pull system is only used to monitor the waveform of the incoming signal read by the power meter. For the absolute power calibration, only a 2-port network between the DUT and the power sensor is necessary to determine the  $P_{out}$  at the microwave transistor reference plane.

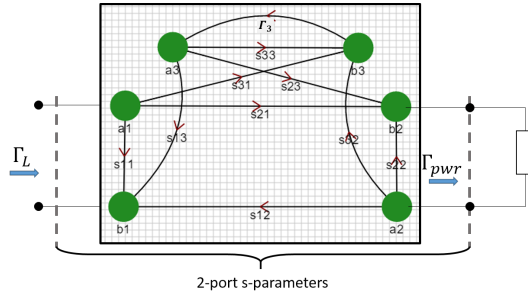


Figure D.1: Conversion of a 3-port network to 2-port network.

To convert a 3-port into a 2-port network, it is only necessary to know the s3p-parameters of the output network and the reflection coefficient,  $\Gamma_3$ , of time-domain/spectrum analyzer, that is given by the following equations:

$$\begin{bmatrix} b_1 \\ b_2 \\ b_3 \end{bmatrix} = \begin{bmatrix} S_{11} & S_{12} & S_{13} \\ S_{21} & S_{22} & S_{23} \\ S_{31} & S_{32} & S_{33} \end{bmatrix} \begin{bmatrix} a_1 \\ a_2 \\ a_3 \end{bmatrix} \quad (\text{D.1})$$

and

$$\Gamma_3 = \frac{a_3}{b_3} \quad (\text{D.2})$$

As a result of the 3-port simplification, the 2-port network is given by:

$$\begin{bmatrix} b_1 \\ b_2 \end{bmatrix} = \begin{bmatrix} S_{11} + \frac{S_{13}S_{31}\Gamma_3}{1-S_{33}\Gamma_3} & S_{12} + \frac{S_{13}S_{32}\Gamma_3}{1-S_{33}\Gamma_3} \\ S_{21} + \frac{S_{31}S_{23}\Gamma_3}{1-S_{33}\Gamma_3} & S_{22} + \frac{S_{23}S_{32}\Gamma_3}{1-S_{33}\Gamma_3} \end{bmatrix} \begin{bmatrix} a_1 \\ a_2 \end{bmatrix} \quad (\text{D.3})$$

## D.2 LPS - Input Network

To convert a 3-port into a 2-port network, it is only necessary to know the s3p-parameters of the input network and the reflection coefficient of the power sensor A. Thus based on the diagram of the Fig. D.2 and the following equations a new s2p-parameters are obtained.

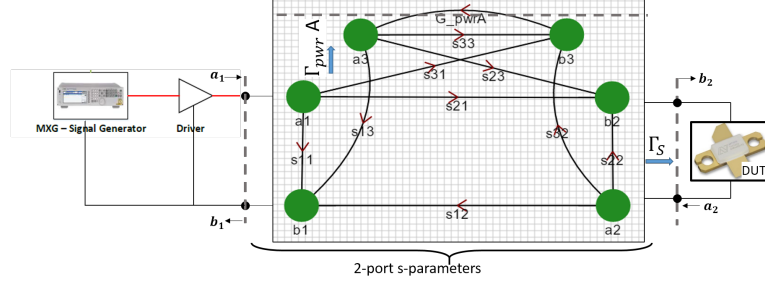


Figure D.2: Conversion from 3-port to 2-port s-parameters of the input network.

$$\begin{bmatrix} b_1 \\ b_2 \\ b_3 \end{bmatrix} = \begin{bmatrix} S_{11} & S_{12} & S_{13} \\ S_{21} & S_{22} & S_{23} \\ S_{31} & S_{32} & S_{33} \end{bmatrix} \begin{bmatrix} a_1 \\ a_2 \\ a_3 \end{bmatrix} \quad (\text{D.4})$$

and

$$\Gamma_{pwr_A} = \frac{a_3}{b_3} \quad (\text{D.5})$$

,where  $\Gamma_{pwr_A}$  represents the power sensor A placed at the input network used to assists the characterization of the device measuring the uncorrected power that is being injected to the DUT.

$$\begin{bmatrix} b_2 \\ b_3 \end{bmatrix} = \begin{bmatrix} S_{22} + \frac{S_{21}S_{12}\Gamma_{pwr_A}}{1-S_{11}\Gamma_{pwr_A}} & S_{23} + \frac{S_{21}S_{13}\Gamma_{pwr_A}}{1-S_{11}\Gamma_{pwr_A}} \\ S_{32} + \frac{S_{12}S_{31}\Gamma_{pwr_A}}{1-S_{11}\Gamma_{pwr_A}} & S_{33} + \frac{S_{31}S_{13}\Gamma_{pwr_A}}{1-S_{11}\Gamma_{pwr_A}} \end{bmatrix} \begin{bmatrix} a_1 \\ a_2 \end{bmatrix} \quad (\text{D.6})$$

# HIGH-POWER AUTOMATED TUNERS

## 0.25 TO 8.0 GHz

### Features

- *Optimized for GSM/EDGE, WCDMA, WiFi, and WiMax In-Fixture and On-Wafer Applications*
- *High Matching Range for GaN, GaAs, LDMOS, and Si Characterization*
- *Simultaneous High-Matching and Low Vibration for On-Wafer Applications*
- *USB Interface for Simple, Fast and Reliable Control*
- *DLL Environment for Automated Applications*
- *Industry's Highest Accuracy Means Your Designs Work Right the First Time*
- *Industry's Best Calibration Frees Your Time for Design*



MT981BU10  
7mm High-Power Automated Tuner

### Applications and Benefits Overview

The MT981 series automated tuners are optimized for high power in-fixture and on-wafer applications requiring low impedance and low vibration simultaneously. Based on Maury's proven non-contacting probe technology, these high-performance tuners evolve beyond outdated contacting probe technology to deliver high VSWR with superb accuracy and reliability.

An integral component of Maury Device Characterization Solutions, these USB-interfaced automated tuners are controlled using one of three Maury Software Solutions; Maury's MT930 series IVCAD Advanced Measurement and Modeling Software; Maury's Device Characterization Software suite (ATS version 5 or later); or Maury's DLL environment.

The MT930 IVCAD software suite is the most advanced measurement and modeling software in the industry, with support for multiple load pull techniques including traditional load pull using external instrumentation, VNA-based load pull, active load pull and hybrid load pull.

The ATS software is an integrated device characterization suite providing front-end and back-end

device characterization tools for power and noise characterization.

The DLL environment enables direct interface with common programming tools such as Agilent VEE™, NI LabVIEW™, MS Visual Basic & C/C++, and Mathworks MATLAB™.

With a tuning resolution in excess of a million impedance points and accuracy better than -50 dB over the entire Smith chart, Maury automated tuners give you the device characterization answers you need with the accuracy necessary to make engineering decisions with confidence. Typical applications include load pull using CW, GSM/EDGE, CDMA, WCDMA, WiMax, and WiFi stimulus for mobile and infrastructure terminal design, RADAR design, and Sat-Com design.

### Controller

For optimum performance, the MT1020B ATS Power Distribution Hub can be used to control up to four (4) MT981xU series tuners. Additionally, the MT1020D Desktop Switching Power Supply can be used to provide power to a single MT981xU series tuner.

Trademarks shown above are the property of their respective owners.



## Specifications

Frequency Range ..... See **Available Models** Table  
 VSWR Matching Range .... See **Available Models** Table  
 Step Size (Probes) .....62.5 microinches<sup>1</sup>  
 Step Size (Carriage) ..... 786 microinches<sup>1</sup>  
 Connectors: ..... Precision 7mm<sup>2</sup>

## Recommended Accessories

2698C2 7mm (3/4-in. hex) torque wrench  
 A028D 7mm connector gage kit  
 8022S 7mm to 3.5mm (female) precision adapter  
 8022T 7mm to 3.5mm (male) precision adapter

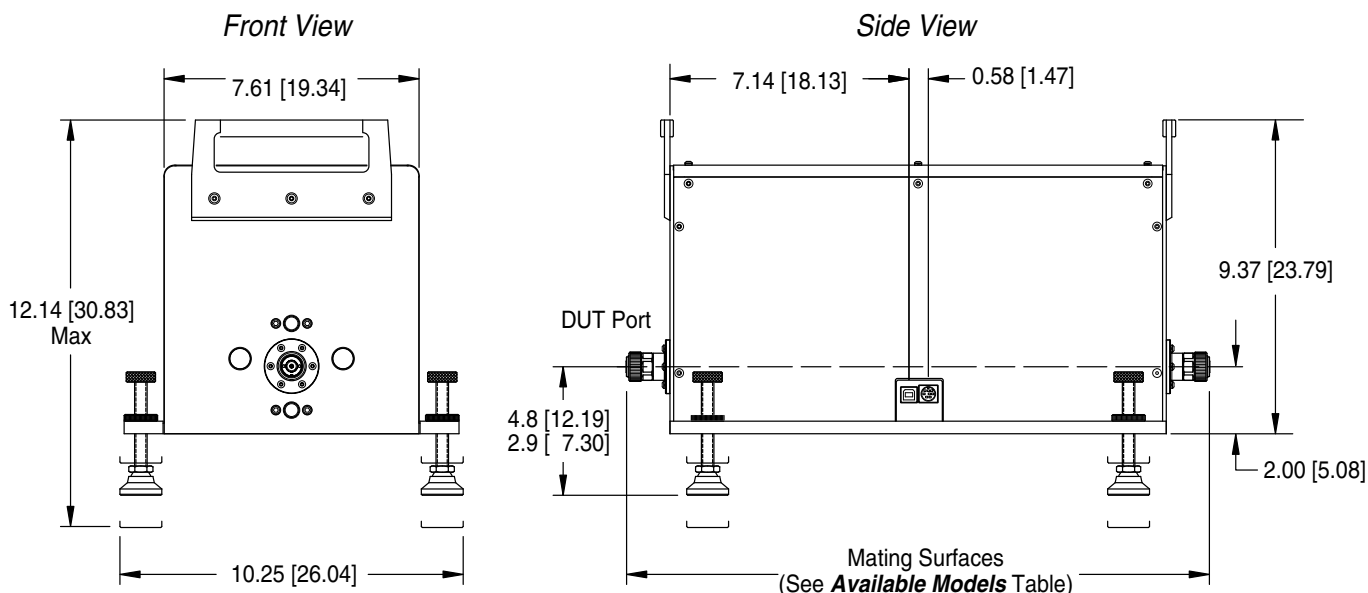
## Accessories Provided

One (1) MT1020D controller, one (1) USB cable and one (1) operating manual.

## Available Models

Model	Frequency Range (GHz)	Matching Range		Power Capability <sup>4</sup>	Vector Repeatability (Minimum)	VSWR <sup>5</sup>	Insertion Loss <sup>5</sup>	Dimensions	
		Minimum	Typical <sup>3</sup>					12.0" [30.5 cm]	10.0" [25.4 cm]
MT981AU11	0.25 – 2.5	15:1	25:1	250 W CW 2.5 kW PEP	-50 dB	1.05:1	0.3 dB	36.9" [93.5 cm]	
MT981BU15	0.40 – 2.5	30:1	45:1					23.0" [58.6 cm]	
MT981BU10	0.40 – 4.0	15:1	25:1					23.0" [58.6 cm]	
MT981BU18	0.40 – 8.0	10:1	25:1		23.0" [58.6 cm]				
MT981WU10	0.60 – 6.0	15:1	25:1		23.0" [58.6 cm]				
MT981EU10	0.80 – 8.0	15:1	30:1	-50 dB	15.9" [40.3 cm]				

## Dimensions – Inches and [cm]



<sup>1</sup> Based on 1/2 stepping the drive motors.  
<sup>2</sup> Precision 7mm per Maury data sheet 5E-060.  
<sup>3</sup> Defined as the minimum VSWR within 70% of the frequency range.

<sup>4</sup> Power rated at maximum VSWR.  
<sup>5</sup> With probes fully retracted.